

Silicification in the Ocean: from molecular pathways to silicifiers' ecology and biogeochemical cycles

Ivia Closset^{1,2}, J. Jotautas Baronas³, Fiorenza Torricella^{4,5}, Félix de Tombeur^{6,7}, Bianca T.P. Liguori⁸, Alessandra Petrucciani^{9,10}, Natasha Bryan¹¹, María López-Acosta^{12,*}, Yelena Churakova¹³, Antonia U. Thielecke^{11,*}, Zhouling Zhang⁸, Natalia Llopis Monferrer^{14,15}, Rebecca A. Pickering¹⁶, Mathis Guyomard¹⁷, Dongdong Zhu¹⁸

¹Finnish Meteorological Institute, Dynamicum Erik Palménin aukio 1, 00560 Helsinki, Finland

²Marine Science Institute, University of California Santa Barbara, Santa Barbara, CA, USA

³Department of Earth Sciences, Durham University, UK

⁴Department of Mathematics, Informatics and Geosciences, MIGe, University of Trieste

⁵Instituto of Polar Sciences, ISP-CNR, Bologna

⁶CEFE, Univ Montpellier, CNRS, EPHE, IRD, Montpellier, France

⁷School of Biological Sciences and Institute of Agriculture, The University of Western Australia, Perth, WA, Australia

⁸GEOMAR, Helmholtz Centre for Ocean Research, Kiel, Germany

⁹Dipartimento di scienze della vita e dell'ambiente, Università Politecnica delle Marche, Ancona, Italy

¹⁰CIRCC, Consorzio Interuniversitario Reattività Chimica e Catalisi, Italy

¹¹Alfred Wegener Institute Helmholtz Centre for polar and marine research, Germany

¹²Instituto de Investigaciones Marinas (IIM), CSIC, C/Eduardo Cabello 6, 36208 Vigo, Spain

¹³Centre for Ecology and Evolution in Microbial Model Systems (EEMiS), Linnaeus University, Kalmar, Sweden

¹⁴Sorbonne University, CNRS, UMR7144 Adaptation and Diversity in Marine Environment (AD2M) Laboratory, Ecology of Marine Plankton team, Station Biologique de Roscoff, Roscoff, France

¹⁵Monterey Bay Aquarium Research Institute, Moss Landing, CA, United States

¹⁶Department of Geological Sciences, Stockholm University, Stockholm, Sweden

¹⁷LOCEAN-IPSL, Sorbonne Université (SU, CNRS, IRD, MNHN), Paris 75005, France

¹⁸Key Laboratory of Marine Chemistry Theory and Technology, Ministry of Education, Ocean University of China, Qingdao 266100, China

Correspondence to: María López-Acosta (lopezacosta@iim.csic.es) and Antonia U. Thielecke (antonia.thielecke@awi.de)

29 **Abstract.** The oceanic silicon (Si) cycle has undergone a profound transformation from an abiotic system in the Precambrian
30 to a biologically regulated cycle driven by siliceous organisms such as diatoms, Rhizaria, and sponges. These organisms
31 actively uptake Si using specialized proteins to transport and polymerize it into amorphous silica through the process of
32 biosilicification. This biological control varies depending on environmental conditions, influencing both the rate of
33 silicification and its ecological function, including structural support, defence, and stress mitigation. Evidence suggests that
34 silicification has evolved multiple times independently across different taxa, each developing distinct molecular mechanisms
35 for Si handling. This review identifies major gaps in our understanding of biosilicification, particularly among lesser-known
36 silicifiers beyond traditional model organisms like diatoms. It emphasizes the ecological significance of these underexplored
37 taxa and synthesizes current knowledge of molecular pathways involved in Si uptake and polymerization. By comparing
38 biosilicification strategies across taxa, this review calls for expanding the repertoire of model organisms and leveraging new
39 advanced tools to uncover Si transport mechanisms, efflux regulation, and environmental responses. It also emphasizes the
40 need to integrate biological and geological perspectives, both to refine palaeoceanographic proxies and to improve the
41 interpretation of microfossil records and present-day biogeochemical models. On a global scale, Si enters the ocean primarily
42 via terrestrial weathering and is removed through burial in sediments and/or authigenic clay formation. While open-ocean
43 processes are relatively well studied, dynamic boundary zones – where land, sediments, and ice interact with seawater – are
44 increasingly recognized as key interfaces regulating global Si fluxes, though they remain poorly understood. Therefore, special
45 attention is given to the role of dynamic boundary zones such as the interfaces between land and ocean, the benthic zone, and
46 the cryosphere, which are often overlooked yet play critical roles in controlling Si cycling. By bringing together cross-
47 discipline insights, this review proposes a new integrated framework for understanding the complex biological and
48 biogeochemical dimensions of the oceanic Si cycle. This integrated perspective is essential for improving global Si budget
49 estimates, predicting climate-driven changes in marine productivity, and assessing the role of Si in modulating Earth’s long-
50 term carbon balance.

51 **1 Introduction**

52 Silicon (Si) is the second most abundant element in the Earth’s crust after oxygen and plays a crucial role in a variety of
53 biological and biogeochemical processes (Struyf et al., 2009; Tréguer et al., 2021). It is a nutrient used by various terrestrial
54 organisms, including plants and mammals, as well as a diverse range of marine life, such as unicellular diatoms and
55 multicellular sponges (DeMaster, 2003; Farooq and Dietz, 2015). These organisms, collectively referred to as silicifiers,
56 produce siliceous structures (also known as biogenic silica, bSi, or opal) through a biologically controlled process known as
57 biosilicification (in the context of this paper biosilicification and silicification are used interchangeably). These silicifiers
58 modulate Si cycling in the ocean through Si uptake and act as vessels of Si sedimentation and burial. While diatoms have
59 received the most attention in biosilicification research due to their ecological importance, abundance, and relative ease to
60 maintain in culture, they are not the only marine silicifiers. Recent studies have highlighted the importance of other key groups

61 such as Rhizaria and sponges (Llopis Monferrer et al., 2020; López-Acosta et al., 2018; Maldonado et al., 2020). Silicon also
62 contributes to other forms of biomineralization beyond siliceous structures made by silicifiers. It plays a role in the calcification
63 of some coccolithophores (Durak et al., 2016; Ratcliffe et al., 2023a) and in the formation of silicified mouthparts in copepods
64 (Naumova et al., 2015). In plants, Si is found at a wide range of concentrations and silicification contributes to the regulation
65 of numerous biotic and abiotic stresses (Currie and Perry, 2007). Furthermore, the use of Si extends beyond eukaryotes, and it
66 has been demonstrated that marine picocyanobacteria are able to accumulate important quantities of bSi (Baines et al., 2012).
67 This growing body of work reveals that biosilicification is a widespread and evolutionary diverse phenomenon. Broadening
68 our focus beyond diatoms is therefore essential to fully capture the complexity and global significance of biosilicification and
69 its influence on the Si cycle in the ocean.

70 Particularly among non-model taxa such as protists, sponges, and picocyanobacteria, the physiological mechanisms
71 underlying Si uptake, transport, and polymerization are still unknown, limiting our ability to generalize across taxa or predict
72 functional responses to environmental change. Moreover, the role of silicifiers in shaping Si dynamics in the modern ocean
73 and over geological timescales remains difficult to quantify. This is due to limited in situ measurements, unknown isotopic
74 fractionation pathways, and the insufficient integration of biological diversity into global biogeochemical models. This
75 includes a limited representation of how silicifiers influence other biogeochemical cycles, particularly the carbon (C) cycle,
76 despite their major role in trapping C in surface waters and contributing to its long-term sequestration into the deep ocean via
77 the biological pump (Laget et al., 2024; Ragueneau et al., 2006; Tréguer et al., 2018). Together, these knowledge gaps hinder
78 our ability to assess how the Si cycle may respond to ongoing environmental changes, including global warming, ocean
79 acidification, and shifts in nutrient availability.

80 In celebration of the Ocean Science Jubilee, we — a group of early-career researchers specializing in biosilicification and
81 Si cycling — have collaborated to produce this review, which synthesizes current understanding of biosilicification across
82 diverse organisms and its influence on the global marine Si cycle. We summarize existing knowledge on Si transport and
83 polymerization at the cellular and molecular levels, the biological functions of bSi, and the environmental and ecological
84 factors that regulate biosilicification. We also explore the taxonomic diversity of marine silicifiers and assess their roles in Si
85 cycling across geological timescales and the modern ocean. Where relevant, we include examples from terrestrial ecosystems
86 to highlight similarities and differences with marine silicifiers and identify opportunities for cross-system knowledge
87 exchange. In addition, we examine key marine Si cycling processes in the different Earth interface zones (i.e., land-ocean,
88 sediment-ocean, and ice-ocean), which are often underrepresented in global models but play a pivotal role in Si transformation
89 and fluxes. In doing so, we highlight how stable (^{29}Si and ^{30}Si) and radioactive (^{32}Si) isotopic tools have been instrumental in
90 uncovering the contributions of these interfaces, as well as the broader biogeochemical impacts of silicifiers across time and
91 space. Finally, we identify major knowledge gaps and unknowns across taxonomic, physiological, ecological, and
92 biogeochemical domains, and propose a framework for future interdisciplinary research to address these challenges and
93 advance our understanding of biosilicification and the global marine Si cycle.

2 Silicification: a widespread yet enigmatic process

Silicification involves the incorporation of inorganic Si into living organisms to form silica structures. This form of biomineralization represents a remarkable feat of biological engineering, characterized by the precise precipitation of amorphous silica within specialized cellular compartments. In the ocean, Si is found in dissolved form as silicic acid, which is readily available for biological uptake by organisms. The silicification process in marine environments occurs at relatively low temperatures, typically ranging from a few degrees Celsius in deep waters or high latitudes to around 30°C in tropical surface waters. In contrast, synthetic silica formation in industrial or laboratory settings generally requires significantly higher temperatures and controlled conditions to facilitate precipitation and structural formation (De Tommasi et al., 2017). This stark difference highlights the efficiency of biological silicification, which occurs under ambient environmental conditions without the need for high temperatures or external catalysts (Livage, 2018).

Understanding silicification reveals the mechanisms by which organisms produce highly intricate and functionally optimized structures (see **Box 1** for tools used to study biosilicification and Si uptake). Studying biological silicification not only deepens our knowledge of biomineralization and evolutionary adaptations but also has potential applications in biomimetic materials, nanotechnology, and sustainable engineering. Despite its broad distribution among marine lineages and the well-recognized benefits, such as protection from predation, light regulation, and enhanced structural support (Ghobara et al., 2019; Pančić et al., 2019; Petrucciani et al., 2022a), the specific requirements for Si and the mechanisms underlying its metabolism remains poorly defined in most living groups.

In marine environments, most work on silicification processes has focused on diatoms, admittedly due to their abundance and the relative ease of culturing them. In these organisms, silicification begins with the intracellular accumulation of Si, which must reach a sufficiently high concentration (19 – 340 mM) for deposition (Kumar et al., 2020a). Dissolved silica (dSi) from the environment is transported across the plasma membrane into the cell and concentrated in specialized intracellular compartments called silica deposition vesicles (SDVs, **Fig 1**; Martin-Jézéquel et al., 2000), where controlled amorphous silica deposition occurs. Given the limited availability of dSi in modern oceans (ranging from under 2 μM in the surface water of central gyres to around 100 μM in polar regions; Tréguer et al., 1995), its uptake is considered the key step in silicification. While most studies have focused on dSi influx, an often-overlooked but crucial process is Si efflux from the cell, which helps prevent excessive intracellular Si accumulation that could lead to auto-polymerization and disrupt cellular function (Petrucciani et al., 2022b). Efflux has been proposed to operate through a mechanism similar to that of the influx but in reverse, although the role of sodium in this process remains unclear (Thamatrakoln et al., 2006).

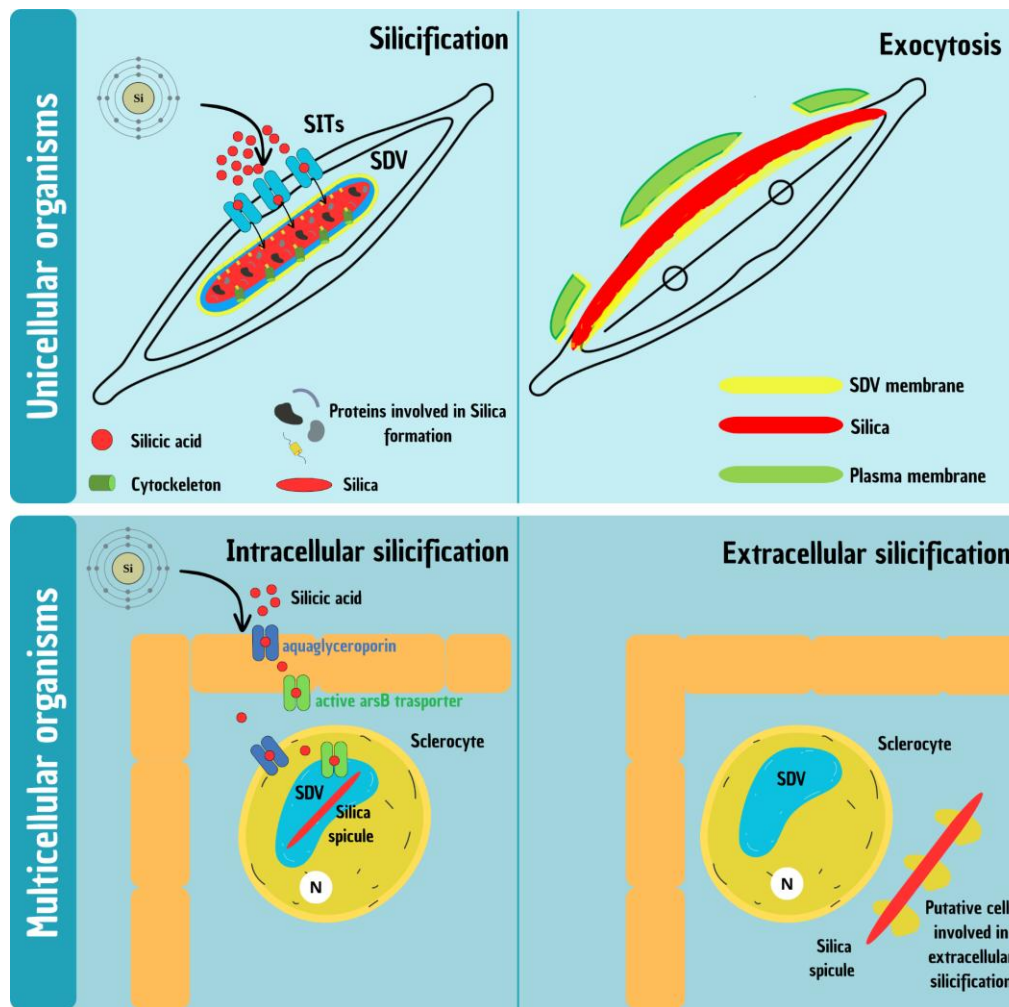


Figure 1. Schematic representation of the silicification process in unicellular and multicellular organisms. (Top) Silicification in unicellular organisms, illustrated with a model diatom. Two main phases are shown: intracellular formation (left) and exocytosis (right) of the silica-based cell wall. In the first phase, dSi is transported via Si transporters (SITs) into the membrane-bound silica deposition vesicle (SDV), where polymerization forms the intricate valve structure. In the second phase, the mature silica element is exocytosed: the distal SDV membrane and plasma membrane gradually detach from the newly formed silica and disintegrate in the extracellular space, while the proximal SDV membrane remains and functions as the new plasma membrane, forming the interface between the cell and its environment. (Bottom) Silicification in multicellular organisms, illustrated using Hexactinellid sponges. Two phases are also depicted: intracellular formation (left) and extracellular elongation (right). During the first phase, dSi is transported to the silica deposition vesicle (SDV) inside specialized cells called sclerocytes, where proteins and enzymes regulate silica polymerization to form spicules. Once spicules outgrow the cell, formation continues extracellularly, though the molecular and cytological mechanisms governing this phase remain largely unresolved.

While silicification in unicellular organisms like diatoms is relatively well understood, the process becomes significantly more complex in multicellular organisms. Unlike single-celled organisms, where dSi is directly taken up from the environment, in multicellular systems, it must traverse multiple cellular barriers before reaching the site for silica deposition (**Fig. 1**). For

example, in sponges, Si uptake and deposition involve several sequential steps. Sponges take up dSi from seawater through their outer epithelial cells and transport it internally across multiple cell layers to specialized silica-secreting cells called sclerocytes. Within sclerocytes, dSi is concentrated in SDVs, where polymerization occurs to form silica spicules, the structural elements of the sponge skeleton (Maldonado et al., 2020).

2.1 Silicon transport

Silicic acid, a small and uncharged molecule, can diffuse freely across membranes at environmentally relevant concentrations, making diffusion the main mode of uptake in diatoms (Thametrakoln and Hildebrand, 2008). However, the average surface seawater silicic acid concentration in marine environments is $10 \mu\text{mol L}^{-1}$ (Conley et al., 2017; Frings et al., 2016), which is relatively low compared to the amounts required for biomineralization. To overcome this limitation, diatoms rely on specialized protein-mediated active transport systems to efficiently take up and concentrate Si within the diatom cell, ensuring the formation of silica-based structures. This process is tightly regulated, with specific proteins preventing premature silica polymerization during the initial stages of silicification.

The first Si transporters (SITs) were identified in the pennate diatom *Cylindrotheca fusiformis* (Hildebrand et al., 1997). These sodium-coupled active transporters facilitate silicic acid uptake from the environment and exhibit variations in cellular localization, binding affinity and transport rates. Diatoms possess multiple SITs (Durkin et al., 2016) with distinct gene expression patterns, potentially corresponding to different silicification roles (Thametrakoln et al., 2006). Structurally, SITs typically contain 10 transmembrane domain segments (TMDs), arranged as two symmetrical 5 TMDs, and operate through a proposed transport model based on well-conserved amino acid motif pairs: EGXQ and GRQ (Thametrakoln et al., 2006), which are believed to play key roles in substrate recognition and translocation across the membrane. The hydroxyl group of silicic acid binds to the carbonyl group of the glutamine in the EGXQ motif in the SIT proteins, triggering a conformational change that allows silicic acid to pass through the membrane (Knight et al., 2016).

SITs have been identified in many eukaryotic supergroups, such as chrysophytes (Likhoshway et al., 2006) and choanoflagellates (Marron et al., 2013). These SITs, along with those from diatoms, are proposed to have evolved from SIT-like (SIT-L) proteins through duplication and fusion events (Knight et al., 2023; Marron et al., 2016). SIT-L proteins resemble half-completed variations of SITs, containing only 5 TMDs and a single EGXQ-GRQ motif pair, and likely originated in bacteria (Marron et al., 2016). Although SIT-Ls share structural similarities with SITs, their role in silicic acid uptake remains uncertain. This uncertainty is reinforced by the observation that eukaryotic lineages containing SIT-Ls tend to be less silicified than those with SITs (Hendry et al., 2018; Marron et al., 2016; Ratcliffe et al., 2023b). Recently, a SIT-L protein from the coccolithophore *Coccolithus braarudii* was confirmed to actively drawdown silicic acid in a heterologous system (Ratcliffe et al., 2023b). However, this study also suggests that SIT-Ls are less efficient transporters than conventional SITs, as their silicic acid uptake remained undetectable even when using highly sensitive radioisotopic methods (^{32}Si) typically used to measure uptake of silicic acid in diatoms and Rhizaria (see **Box 1**).

171 While SITs and SIT-Ls play a crucial role in Si transport in unicellular silicifiers, the mechanisms governing this process
172 in multicellular organisms appear to be fundamentally different, suggesting independent evolutionary pathways for
173 silicification. In sponges, Si transport involves both passive and active transport mechanisms. Passive transport occurs via
174 aquaglyceroporins, facilitating Si diffusion along its concentration gradient. Active transport is mediated by Na⁺-coupled co-
175 transporters, enabling Si accumulation against its gradient. This dual transport system allows sponges to acquire dSi from
176 seawater and transport it through the various cell barriers to the sites of spicule formation, where polymerization is initiated
177 (Maldonado et al., 2020).

178 Research on Si transport in marine macrophytes is rather limited, despite recent evidence that they may play a key role in
179 marine Si biogeochemistry (e.g. macroalgae; Yacano et al., 2021). In seagrasses, a protein called Siliplant1 has been associated
180 with the vesicular transport of silica into the apoplast, the network of cell walls and intracellular spaces outside the plasma
181 membrane, facilitating its incorporation into the extracellular matrix (Kumar et al., 2020b; Nawaz et al., 2020). For example,
182 in *Zostera marina*, this mechanism likely facilitates the deposition of amorphous silica within cell walls and intercellular spaces
183 that can persist even after harsh chemical treatments like alkaline digestion (Roth et al., 2025). Despite such evidence of “active
184 Si transport”, more research is needed to better understand and characterize Si accumulation in marine macrophytes. In this
185 respect, research on terrestrial plant species may provide valuable information. In particular, the tremendous variation in plant
186 Si accumulation between terrestrial plant species (e.g. in leaves, Si concentration ranges from negligible amounts to over 10%
187 of dry weight; de Tombeur et al., 2023b) is classically attributed to the relative importance of passive and active transport
188 (Liang et al., 2006). In short, the presence of specific influx and efflux channels encoded by specific genes would allow silicic
189 acid uptake from the soil solution. Notably, a gene coding for cell-specific silica deposition has been recently identified in rice
190 (Mitani-Ueno et al., 2023), shedding light on why certain taxa accumulate significantly more Si than others (Deshmukh et al.,
191 2020; Hodson et al., 2005). However, such gene-based mechanisms remain poorly explored in marine plants. For instance,
192 only a few proteins, such as Siliplant1, have been tentatively linked to Si transport in seagrasses (Kumar et al., 2020b; Nawaz
193 et al., 2020), with homologues of other known Si transporter genes in plants yet to be found.

194 **2.2 Silica polymerization**

195 Extensive research has sought to understand how silicic acid is internalized by silicifying organisms. This process is still being
196 actively studied to better understand its details, even though a lot of research has already been done in model diatoms
197 (Hildebrand et al., 2018; Mayzel et al., 2021; McCutchin et al., 2025), as well as in sponges (Shimizu et al., 2015, 2024; Wang
198 et al., 2012), and plants (Kumar et al., 2017a, b, 2021; Zexer et al., 2023). Silicification can occur intracellularly or
199 extracellularly, but in all cases, specialized proteins guide the formation of silica into intricate nanoscale shapes.

200 Diatoms are characterised by their ability to exploit silicic acid to build a siliceous external cell wall, called a frustule. In
201 diatoms, silica polymerization and frustule synthesis occur within SDVs. These vesicles have been visualized using
202 transmission electron microscopy but have yet to be biochemically isolated (Hildebrand et al., 2018; Hildebrand and Lerch,
203 2015). The internal environment of the SDVs is slightly acidic, facilitating the polymerization of silicic acid into a gel-like

204 silica network (Iler, 1979). Once inside the cells, yet unidentified binding components –potentially ligands or proteins– are
205 thought to maintain silicic acid in solution and prevent premature autopolymerisation, which occurs at concentrations
206 exceeding 2 mM (Martin-Jézéquel et al., 2000). Although polymerization was long assumed to be restricted to SDVs, recent
207 discoveries in certain diatom species with elaborate silica appendages suggest that silicification may also occur extracellularly
208 (Mayzel et al., 2021).

209 Silicon polymerization in diatoms is finely controlled by specialized proteins, with silaffins being the most extensively
210 studied. These small, lysine- and serine-rich peptides catalyse silica polymerization, and the morphology of the resulting silica
211 structure depends on their concentration and specific combination (Kröger et al., 1999, 2002). Other key proteins include long-
212 chain polyamines (LCPAs), which catalyse silica polymerization in the presence of polyanions, and silacidins, proteins rich in
213 serine and acidic amino acids that catalyse silica formation in the presence of LCPAs (Wenzl et al., 2008). Additional proteins
214 contribute to specific steps in the process: 1) Cingulins, which are rich in tryptophan and tyrosine, localize to the girdle bands
215 of diatom frustules; 2) Ammonium fluoride insoluble proteins (AFIM) are hypothesized to serve as pattern-forming base
216 layers, and 3) silicalemma associated proteins (SAPs), including Silicanin-1, probably function as intermediaries between the
217 cytoskeleton and the SDV (Görlich et al., 2019; Kotzsch et al., 2017; Tesson et al., 2017).

218 Silica polymerization in sponges is also biologically regulated and occurs both intracellularly and extracellularly.
219 Generally, intracellularly polymerization occurs within SDVs located in sclerocytes: The formation of longer spicules (i.e.
220 250-300 μm), known as megascleres, is completed outside the cell, where silica is deposited externally (Schröder et al.,
221 2007). Initial formation begins inside the sclerocyte but is transported out of the cell for further elongation, although the
222 mechanisms underlying extracellular silicification remain poorly understood. Some studies suggest that sclerocytes may either
223 release exosome-like, silica-rich vesicles (silicasomes) or physically migrate along the growing spicule, depositing silica
224 directly without the need for protein mediation (Müller et al., 2013; Schröder et al., 2007; Wang et al., 2012). More recently,
225 specific enzymes involved in extracellular silica deposition have been identified in hexactinellid sponges (Shimizu et al., 2024),
226 suggesting a more complex and regulated process than previously assumed. However, some evidence also indicates that not
227 all large hexactinellid spicules are completed extracellularly, challenging the assumption that size alone determines the
228 transition from intra- to extracellular silicification (Mackie and Singla, 1997).

229 Most research on the enzymatic control of silica polymerization in sponges is relatively recent. The first enzyme identified
230 in this process, silicatein, was described by Shimizu et al. (1998). Silicateins are cathepsin-like proteins that catalyze the
231 hydrolysis and condensation of silicic acid, facilitating controlled silica polymerization (Müller et al., 2007; Riesgo et al.,
232 2015; Wang et al., 2012). These enzymes regulate polymerization through their surface hydroxyl groups and exhibit species-
233 specific variants that influence spicule morphology (Shimizu et al., 2015). Sponges also produce silicase, an enzyme that
234 hydrolyzes silica under specific physiological conditions, potentially regulating silica solubility and remodeling during spicule
235 growth (Ehrlich et al., 2010). Recent findings have identified additional proteins involved in silica polymerization, including
236 silicatein-interacting proteins that modulate polymerization efficiency and structural integrity (Shimizu et al., 2024).

Furthermore, collagen-like and lectin-like proteins may play auxiliary roles in silica deposition by modulating silica-protein interactions (Shimizu et al., 2024; Wang et al., 2012).

These biomineralization mechanisms evolved independently across the three classes of siliceous sponges. Demosponges rely on silicateins for silica deposition, whereas hexactinellid sponges lack silicateins and instead use hexaxilin for intracellular polymerization, along with glassin and perisilin for extracellular silica deposition that thickens spicules (Shimizu et al., 2015, 2024). Homoscleromorph sponges also display unique silica polymerization mechanisms, though the enzymes involved remain unidentified. The presence of unrelated enzymes in the Class Demospongiae and Hexactinellida, along with the distinct mechanisms observed in Homoscleromorpha, suggests that silicification has evolved multiple times independently in sponges (Shimizu et al., 2024). This convergent evolution underscores the adaptive significance of silica biomineralization in marine environments and highlights the diverse molecular strategies underpinning sponge silicification.

In plants, it is increasingly accepted that some cell wall polymers and proteins can initiate and control silicification (Zexer et al., 2023). For instance, the deposits of silica in the so-called silica cells found in many grass species are thought to be controlled by a protein named Siliplant1 (Kumar et al., 2020b; Zexer et al., 2023). These works have been pivotal to further understanding plant silicification and its potential links to other silicifying organisms (Kumar et al., 2020a).

2.3 Environmental and ecological influences on silicification

While the regulated flow of silica ions is crucial for biomineralization, it is not the only factor determining this process. Biomineralization is influenced by a complex interplay of environmental and ecological conditions. Although most studies have again focused on diatoms, similar mechanisms likely occur in other silicifying organisms. Silica deposition depends directly on dSi availability, with its limitation resulting in reduced silicification (Brzezinski et al., 1990; McNair et al., 2018; Shrestha et al., 2012). Lower temperatures have also been associated with increased silicification in diatoms (Durbin, 1977). Additionally, under replete silica conditions, silicification tends to be inversely correlated with growth rate, suggesting that other growth-limiting factors, such as the availability of iron ($\text{Fe}^{2+}/\text{Fe}^{3+}$) and zinc (Zn^{2+}), may indirectly regulate frustule formation (Flynn and Martin-Jézéquel, 2000; Martin-Jézéquel et al., 2000). Light intensity further influences silicification in a complex manner, with increased silicification observed under both low ($15 \mu\text{mol photons m}^{-2} \text{ s}^{-1}$) and high ($300 \mu\text{mol photons m}^{-2} \text{ s}^{-1}$) light conditions (Petruciani et al., 2023; Su et al., 2018; Xu et al., 2021). Other environmental factors, such as salinity (Vrieling et al., 2007) and pH (Hervé et al., 2012), can also modulate silicification, emphasizing the intricate interplay between environmental conditions and biomineralization.

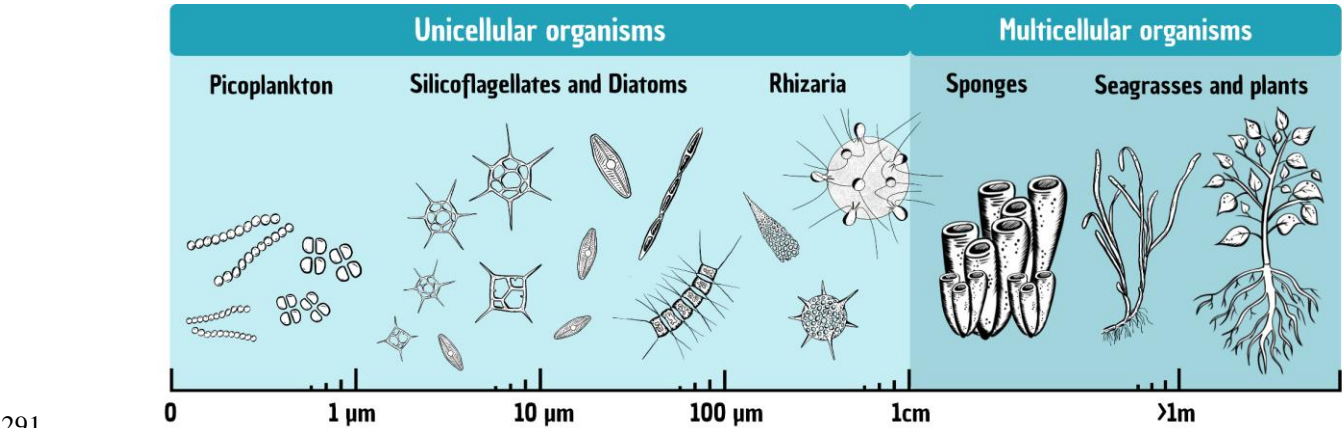
Beyond its biochemical and environmental determinants, silicification plays a fundamental ecological role for silicifying organisms contributing to their overall fitness. In diatoms, frustules act as protection against predators due to high mechanical strength (Hamm et al., 2003). More heavily silicified diatoms are often rejected as food sources by copepods (Ryderheim et al., 2022), and increased silicification has been observed in response to predator presence (Petruciani et al., 2022a; Pondaven et al., 2007). This suggests that the trophic chain can influence biomineralization processes and affect Si bioavailability. Similarly, some sponge species allocate more resources to skeleton formation as a defence strategy against

270 predation, thereby enhancing their chances of survival (Ferguson and Davis, 2008; Rohde and Schupp, 2011). In terrestrial
271 plants, silica deposition enhances resistance to herbivory by making leaves more abrasive and harder to digest (Hartley and
272 DeGabriel, 2016; Massey et al., 2006). However, studies on silica-based defences in seagrasses are currently lacking, and it
273 remains unclear whether these marine plants use similar strategies.

274 **3 Diversity of marine silicifiers**

275 Over the past decade, research has transformed our understanding of the marine Si cycle by revealing that multiple groups of
276 organisms contribute to silica dynamics, challenging the long-standing paradigm that diatoms were the sole important
277 silicifiers. Historically, diatoms have been considered the primary drivers of bSi production and recycling in the ocean (Nelson
278 et al., 1995; Tréguer et al., 1995; Tréguer and De La Rocha, 2013). However, recent studies have highlighted the significant
279 role of other groups, such as Rhizaria and sponges (e.g. Laget et al., 2024; Llopis Monferrer et al., 2020; Maldonado et al.,
280 2019). Additionally, many other taxa have been identified as interacting with Si (Baines et al., 2012; Churakova et al., 2023;
281 **Fig. 2**), however, their contributions to Si cycling have yet to be quantified on regional and global scales. Beyond their
282 contributions to Si cycling, the ecophysiological functioning of these groups is often poorly understood.

283 Understanding the taxonomic and functional diversity of silicifiers is not only crucial for ecological and evolutionary
284 perspectives, but also provides essential inputs for functional trait models that incorporate silicic acid cycling and silicifying
285 organisms (see also **Box 3**), thereby improving the predictive power of global biogeochemical models. For example, Naidoo-
286 Bagwell et al. (2024) recently demonstrated this by extending the Earth system model cGENIE with a diatom functional group,
287 therefore requiring dSi, which improved the model’s ability to reproduce observed nutrient fields, export production, and
288 global distributions of diatoms. This expanding knowledge emphasizes the need to integrate multiple biological contributors
289 into the Si biogeochemical cycle to better understand its functioning and enhance our ability to predict the effects of climate
290 change and anthropogenic impacts (Tréguer et al., 2021).



291
292 **Figure 2. Total size range of silicifiers, from the smallest unicellular organisms (picoplankton) up to multicellular terrestrial plants.**

293
294
295
296

The following paragraphs provide an overview of the main groups of silicifiers, ordered by their average size ranges and the current state of the art regarding their ecology and contributions to Si and C cycling.

297 **3.1 Picoplankton**

298 Picoplankton is a broad size category encompassing all planktonic or floating organisms measuring under 2 μm , though this
299 is often extended to 3 μm due to the filter sizes used in field studies (Vaulot et al., 2008). The three main groups of picoplankton
300 include heterotrophic bacteria, autotrophic bacteria (picocyanobacteria from the genera *Prochlorococcus* and *Synechococcus*),
301 and autotrophic eukaryotes (picoeukaryotes). Picocyanobacteria and picoeukaryotes are typically grouped together under the
302 moniker picophytoplankton. The discovery of large abundances of heterotrophic bacteria in the oceans, larger than previously
303 estimated, first put these tiny unicellular organisms on the map (Hobbie et al., 1977). Since then, picoplankton have been
304 discovered to be the base of the microbial food web, and their significant contributions in terms of biomass and productivity
305 make them influential players in global biogeochemical cycling (Azam et al., 1983; Falkowski et al., 2008; Le Quéré et al.,
306 2005).

307 Picoplankton are distributed widely in oceanic and freshwater environments, often described as ubiquitous or cosmopolitan.
308 However, different picoplankton groups fill different environmental niches. For example, *Synechococcus* and picoeukaryotes
309 prefer lower temperatures, while *Prochlorococcus* thrives in higher temperatures and lower latitudes (Buitenhuis et al., 2012;
310 Flombaum et al., 2020; Visintini et al., 2021). *Prochlorococcus* abundances are notoriously high in oligotrophic (low nutrient)
311 areas of the ocean, which can be explained by their competitive advantages (e.g. extremely small size, high diversity; Biller et
312 al., 2015). Meanwhile, in nutrient-replete upwelling areas picoeukaryote growth is favoured (Li et al., 2023; Painting et al.,
313 1993). Additional environmental factors that can affect picoplankton distribution patterns are light intensity and water mass
314 events, as well as biological factors; such as the presence of predatory microplankton and viruses (Fuhrman, 1999; Otero-
315 Ferrer et al., 2018; Sieradzki et al., 2019). Models predicting the impact of climate change on picoplankton suggest a global
316 increase in picophytoplankton abundances, particularly in areas like the Arctic and Indian Oceans (Flombaum et al., 2020). In
317 contrast, heterotrophic bacterial biomass in surface waters is expected to slightly decline, though this decrease is minor
318 compared to the predicted reductions in microplankton and larger organisms (Heneghan et al., 2024; Kim et al., 2023). Overall,
319 these findings indicate that future oceans will be increasingly dominated by picoplankton.

320 Picoplankton generally lack structural cellular components made of Si. However, some exceptions exist, such as *Triparma*
321 *laevis* from the class Bolidophyceae, a close relative of diatoms that can measure less than 3 μm in size (Booth and Marchant,
322 1987; Kuwata et al., 2018; Yamada et al., 2014). Nevertheless, there is strong evidence that picoplankton interact with dSi in
323 their environments regardless of whether or not they possess siliceous structures. Both extracellular and intracellular
324 incorporation of dSi has been observed in heterotrophic bacteria. In some species of the bacterium *Bacillus*, dSi uptake occurs
325 during an early stationary phase and is used for spore formation (Hirota et al., 2010). Environments where dSi is saturated,

particularly geothermal hot springs, are sites of extracellular silica polymerization in different bacterial species (Inagaki et al., 2003; Lalonde et al., 2005; Phoenix et al., 2000). In the marine environment, *Synechococcus* cells from the Sargasso Sea were found to harbour highly concentrated quantities of bSi (Baines et al., 2012). BSi accumulation and/or dSi uptake has been demonstrated by marine *Synechococcus* strains in both the natural environment and in laboratory experiments (Aguilera et al., 2025; Krause et al., 2017; Ohnemus et al., 2016).

The effect of dSi on picoplankton has generally been considered neutral, as *Synechococcus* growth rates do not change when cultured in a wide range of dSi concentrations, though a new study demonstrates that high silicic acid concentrations can have negative effects on cell physiology (Ou et al., 2025). BSi accumulation has also been demonstrated by cultures of marine and brackish picoeukaryotes, including the smallest known marine eukaryote *Ostreococcus tauri* (Churakova et al., 2023). Curiously, in freshwater, *Synechococcus* bSi accumulation was not observed, suggesting that *Synechococcus* strains in this environment lack the same mechanism for dSi uptake or do not utilize dSi in ways similar to marine or brackish *Synechococcus* (Aguilera et al., 2025). A mechanistic explanation for Si uptake in these non-silicifying organisms can partially be explained by the SIT-Ls found in a limited number of bacterial and picocyanobacterial genomes (see **Section 2** and Marron et al., 2016). However, in the majority of species and strains studied, the mechanisms by which picoplankton uptake and utilize dSi need further investigation and more relevant methodologies for studying picoplankton need development.

3.2 Silicoflagellates

Silicoflagellates are marine planktonic organisms belonging to the class Dictyochophyceae (Silva, 1982), order Dictyochaales (Haeckel, 1887), which are characterised by a distinctive star-shaped silica skeleton (mostly 20–100 µm). They are exclusively marine unicellular protists and mostly considered photosynthetic, however, studies also show mixotrophic behaviour or non-photosynthetic bacterioivory (Eckford-Soper and Daugbjerg, 2016; Gereá et al., 2016; Sekiguchi et al., 2002). They have chromatophores for photosynthesis, but also possess pseudopodia, a typical feature of zooplankton, further complicating their classification (Sheath and Wehr, 2003).

Almost all of their protoplasm is located inside the skeleton, which is composed of hollow tubular elements joined at triple junctions to create a tridimensional star-shaped structure constructed outside of the cytoplasm. They have a single flagellum situated at the anterior end of the cell, which extends outside the skeleton itself (Chang et al., 2017a). In culture, they have occasionally been observed to shed their skeletons, especially at high cell abundances, and continue swimming either as flagellated cells or as unflagellated amoeboid cells. These cells can divide without cytokinesis and develop into multinucleate organisms (Henriksen et al., 1993; Van Valkenburg and Norris, 1970). This naked stage has since been described in nature and has been found to occasionally occur in significant blooms (Jochem and Babenerd, 1989; Moestrup and Thomsen, 1990). Reproduction occurs through binary fission (Van Valkenburg and Norris, 1970). In rare cases, the formation of double skeletons has been observed with the two skeletons joined at the basal ring (McCartney et al., 2014). Though other modes of reproduction have not been observed, the possibility of a sexual reproduction phase — similar to that of other phytoplanktonic organisms (e.g. diatoms) — cannot be ruled out. Silicoflagellate cell physiology remains largely understudied (Sancetta, 1990),

359 partially due to challenges in maintaining them in culture. Despite the first successful culture in 1970 (Van Valkenburg and
360 Norris, 1970), few cultures exist today, so individuals must be isolated from field samples for physiological experiments
361 (Chang and Gall, 2016; Taguchi and Laws, 1985a).

362 Silicoflagellates first appeared in the Early Cretaceous (115 million years ago; McCartney et al., 2014) and showed great
363 diversification throughout the Cenozoic (<66 Ma) (McCartney et al., 1995, 2018). Their distinct skeleton structure and
364 morphology are the basis for taxonomic identification (Malinverno, 2010) and due to their high abundance in sediments, they
365 are used in micropalaeontology as proxies for palaeotemperature reconstructions (see **Box 2** for further details). In the modern
366 ocean, silicoflagellates are thought to be composed of four extant genera: *Dictyocha* (Ehrenberg, 1837), *Octactism* (Schiller,
367 1925), *Vicicitus* (Chang et al., 2012), and *Stephanocha* (Jordan and McCartney, 2015). However, as there is strong variability
368 and plasticity in the skeleton (Dumitrica, 2014; McCartney et al., 2014; Van Valkenburg and Norris, 1970), in addition to the
369 presence of the naked stage, this has led to considerable controversy regarding the number of species and genera (Chang et al.,
370 2012, 2017a; Jordan and McCartney, 2015).

371 The abundances of different silicoflagellate species are influenced by variations in temperature and salinity, both in cultures
372 (Henriksen et al., 1993; Van Valkenburg and Norris, 1970) and natural environments (Hernández-Becerril and Bravo-Sierra,
373 2001; Ignatiades, 1970; Rigual-Hernández et al., 2016; Sancetta, 1990). However, the responses of individual species to these
374 environmental factors are not always consistent (Sancetta, 1990). Additionally, Malinverno et al. (2010) demonstrated that the
375 same species, *Stephanocha speculum*, can present different varieties linked to their precise ecological niches, with some
376 varieties (*S. speculum* var. *monospicata*, var. *bispicata*, and var. *speculum*) being found in open ocean conditions, while *S.*
377 *speculum* var. *coronata* is associated with sea ice cover.

378 Silicoflagellates are most abundant in nutrient-rich areas of the ocean at high latitudes (Fagerness, 1984; Henriksen et al.,
379 1993; Onodera et al., 2016; Takahashi et al., 2009) and in upwelling systems (e.g. Hernández-Becerril and Bravo-Sierra, 2001;
380 Murray and Schrader, 1983; Sancetta, 1990). Their C uptake rates have been shown to be comparable to other phototrophic
381 phytoplankton (e.g. for *Dictyocha perlaevis*; Taguchi and Laws, 1985b), though there are no studies to date comparing
382 different species of silicoflagellates or changes in environmental conditions. Despite occasional high abundances, they are
383 mostly considered insignificant contributors to primary production, planktic dynamics, and export fluxes. For example, in the
384 Arctic Ocean, while they have been shown to contribute less than 1% of the flux of particulate organic C (Onodera et al.,
385 2016), they are regionally important prey for different copepod and krill species (Nakagawa et al., 2002; Passmore et al., 2006;
386 Pasternak and Schnack-Schiel, 2001) as well as gelatinous grazers (Hiebert et al., 2025). Some species of silicoflagellates
387 (e.g. *Dictyocha* spp.) have additional ecological significance through their role as harmful algae bloom (HAB) species with
388 significant ichthyotoxicity (Esenkulova et al., 2020; Henriksen et al., 1993).

389 While the ecological relevance of silicoflagellates has been recognised, their mechanisms of silicic acid uptake remain
390 unexplored, and their contribution to the Si and C cycles has yet to be quantified. While some previous studies focused on
391 quantifying the regional contribution of silicoflagellates to Si export (Takahashi, 1989), their role in global Si cycling is
392 entirely unconstrained (Tréguer et al., 2021).

3.3 Diatoms

Diatoms are a greatly diversified group of eukaryotic phytoplankton (Bacillariophyceae) belonging to the supergroup Stramenopiles (Bowler et al., 2010). They were first observed in 1703 (Round et al., 1990) and, since then, have attracted scientific interest across multiple disciplines, from taxonomists, oceanographers, geologists, engineers, and chemists, establishing them as the by far best-studied group of marine silicifiers. To date around 18,000 species of diatoms have been described, while their total diversity is estimated between 100,000 to 200,000 genera (Jeong and Lee, 2024; Mann and Vanormelingen, 2013). These photoautotrophic unicellular microorganisms are ubiquitous and can be found in all aquatic environments, including in sea ice, soils, lichens, biofilms, and airborne; denoting their extensive adaptive capabilities (Lohman, 1960).

Diatom taxonomy is based on frustule morphological traits and categorizes the species in two groups based on cellular symmetry: centric diatoms, with a radial symmetry, and pennate diatoms, with an elongated and bilateral symmetry (Round et al., 1990). Diatoms are thought to be secondary endosymbionts (Gentil et al., 2017; Morozov and Galachyants, 2019), meaning that their precursor was a eukaryote that phagocytized another eukaryote (which became an organelle), resulting in chloroplasts surrounded by 4 membranes. The earliest known fossil record of diatoms is still widely debated (Brylka et al., 2023), but molecular clock and sedimentary evidence suggest an origin near the Triassic-Jurassic boundary (Nakov et al., 2018), when a greater availability of niches occurred. The gap in fossil records during this period has been hypothesized to relate to non-silicified or lightly silicified diatoms (Armbrust, 2009).

Diatoms are key primary producers in the oceans nowadays and their ability to adapt to different environmental conditions allows them to outcompete other phytoplanktonic groups during blooms. They are highly efficient primary producers constituting 40% of marine primary production or 20 – 25% of global Earth's primary production, despite representing only 1% of Earth's photosynthetic organic biomass (Falkowski et al., 2004; Field et al., 1998). Their intricate frustules, provide improve fitness compared to other microorganisms (Martin-Jézéquel et al., 2000) including but not limited to providing mechanical protection, allowing hydrodynamic control of particle diffusion and advection, or increasing photosynthetic efficiency.

Nutrient uptake in diatoms is facilitated by their large vacuoles, which store essential elements like nitrogen (N) and Si. This storage capacity supports rapid growth during favourable conditions, contributing to their ecological success (Behrenfeld et al., 2021). Diatoms reproduce asexually through mitotic division, which progressively reduces cell size due to the constraints of their rigid silicious frustules. During each division, the daughter cell inherits one parental valve and forms a new, smaller valve within it, leading to a gradual decrease in cell dimensions over successive generations (Jewson, 1997). When cells approach a critical minimum size threshold, sexual reproduction is triggered to restore maximal cell dimensions. This process involves the formation of auxospores, specialized zygotic cells that expand and produce the initial large vegetative cells for the next cycle (Chepurnov et al., 2002). Auxospore formation is influenced by environmental factors such as light, nutrient availability, and cell density, as well as endogenous chemical signals (Assmy et al., 2006; Mouget et al., 2009). The interplay

426 between asexual size reduction and sexual size restoration ensures diatom populations maintain their ecological and
427 evolutionary success. This unique life cycle strategy contributes to their adaptability and widespread distribution in aquatic
428 ecosystems.

429 Nutrient limitation, particularly of Si, Fe, and N, is a key driver of diatom growth and silica production. In oligotrophic
430 gyres, low dSi concentrations (0.9 – 3.0 μM) limit silica production, despite rapid diatom growth rates. In nutrient-rich zones,
431 diatom blooms significantly enhance silica and C export, with Si:C ratios ranging from 0.09 to 0.15 depending on species and
432 environmental conditions (Brzezinski, 1985). Their regionally high abundance and ubiquitous distribution make them a key
433 source of organic C for higher trophic levels, including zooplankton and fish larvae. Moreover, diatoms are an important vector
434 for C export (~20–40%; Jin et al., 2006) due to their ability to form aggregates and their dense frustule, which improves sinking.
435 As they sink, they rapidly transport organic matter to deeper ocean layers, and eventually are sequestered in sediments over
436 geological time scales thanks to their siliceous frustules that enhance their preservation within the sedimentary records. Due
437 to the well-defined ecological niches occupied by individual diatom species, their fossil assemblages serve as a reliable proxy
438 for reconstructing past environmental conditions and tracking climate evolution (see **Box 2** and e.g. Crosta et al., 2021;
439 Torricella et al., 2025).

440 **3.4 Siliceous Rhizaria**

441 Rhizaria, a diverse ‘supergroup’ of unicellular eukaryotes, represents a fascinating and largely unexplored realm of biodiversity
442 (Burki and Keeling, 2014). This supergroup is subdivided in three phyla: Endomyxa, Cercozoa, and Retaria. A key unifying
443 morphological feature within these phyla is the production of very fine pseudopodia, often numerous, and typically supported
444 by microtubules called filopodia (Adl, 2024). The major taxa of siliceous Rhizaria are represented by organisms belonging to
445 the Cercozoa and Retaria phyla. Among Cercozoans with skeletons, those belonging to the Thecofilosaria, especially the
446 Phaeodaria, possess skeletons that take the form of spicules or bars, which vary in size and shape. Although Phaeodaria were
447 traditionally classified as Radiolaria due to morphological similarities, molecular phylogenetic analyses have demonstrated
448 that they are not closely related to Radiolaria and are instead affiliated with the Cercozoa (Nikolaev et al., 2004). The phylum
449 Retaria includes organisms with skeletons of various compositions, and is divided into Foraminifera and Radiolaria. The
450 skeletons of Foraminifera are primarily made of calcium carbonate, while Radiolaria exhibit skeletons of various nature,
451 including strontium sulfate (exclusive to the Acantharia class) or opaline silica (found in the Polycystine and Sticholonche
452 classes).

453 Phaeodaria and Radiolaria, both characterized by an intricate siliceous skeleton, exhibit a remarkable range of lifestyles
454 (solitary and colonial) and trophic diversity (heterotrophic or mixotrophic with photosynthetic symbionts). They also present
455 great morphological variability, with sizes spanning from a few tens of micrometres to several millimetres, a gigantic size for
456 protists. A key structural distinction lies in their skeletons. While Radiolaria skeletons are composed of robust, solid amorphous
457 silica, Phaeodaria skeletons are hollow (Takahashi, 1983). Among the Polycystine Radiolaria, Spumellaria and Nassellaria are
458 the most extensively studied groups, largely due to their robust skeletons and continuous fossil record dating back to the early

459 Cambrian (De Wever et al., 2001). Spumellaria are characterized by concentric, generally spherical skeletons and were the
460 first to appear in the Cambrian period. In contrast, Nassellaria display bilateral symmetry and possess conical skeletal
461 structures with a limited number of spicules, first emerging in the Early Triassic (Anderson, 2001). Nassellaria are also known
462 for their ability to form colonies, such as those seen in Collodaria, or large solitary skeletons, such as those
463 of Orodaria (Nakamura et al., 2021).

464 Siliceous Rhizaria are widely distributed across the world's oceans, from tropical to polar regions, and are especially
465 abundant in open-ocean environments. These protists are commonly found in the upper layers of the ocean, where sunlight
466 supports the photosynthetic symbionts hosted by many Rhizaria species (Decelle et al., 2021). However, they are also well
467 represented in deeper zones, including the mesopelagic (Biard and Ohman, 2020). Global assessments indicate that Rhizaria
468 play a substantial role in zooplankton abundance, contributing up to 33% (Biard et al., 2016). More recent studies, also using
469 advanced imaging techniques to quantify large Rhizaria, indicate that they represent up to 1.7% of mesozooplankton C biomass
470 within the upper 500 m of the water column (Laget et al., 2024). Interestingly, Rhizaria biomass, particularly that of Phaeodaria,
471 is more than twice as high in the mesopelagic than in the epipelagic layer (Laget et al., 2024). In marine ecosystems, Rhizaria
472 have also been shown to dominate the eukaryotic community captured in sediment trap samples collected below the euphotic
473 zone, as revealed by metabarcoding analyses (Gutierrez-Rodriguez et al., 2019; Preston et al., 2020).

474 The reproductive biology of Rhizaria remains poorly understood, primarily due to the challenges of maintaining most
475 species under laboratory conditions. Although various life stages and lineage-specific cellular innovations have been observed
476 in natural environments, their functional roles, as well as their physiological and ecological significance, remain largely
477 uncharacterized (Rizos et al., 2024). Evidence suggests that both sexual and asexual reproduction occur across different
478 Rhizaria lineages. Sexual reproduction involves the production and release of haploid gametes, which fuse to form a zygote
479 with genetic material from both parent organisms. Asexual reproduction occurs by cell division during mitosis, resulting in
480 two identical organisms. In colonial forms, asexual growth may occur through fission of the central capsules, contributing to
481 colony expansion or fragmentation into multiple new colonies. In several species, reproduction involves the release of
482 numerous flagellated swarmer cells that are considered to be gametes, produced via multiple nuclear divisions within the parent
483 cell. These swarmers are released simultaneously and are presumed to fuse into zygotes, although the exact mechanisms of
484 gamete fusion and early development remain poorly understood (Suzuki and Not, 2015). While the early ontogenetic stages
485 are still not fully documented, the process of skeletal formation during growth has been extensively studied in several species
486 under laboratory conditions (Anderson, 2001).

487 The widespread distribution of siliceous Rhizaria across marine ecosystems underpins their ecological importance in both
488 food web dynamics and biogeochemical cycles. As basal components of planktonic communities, they serve as essential food
489 sources and can act as vectors for energy transfer to higher trophic levels. Many Rhizaria host photosynthetic symbionts,
490 enhancing primary production in oligotrophic waters (e.g. Llopis Monferrer et al., 2025). For instance, Collodaria are
491 particularly abundant in nutrient-poor, tropical epipelagic zones and contribute significantly to zooplankton biomass (Faure et
492 al., 2019). In deeper waters, Rhizaria play an important role in transforming sinking particles and serve as a key source of

organic C in the mesopelagic zone (Laget et al., 2024; Lampitt et al., 2023). Their ecological significance extends to the Si cycle, as many Rhizaria species take up silicic acid from seawater to build their intricate skeleton (Llopis Monferrer et al., 2020) contributing up to approximately 20% of the bSi production in the global ocean (Tréguer et al., 2021). Through both biological uptake and export, Rhizaria facilitate the vertical transport of silica and C to the deep ocean, reinforcing their role in long-term elemental cycling (Biard et al., 2018; Stukel et al., 2018). The opaline silica skeletons they produce also contribute to a rich and continuous fossil record since the Cambrian, more than 500 million years ago (**Box 2**; De Wever et al., 2001).

3.5 Sponges

Sponges belong to the phylum Porifera, which comprises approximately 9750 species classified into four distinct classes: Demospongiae, Calcarea, Hexactinellida, and Homoscleromorpha (Hooper and Van Soest, 2002; de Voogd et al., 2025). The largest and most diverse class, Demospongiae, accounts for nearly 84% of all known sponge species. The remaining species are distributed among the classes Calcarea (8%), Hexactinellida (7%), and Homoscleromorpha (1%; Van Soest et al., 2012). Sponges have been part of marine fauna since the late Precambrian (890-540 Ma) and are among the earliest known multicellular organisms on Earth (Wörheide et al., 2012). Since the Early Cambrian, many sponges have evolved siliceous skeletons, a trait present in over 80% of extant species (Neuweiler et al., 2014). These sessile filter feeders inhabit a vast range of marine habitats, from intertidal zones to the deep sea, across all latitudes (Maldonado et al., 2017; Van Soest et al., 2012). While some species have broad distributions, others are highly specialized, restricted to specific substrates or environmental conditions such as deep-sea sponge reefs, coral-associated habitats, or high-silica environments.

Due to their ubiquity and substantial biomass, sponges are increasingly recognized as key functional components of ocean ecosystems (Bell, 2008; Bell et al., 2023; Folkers and Rombouts, 2020). Their complex body structures provide habitat for a diverse array of sessile and mobile organisms, making sponge-dominant communities biodiversity hotspots (Beazley et al., 2013; Klitgaard, 1995). Additionally, sponges contribute significantly to biogeochemical cycling by filtering and recycling dissolved organic and inorganic matter and nutrients, thereby influencing the fluxes of essential elements such as C, N, P, and Si (Busch et al., 2022; De Goeij et al., 2013; Maldonado et al., 2012).

Sponges reproduce both sexually and asexually. In sexual reproduction, gametes are released into the water column for external fertilization, although some species exhibit internal fertilization (Maldonado and Riesgo, 2008). Asexual reproduction occurs through budding, fragmentation, or gemmule formation, contributing to their resilience in dynamic environments (Battershill and Bergquist, 1990). Sponges exhibit a biphasic life cycle, alternating between a pelagic larval stage and a sessile adult stage. Larvae are typically short-lived, ranging from hours to a few days, and rely on passive dispersal by ocean currents (Maldonado and Abdul Wahab, 2025). Upon settlement, larvae undergo metamorphosis into juvenile sponges, attaching to a substrate where they develop into mature, filter-feeding adults. Sponges generally live for several years to decades, with some species known to survive even for centuries (Leys and Lauzon, 1998; McGrath et al., 2018; McMurray et al., 2008).

For decades, the role of sponges in Si cycling was considered negligible. However, recent research has demonstrated their significant contribution at both regional and global scales (López-Acosta et al., 2022; Maldonado et al., 2019, 2021). Siliceous

sponges actively assimilate large amounts of dSi, transforming it into bSi for skeletal formation. Upon their death, this silica can either dissolve back into the water column, sustaining other silicifiers, or be buried in sediments, influencing long-term silica sequestration. This process is particularly relevant in deep-sea sponge grounds and continental shelf ecosystems, where sponges are particularly abundant and act as major reservoirs facilitating benthic-pelagic coupling of the Si cycle (Tréguer et al., 2021). Furthermore, sponge-mediated Si cycling interacts with other major biogeochemical cycles such as those of C and N, as sponge excretion and microbial symbionts further contribute to matter and nutrient transformations (Busch et al., 2022; Maldonado et al., 2012).

3.6 Plants

In the last two decades, an important number of functions has been assigned to leaf silicification (Cooke and Leishman, 2016; Johnson et al., 2024; de Tombeur et al., 2023b), including for wetland and aquatic plants (Schoelynck et al., 2012; Schoelynck and Struyf, 2016). Interestingly, species that are emergent (only basal stem parts in the water) and submerged tend to accumulate more Si compared with species that mostly have floating organs (Schoelynck and Struyf, 2016). In emergent and submerged species, silicification could be used to increase strength in order to overcome different physical stresses (gravity, horizontal force, etc.; Schoelynck and Struyf, 2016). In floating species, on the contrary, silicification is considered less important because they are less impacted by hydrodynamics forces (Schoelynck and Struyf, 2016). Beyond the structural role of Si in wetland and aquatic species, Si is also used for resisting herbivory. For instance, the bSi concentration of different *N. lutea* individuals is negatively correlated with the damages caused by *Galerucella nymphaeae* (Schoelynck and Struyf, 2016). Whether silicification is an adaptation or exaptation to grazing is, however, still debated (de Tombeur et al., 2023b). While trait-based approaches have recently advanced our understanding of silicification strategies in plants, applying similar frameworks to other marine silicifiers such as diatoms remains challenging due to fundamental differences in morphology and silica utilization patterns (see **Box 3**).

In coastal systems, seagrass meadows provide vital ecological services, including nutrient cycling and climate regulation, and may influence Si dynamics in estuarine and marine environments. Despite their ecological importance and proximity to riverine Si inputs, the role of seagrasses in the Si cycle remains understudied. While the elemental composition of seagrass leaves has been widely analysed for macronutrients like N and phosphorus, only a few studies have quantified Si concentration in seagrass (see Herman et al., 1996; Roth et al., 2025; Vonk et al., 2018), leaving an important gap in understanding their role in biogeochemical Si cycling. The mechanisms of Si accumulation in seagrasses are not yet fully understood, but recent research in *Zostera marina* has identified phytoliths in its roots, stems, and leaves (Rong et al., 2024) and suggests a functional dSi uptake pathway involving the Slp1 protein and vesicular transport (Kumar et al., 2020b; Nawaz et al., 2020). By measuring bSi in four families of seagrass species, Vonk et al. (2018) showed that *Z. marina* tends to accumulate more silica than other seagrasses, though still less than freshwater vegetation. This species displays a relatively low bSi content but may still play a significant role in coastal Si cycling, especially since some of its Si resists dissolution and could buffer the transport of dSi to the ocean (Roth et al., 2025).

559 **4 Impact of living organisms on marine silicon cycling**

560 Understanding the diversity, biology, and ecological roles of silicifying organisms is essential to contextualize their broader
561 influence on Earth system processes. In the following section, we examine how the biogeochemical cycle of Si has evolved
562 from abiotic to biologically mediated control, highlighting the role of silicifying taxa in transforming Si fluxes, sedimentation
563 patterns, and ocean chemistry across Earth's history and into the modern era.

564 **4.1 Evolution of the silicon cycle across geologic time**

565 Researchers began trying to better understand the evolution of the oceanic Si cycle just over three and a half decades ago
566 (Maliva et al., 1989; Siever, 1991, 1992), with considerable effort since then focused on standing stocks and how the current
567 cycle evolved (Conley et al., 2017; Trower et al., 2021). The modern oceanic Si cycle is relatively well studied (Tréguer et al.,
568 2021), with Si mainly occurring in the marine environment in the form of dSi. The amount of dSi available in the ocean is a
569 balance between inputs (e.g. rivers, aeolian, submarine groundwater, glaciers, and hydrothermal activity), biological
570 circulation via silicifiers (e.g. diatoms, sponges, and Rhizaria), and removal (e.g. burial, biogenic uptake, and secondary
571 formation; see **Fig. 3**). Overall, modern oceanic dSi concentrations are low, averaging less than 10 μM at the surface and
572 around 70 μM in the deep ocean (Gouretski and Koltermann, 2004; Tréguer et al., 1995), primarily regulated by biological
573 activity, but this has not always been the case. In the absence of silicifiers, the oceans must have had higher dSi concentrations
574 in the Precambrian compared to the Phanerozoic (Maliva et al., 2005). Understanding the evolution of silicifiers is therefore
575 crucial to understanding the geologic history of the oceanic Si cycle.

576

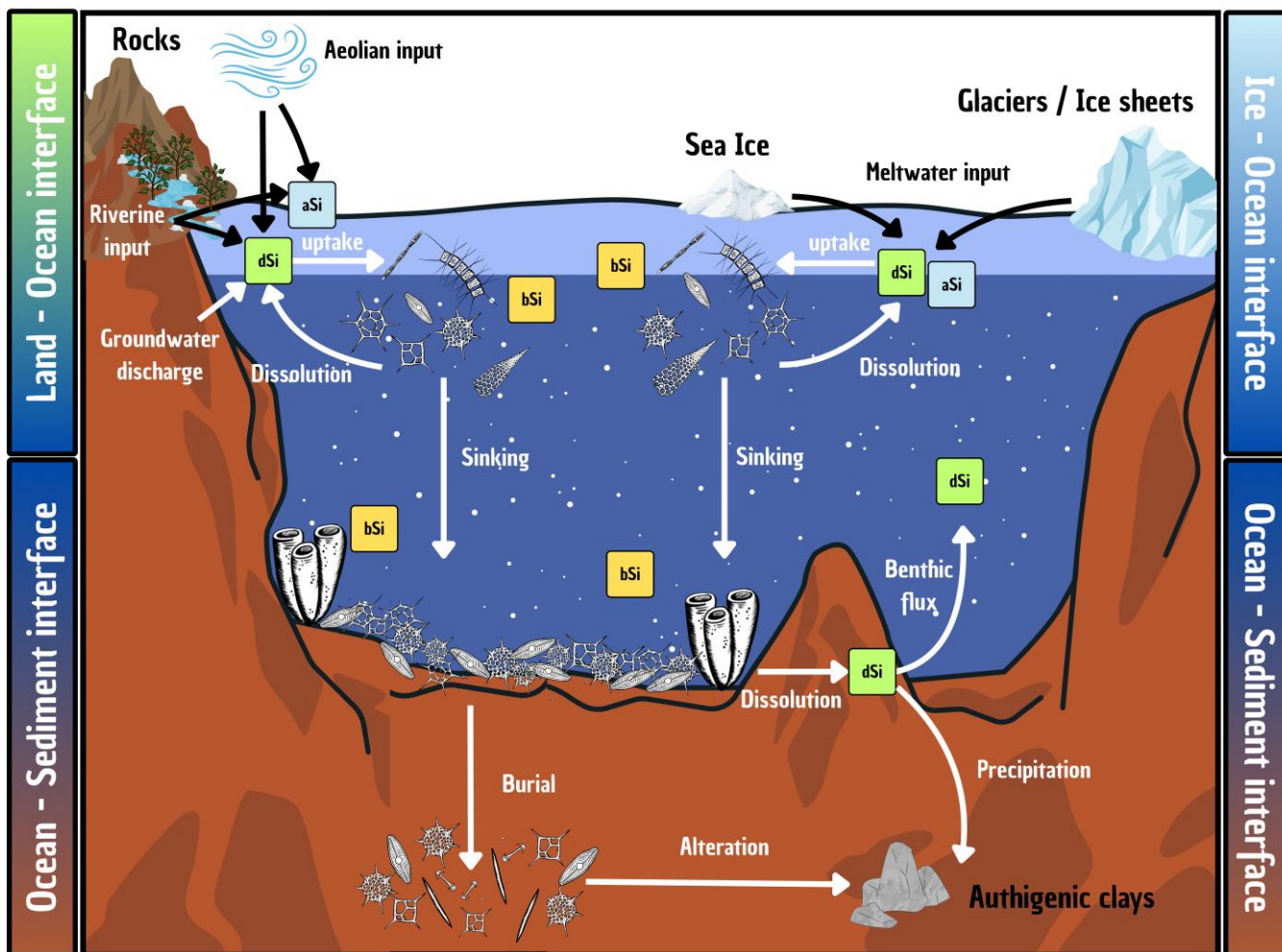


Figure 3. Schematic representation of the Si cycle in the modern global ocean, illustrating key processes occurring at the interface between the ocean and other environments (e.g. sediments, land, ice). Particular attention is given to the transformations and transfers of Si in both dissolved (dSi; green boxes) and particulate forms (e.g. biogenic silica, bSi - yellow boxes - and amorphous silica, aSi - blue boxes) as it moves between the surface and deep ocean. Details are given in section 4.3 and quantification of the fluxes are presented in Table 1.

The Precambrian era (>540 Ma) covers most of the Earth's history with little to no complex life forms in the oceans and is characterized by its widespread abiotic silica-rich chert formations. Precambrian cherts are chemically precipitated sedimentary rocks that formed in peritidal and shallow shelf environments mainly during the Proterozoic (2500 – 540 Ma) (Perry and Lefticariu, 2007). Due to continental weathering, volcanism, and hydrothermal activity, the oceans were saturated with respect to dSi, and the Si cycle was mainly controlled by the solubility of mineral phases precipitating out of the seawater (Siever, 1991, 1992). For this reason, there is one main difference between the Precambrian and the Phanerozoic (<540 Ma): bSi precipitation. Silicifiers had not yet fully evolved in an abundance to efficiently remove dSi from the oceans and influence

the Si cycle as they do today. Pinpointing the exact evolutionary timeline of dSi utilizing organisms is tricky, as fossil evidence for early biogenic silicification is viewed as controversial (Chang et al., 2017b; Porter and Knoll, 2000; Sperling et al., 2010). There are some Neoproterozoic (1000 – 540 Ma) protists which had scales that were probably siliceous (Morais et al., 2017), and Ediacaran (635 – 540 Ma) sponges with siliceous spicules (Chang et al., 2019; Chen et al., 2023), but the full extent of their influence on the Si cycle is still unknown.

The appearance of biogenic tools used during silicification challenges the idea that dSi in the Precambrian oceans was only controlled by inorganic reactions, and suggests that oceanic dSi could have been influenced by biology before the Phanerozoic began. The Precambrian Si cycle may therefore not only be abiotically controlled by inorganic reactions, volcanism, hydrothermal activity, and reverse weathering (Isson and Planavsky, 2018; Jurkowska and Świerczewska-Gładysz, 2024; Maliva et al., 1989, 2005), but potentially by the appearance of organisms capable of using Si (Conley et al., 2017; Marron et al., 2016). While the exact timeline and quantity is widely debated in the literature (e.g. Conley et al., 2017; Grenne and Slack, 2003; Maliva et al., 2005; Trower et al., 2021), following the Precambrian, a decrease in oceanic dSi concentrations (~500 – 1000 μM) occurred with the widespread evolution of large-scale skeletal marine silicification and the appearance and radiation of siliceous sponges.

The expansion of silica biomineralization via sponges at the beginning of the Paleozoic (540 – 420 Ma) (Chang et al., 2019) lowered dSi concentrations below saturation and changed the oceanic Si cycle to a biologically dominated system, which we continue to see today (Tréguer et al., 2021; Trower et al., 2021). Fossil evidence confirms this biological switch as it was observed that, as sponge populations began to increase, the thick layers of shallow abiotic silica-rich chert became less common and were replaced by deep ocean patchy hydrothermally influenced biogenic chert formations (Chang et al., 2019). Just after the appearance of sponges, a siliceous zooplankton group, Radiolaria, emerged and quickly expanded worldwide during the Ordovician (485 Ma) (Fortey and Holdsworth, 1971; Kidder and Tomescu, 2016), resulting in an additional parallel drop in oceanic dSi concentrations. From there, sponges and radiolarians regulated dSi in the oceans for several million years via biomineralization and the uptake and burial of bSi.

The Mesozoic Era (250 – 145 Ma) saw a massive change in the oceanic ecosystem, with a significant decrease in dSi concentrations. It is believed that the Mesozoic Si cycle was closer to modern day values due to the radiation of diatoms (Harper and Knoll, 1975; Maliva et al., 1989; Siever, 1991). The exact timeline of this major dSi drawdown is largely questioned (Conley et al., 2017; Trower et al., 2021; Yager et al., 2025), as the evolution and worldwide radiation of diatoms is still widely debated (Brylka et al., 2023). Molecular clocks suggest that diatoms originated 200 million years ago near the Triassic-Jurassic boundary (Nakov et al., 2018), but the first widespread fossil deposits were found in the Lower Cretaceous (121 Ma) (Brylka et al., 2024), causing uncertainty in when their abundance took control of the global oceanic Si cycle.

While the major players remain the same, the current oceans differ from those of the Mesozoic in many aspects including sea level, tectonic seafloor spreading and a lack of epicontinental seas. Our present-day marine Si cycle, as presented in the next section, is likely the result of not only biological evolution but also tectonic and palaeoenvironmental conditions

established in the Eocene (33.9 Ma), with low dSi concentrations and biological control of uptake, circulation and burial (Jurkowska and Świerczewska-Gładysz, 2024).

4.2 The modern ocean Si cycle and its fluxes

4.2.1 Biogenic silica production of different silicifiers

Silicic acid levels in modern oceans are largely regulated by diatoms (Krause et al., 2011; Kristiansen et al., 2000; Ng et al., 2024). Direct measurements of bSi production by diatoms have often relied on radioisotope tracer methods using ^{32}Si , which allow precise quantification of Si uptake and bSi production rates in natural assemblages. In the modern ocean, pelagic diatoms consume Si more efficiently and produce bSi at a rate of $255 \pm 52 \text{ Tmol-Si yr}^{-1}$ (Tréguer et al., 2021), which is higher than the annual production rate of picocyanobacteria ($<20 \text{ Tmol-Si yr}^{-1}$; Brzezinski et al., 2017; Krause et al., 2017), rhizarians ($2\text{--}58 \text{ Tmol-Si yr}^{-1}$; Llopis Monferrer et al., 2020), siliceous sponges ($6.2 \pm 5.9 \text{ Tmol-Si yr}^{-1}$; Tréguer et al., 2021), benthic diatoms ($6.1 \pm 0.7 \text{ Tmol-Si yr}^{-1}$; Tréguer et al., 2021), and macroalgae ($0.27\text{--}1.33 \text{ Tmol-Si yr}^{-1}$; Yacano et al., 2021). As the bSi production of non-diatom silicifiers is minor and falls within margin of error for pelagic diatom production, Tréguer et al. (2021) set the preferred estimate for global pelagic bSi production at $255 \pm 52 \text{ Tmol-Si yr}^{-1}$.

Although pelagic diatoms are the primary producers of bSi in the global ocean, the contributions of other silicifiers to the marine bSi production are also important at both regional and global scales when considering their role in the marine food web and the export of C to depth via the biological Si pump. For instance, the accumulation of Si by picocyanobacteria accounts for around 10% of the bSi produced in the mid-latitude ocean gyres and oligotrophic oceans (Baines et al., 2012; Krause et al., 2017; Wei et al., 2023). A recent estimate based on the Si:C ratio and picocyanobacteria cell abundances found that Si accumulation by picocyanobacteria may account for 12% of the global Si inventory and 45% of the global annual bSi production (Wei et al., 2023). However, it should be noted that Wei et al. (2023) applied the Si:C ratio of *Synechococcus* to *Prochlorococcus* (the most abundant species) in nutrient-depleted waters, where competition for dSi by diatoms is undermined, to the global ocean, which likely overestimates the role of picocyanobacteria in the marine Si cycle.

Benthic diatoms are another important group of silicifiers living in the coastal photic zone (Cahoon, 1999). The first estimate of global benthic diatom production was calculated based on: 1) a normalised production rate of benthic diatoms ($1 \text{ mol-Si m}^{-2} \text{ yr}^{-1}$ applied to the global coastal photic zone, yielding $6.8 \text{ Tmol-Si yr}^{-1}$) and 2) global benthic microalgal primary production and the Si:C ratio of the diatom cells (i.e. $(0.13 \text{ mol-Si mol-C}^{-1} \times 514 \times 10^{12} \text{ g-C yr}^{-1})/12 \text{ g-C mol}^{-1} = 5.4 \text{ Tmol-Si yr}^{-1}$; see Tréguer et al., 2021).

Due to their long lifespans and low dissolution rate, siliceous sponges store a considerable amount of Si within their skeletons (Chu et al., 2011; López-Acosta et al., 2022; Maldonado et al., 2019). However, the quantification of the sponge bSi production on the global scale remains highly uncertain (DeMaster, 2019; Tréguer et al., 2021) because of the large variations in Si consumption among sponge species at different growth stages and in different regions (López-Acosta et al., 2016; López-Acosta et al., 2018; Maldonado et al., 2011), and the poorly constrained standing crop of siliceous sponges on the seafloor.

Thus, Tréguer et al. (2021) estimated the sponge bSi production by assuming the deposition rate of sponge bSi was equal to the sponge production rate, a method that does not require information on the sponge standing crop.

Marine macroalgae and seagrasses also contain Si, and may contribute significantly to bSi production in the global neritic zone. By analysing the Si content of various macroalgae genera, Yacano et al. (2021) found large variability in the Si content (ranging from 0.13% to 39.4% by dry weight). By scaling the global net primary production of macroalgae (80 – 210 Tmol-C yr⁻¹; see Raven, 2018) by the mean C:Si ratio of macroalgae (295.6) and the median C:Si ratio of macroalgae (157.4), Yacano et al. (2021) estimated the global macroalgae bSi production to be 0.27 – 1.33 Tmol-Si yr⁻¹. This is similar in magnitude to the global bSi production of sponges and benthic diatoms.

The area of seagrasses in the global ocean was estimated using field survey data (160,387 – 266,562 km²; McKenzie et al., 2020) and modelling results (917,169 km²; Gouvêa et al., 2024), yielding large variations in the estimated seagrass meadow area. Based on the previously reported global seagrass shoot production rate (0.34 g DW m⁻² d⁻¹; Strydom et al., 2023), the Si content of seagrass leaves (0.082% DW; Vonk et al., 2018), and the Si reservoir in seagrass meadows (0.18 g-Si m⁻²; Roth et al., 2025) of the North Atlantic, a conservative estimation of the annual global seagrass bSi production would range from 0.58 – 3.33×10⁻³ Tmol-Si yr⁻¹ and the resulting seagrass bSi reservoir would range from 0.33 – 1.86×10⁻³ Tmol-Si. This represents a lower limit of the global seagrass bSi production due to the low seagrass Si content (Vonk et al., 2018) used in the calculation and the low production rate in the North Atlantic compared to other regions such as the temperate North Pacific and the temperate Southern Hemisphere (Strydom et al., 2023). Further research is necessary to understand the bSi production of these silicifiers at different seasonal and regional scales.

4.2.2 Fluxes and budget of Si in the modern ocean

Silicon, which is ultimately derived from the weathering of the Earth's crust, is transported to the ocean via various pathways (Fig. 3 and Table 1). It is then removed from the ocean through the burial of bSi (Tréguer et al., 2021) and the formation of authigenic clays (Aller and Wehrmann, 2025; Rahman et al., 2017). Accurately quantifying the different fluxes of the marine Si budget is important for understanding how it evolves in response to global warming, ocean acidification, and anthropogenic impacts (e.g. river damming and changes in land use).

The first Si budget was evaluated by Calvert (1968) and considered river and seafloor basalt weathering to be major marine Si sources. The burial of bSi on the seafloor was identified as the only ocean Si sink (Table 1). However, further research has identified several additional significant sources of Si, including hydrothermal activity (DeMaster, 1981), aeolian input (Tréguer et al., 1995), submarine groundwater discharge (Tréguer and De La Rocha, 2013), glacial meltwater in the polar regions (Tréguer et al., 2021), and the release of Si from sandy beaches (Aparicio et al., 2025). Several important sinks were also identified, including siliceous sponges (Maldonado et al., 2019; Tréguer and De La Rocha, 2013) and authigenic clay formation (Michalopoulos and Aller, 1995; Tréguer et al., 2021; Tréguer and De La Rocha, 2013) (see Table 1 and Section 4.3.3).

687 **Table 1. Si sources and sinks of the global ocean accessed during the past 60 years. The unit of the flux is expressed as Tmol-Si yr⁻¹**
688 **(10¹² mol-Si yr⁻¹). The numbers marked with “*” represent values calculated in this study, and values in parentheses are fractions**
689 **of the total Si source or sink.**

Marine Sources	Si Calvert (1968)	DeMaster (1981)	Tréguer et al. (1995)	DeMaster (2002)	Tréguer and De La Rocha (2013)	Frings et al. (2016)	DeMaster (2019)	Tréguer et al. (2021)	Aparicio et al. (2025)
River	7.2 (99%)	5.6 (90%)	5.0±1.1 (82%)	5.6 (84%)	7.3±2.0 (67%)	6.33±0.36 (62%)	6.3±0.4 (53-81%)	8.1±2.0 (55%)	8.1±2.8 (38%)
Riverine amorphous Si	-	-	-	-		1.90±1.00 (19%)	0.2±0.5 (2-3%)		
Hydrothermal sources	-	0.6 (10%)	0.2±0.1 (3%)	0.6 (9%)	0.6±0.4 (6%)	0.60±0.40 (6%)	0.4±0.2 (3-5%)	1.7±0.8 (11%)	1.7±0.9 (8%)
Basalt weathering	0.1 (1%)	-	0.4±0.3 (7%)		1.9±1.7 (17%)	0.40±0.30 (4%)	0.1±0.2 (1%)	1.9±0.7 (13%)	1.9±0.7 (9%)
Aeolian input	-	-	0.5±0.5 (8%)	0.5 (7%)	0.5±0.5 (5%)	0.30±0.20 (3%)	0.2- 1.0±0.3 (3-8%)	0.5±0.5 (3%)	0.5±0.5 (2%)
Submarine ground water	-	-	-	-	0.6±0.6 (6%)	0.65±0.54 (6%)	0.6- 3.8±2.0 (8-32%)	2.3±1.1 (16%)	0.4±0.3 (2%)
Glacial meltwater in polar area	-	-	-	-	-	-	-	0.3±0.3 (2%)	0.3±0.3 (1%)
Sandy beaches	-	-	-	-	-	-	-	-	8.3±3.0 (39%)
Total Si input flux	7.3 (100%)	6.2 (100%)	6.1±2.0 (100%)	6.7 (100%)	10.9±4. 7 (100%)	10.20±1.3 0 (100%)	7.8- 11.8±2.1 (100%)	14.8±2. 6 (100%)	21.3±8.5 (100%)

*

Marine Si

Sinks

Diatom	6.0 (100%))	5.5-7.5 (100%)	7.1±1.8 (100%)	6.5-7.4 (100%)	6.3±3.6 (55%)	-	7.4- 8.8±1.5 (91- 100%)	9.2±1.6 (59%)	9.2±2.8 (59%)
Sponges	-	-	-	-	3.6±3.7 (32%)	-	0.04- 0.9±0.9 (0-9%)	1.7±1.6 (11%)	1.7±1.6 (11%)
Reverse weathering	-	-	-	-	1.5±0.5 (13%)	-	0 (0%)	4.7±2.3 (30%)	4.7±2.3 (30%)
<i>Total Si output flux</i>	6.0 (100%))	5.5-7.5 (100%)	7.1±1.8 (100%)	6.5-7.4 (100%)	11.4±7. 6 (100%)	-	7.4- 9.7±1.8 (100%)	15.6±2. 3 (100%)	15.6±6.7 (100%)
Total marine dSi reservoir (Tmol Si)	97000 *	97000*	97000	97000*	97000	112000	112000	120000	90000
<i>Marine geological residence time of Si (yrs)</i>	15000 *	15400*	15000	14000*	10000	12000	9500- 14400	7700	4200- 7000

Based on the evaluations of marine Si sources and sinks, the modern marine Si cycle was long considered to be in a steady state, with an equal input and output flux of Si (see **Table 1** and references therein). However, recent studies suggest that the dissolution of Si from sandy beaches in the intertidal surf zones contributes a significant flux of dSi to the ocean (Aparicio et al., 2025; Fabre et al., 2019). This leads to an imbalanced global ocean Si budget (Si input flux: 21.3 Tmol-Si yr⁻¹, Si output flux: 15.6 Tmol-Si yr⁻¹; see **Table 1**). However, Tréguer et al. (2021) found that Fabre et al. (2019) overvalued the dSi from sandy beaches due to the complex composition of world ocean beaches, variable sand and seawater mixing conditions at both spatial and temporal scales, and the likely overestimation of coastal water dSi concentration (85.4 μmol L⁻¹). Furthermore, Si efflux from sandy beaches was included in the submarine groundwater discharge by Cho et al. (2018). Thus, the potential double counting of the coastal zone's Si input flux may lead to an overestimation of the world ocean's Si sources.

Due to the identification of new pathways and processes, as well as important bSi sinks (e.g. siliceous sponges), the estimation of Si input and output fluxes has doubled since the study by Calvert (1968) (**Table 1**). This has resulted in a shorter residence time of Si in the ocean, from 15000 years to approximately 7000 years. Ultimately, more accurate estimates of the biotic and abiotic fluxes and processes that drive the global Si cycle are needed to assess whether it is in a steady state or if the ocean is becoming more enriched or gradually depleted of dSi. However, this task is challenging, given the complexity of the large number of interconnected processes, coupled with both natural variability and anthropogenic perturbation.

4.3 Interfaces in the oceanic silicon cycle: processes, pathways, and perturbations

Beyond the open ocean, the global Si cycle is shaped by dynamic exchange zones — interfaces where land, sediments, and ice meet the sea. These interfaces host complex physical, chemical, and biological processes that modulate the pathways and reactivity of Si entering or leaving the ocean. Exploring these often-overlooked boundaries reveals critical controls on Si availability and ecosystem function and is essential to constrain the spatial heterogeneity and long-term evolution of the marine Si cycle.

4.3.1 Land–ocean interface: biogeochemical filters and emerging pathways in the silicon cycle

The land-ocean interface plays a critical role in the global Si cycle, serving as a dynamic transition zone where terrestrial inputs, biological transformations, and sedimentary processes interact to modulate Si fluxes to the coastal and open ocean. Rivers, the primary source of Si to the ocean, transport Si derived from continental weathering, with an increasing number of studies using germanium (Ge)/Si ratios, and Si and Ge isotopes to understand Si cycling during weathering and Critical Zone processes on land (Baronas et al., 2018; Fernandez et al., 2022; Frings et al., 2016, 2021). Recent studies have identified a number of previously overlooked Si sources, including submarine groundwater (Cho et al., 2018; Rahman et al., 2019; Santos et al., 2021; Zhu et al., 2025), salt marshes (Williams et al., 2022), and sandy beaches (Aparicio et al., 2025). These new sources challenge the view that land-ocean inputs are dominated by silicifier-modulated riverine fluxes, suggesting that physical processes may play a larger role than previously assumed. The effect of submarine groundwater discharge and beach sand dissolution on the productivity of silicifiers is yet to be investigated.

Silicifying organisms exert substantial control over Si retention, recycling, and export from land. For example, diatoms play a key role in Si cycling in large estuaries, making them effective Si filters that sequester a significant fraction of terrestrial Si before it reaches the ocean (Baronas et al., 2016; Chong et al., 2014; Zhang et al., 2020a). Similarly, plant Si accumulation exerts a major control on the terrestrial Si cycle (Alexandre et al., 1997; de Tombeur et al., 2020), with probable consequences for the land-to-ocean transfer of dSi (Conley, 2002; Conley and Carey, 2015). In fact, the annual soil-plant systems recycle much more Si (global annual Si uptake by vegetation ranges from 60 to 200 Tmol Si yr⁻¹; Conley, 2002) compared to what is transferred from land to oceans through rivers (**Table 1**). Ge and Si isotope mass balances also indicate 12 – 54% of all Si released during terrestrial weathering is taken up by terrestrial vegetation (Baronas et al., 2018; Frings et al., 2021). Such phenomena are often referred to as the “terrestrial ecosystem silica filter” (Struyf and Conley, 2012). In addition to retaining

733 and enhancing the formation of secondary weathering products on land (Baronas et al., 2020; Cornelis and Delvaux, 2016),
734 plants also increase silicate weathering rates through a wide range of processes (i.e. bio-weathering; Wild et al., 2022). In
735 contrast to the numerous studies on marine and terrestrial silicifiers, there have been relatively few studies of lacustrine Si
736 cycle, with most studies focusing on bSi oxygen isotope analyses or palaeoproductivity reconstructions (Frings et al., 2024;
737 Meister et al., 2024). As a result, the impact of freshwater bSi cycling on the land-to-ocean Si flux is relatively unconstrained.

738 Anthropogenic activities, including land use change, eutrophication, and damming, are reshaping Si fluxes at the land-
739 ocean interface, with implications for diatom productivity and coastal ecosystem health (Laruelle et al., 2009; Maavara et al.,
740 2014). New evidence continues to demonstrate the effects of eutrophication and damming on Si trapping in both river channels
741 and reservoir systems (Ran et al., 2022). Zhang et al. (2020b) showed that damming and eutrophication have altered the Si
742 isotopic signature in the Baltic Sea due to shifts in diatom-driven Si utilization and sedimentary Si regeneration. Additionally,
743 research has shown that coastal Si cycling is amplified by oyster aquaculture, which drives rapid recycling of dSi to the water
744 column (Ray et al., 2021). Climate change also impacts Si dynamics at the land-ocean interface. Palaeo-records from
745 Chesapeake Bay, the largest estuary in the US, indicate that estuarine Si cycling is sensitive to changes in sedimentation rate
746 over the Holocene, influenced by both climatic shifts (e.g. sea level rise, runoff changes) and human activities (e.g.
747 deforestation) (Nantke et al., 2019). Geilert et al. (2023) demonstrated how climatic events such as coastal El Niño can
748 accelerate marine silicate alteration, driving rapid authigenic clay formation that modifies Si availability in continental margin
749 sediments. This underscores the sensitivity of coastal Si cycling to episodic disturbances, which are becoming more frequent
750 due to climate change.

751 **4.3.2 Benthic interface: silicon recycling and burial at the seawater–sediment boundary**

752 The flux and efficiency of bSi burial in marine sediments primarily depends on 1) the bSi delivery rate to the sediment (itself
753 a function of productivity and pelagic recycling rates; Van Cappellen et al., 2002); 2) the type of bSi (e.g. diatom, Rhizaria,
754 sponges, etc.) and its inherent solubility, surface area, and dissolution rates (Aller and Wehrmann, 2025; Maldonado et al.,
755 2019, 2022); 3) detrital sediment supply and overall sediment accumulation (Loucaides et al., 2010; Presti and Michalopoulos,
756 2008); and 4) diagenetic and redox conditions in marine sediments (McManus et al., 1995; Van Cappellen and Qiu, 1997; Zhu
757 et al., 2024). Regarding the contribution of different organisms to the benthic bSi burial flux, the long-term general consensus
758 of diatom dominance has recently been challenged by a number of studies on other silicifying organisms, notably rhizarians
759 and sponges. Maldonado et al. (2019) have shown that, due to the high preservation efficiency ($45.2 \pm 27.4\%$), sponge spicules
760 could contribute a burial flux of $1.71 \pm 1.61 \text{ Tmol-Si yr}^{-1}$ globally, more than an order of magnitude higher than previously
761 estimated. While dissolution rates can vary significantly between different sponge types, bSi of the dominant demosponges is
762 orders of magnitude more resistant to dissolution compared to diatom bSi under seafloor-like conditions, although the cause
763 is yet to be identified (Maldonado et al., 2022). While rhizarians have a much lower preservation efficiency of $6.8 \pm 10.1\%$
764 (Maldonado et al., 2019), a recent study has significantly revised their global productivity upwards to $2 - 58 \text{ Tmol-Si yr}^{-1}$

(Llopis Monferrer et al., 2020). Assuming a similar benthic export efficiency to diatoms (33%), rhizarian bSi could thus theoretically contribute $0.1 - 3.4 \text{ Tmol-Si yr}^{-1}$ to the benthic bSi burial flux. The lower end of this range is consistent with the $0.09 \pm 0.05 \text{ Tmol-Si yr}^{-1}$ estimated by Maldonado et al. (2019), using direct observations of rhizarian skeletons in marine sediments from across the global ocean.

Once deposited, bSi undergoes (partial) dissolution, often coupled with diagenetic alteration (see the recent review by Aller and Wehrmann (2025) and **Fig. 3**). The latter includes the direct alteration of bSi and/or the formation of authigenic silicate (clay) phases, frequently as coatings and partial replacement of the initial bSi phases. Recent studies have attempted to quantify the relative contribution of these different processes by investigating the Si and Ge isotopic signature of both sediments and pore waters (Baronas et al., 2019; Cassarino et al., 2020; Closset et al., 2022; Ward et al., 2022). Indeed, unique isotopic fractionation during these processes could lead to predictable shifts in the Si isotopic composition ($\delta^{30}\text{Si}$) of pore water values, helping decipher the complex Si cycle in surface sediments (see **Box 4**). Most of the studies targeted the Southern Ocean or upwelling areas that are known to play a dominant role in the global marine Si cycle, hosting abundant diatom populations and exporting large quantities of bSi. For example, the Southern Ocean produces $\sim 30\%$ of global silica and acts as the largest sedimentary sink of Si ($\sim 2 \text{ Tmol-Si yr}^{-1}$; Tréguer, 2014).

The main output of these studies is that most settling bSi dissolves within the upper few centimetres of the sediment directly below the sediment-water interface, regulating pore water dSi concentrations and deep ocean Si fluxes. For example, in the Southern Ocean, diffusive Si fluxes from the sediment show a zonal trend, peaking near the Polar Front and correlating with sediment bSi content likely reflecting diatom productivity in the overlying water column (Closset et al., 2022). However, isotopic compositions of both pore water and bSi preserved in the sediment indicate that secondary processes such as the formation of authigenic aluminosilicates from the dissolving bSi, dissolution of reactive lithogenic silica, and adsorption onto particles can play a significant role in both shallow and deep benthic marine environments (Frings et al., 2024; Luo et al., 2022; Ward et al., 2022).

When authigenic silicate clay formation incorporates major cations, it lowers the pH of surrounding pore waters and therefore reduces seawater alkalinity, which is termed “reverse weathering” (Mackenzie and Garrels, 1966). It is important to recognize that not all authigenic mineral formation results in reverse weathering, but only that which consumes alkalinity and therefore drives an increase in atmosphere-ocean pCO_2 (Hong et al., 2025). While there is ample evidence that clay authigenesis is a major sink of Si and some trace elements (Baronas et al., 2019; Lauchli et al., 2025; Rahman et al., 2017), only a few studies have directly evidenced the associated consumption of cations (Michalopoulos and Aller, 1995, 2004; Wu et al., 2025). Nevertheless, it has recently been proposed that reverse weathering has played a crucial role in stabilizing marine pH and regulating climate over geological timescales (Isson and Planavsky, 2018).

Despite its importance, the formation of authigenic (newly precipitated) clays is difficult to detect in sediments dominated by detrital clays but it can occur relatively quickly (less than one year; Michalopoulos et al., 2000). However, a re-estimate of both forward and reverse weathering rates in marine sediments has suggested that there is no net alkalinity flux in marine sediments, and both processes must be tightly coupled to enable each other (Wallmann et al., 2023). Furthermore, forward and

reverse silicate weathering exhibits only a secondary role, and is strongly influenced by organic matter degradation and carbonate mineral reactions in marine sediments (Hong et al., 2025; Luo et al., 2025). Therefore, the role that bSi diagenesis-enabled reverse weathering plays in controlling Earth's long-term C cycle balance is still open for debate.

4.3.3 Cryospheric interface: the role of glacial and sea-ice systems in silicon cycling

The cryosphere includes all of Earth's frozen systems, both on land and in the ocean. This encompasses snow, glaciers, ice sheets, icebergs, sea ice, frozen rivers and lakes, permafrost, and seasonal frozen grounds. While the role of each of these systems on the Si cycle is not yet fully understood, significant progress has been made in studying glaciers, ice sheets, sea ice and permafrost (Alfredsson et al., 2015; Hatton et al., 2019b; Hawkings et al., 2017; Pokrovsky et al., 2013).

Glaciers and ice sheets cover up to 30% of Earth's land during glacial cycles, releasing significant amounts of freshwater and sediment impacting downstream ecosystems (Hopwood et al., 2025; Tréguer, 2014). This discharge can limit light penetration into the water column (Halbach et al., 2019) but it also supplies essential nutrients to marine environments, increasing primary production (Hawkings et al., 2017). Recent studies highlighted the significant contribution of glaciers and ice sheets to the global Si cycle, supplying both dSi and amorphous silica (aSi) to marine environments (Hawkings et al., 2017; Meire et al., 2016; Tréguer et al., 2021). These contributions rival other inputs such as dust deposition, groundwater discharge and hydrothermal input (Hawkings et al., 2017). The magnitude and reactivity of glacial Si fluxes have a direct influence on the dissolution rates and availability of bioavailable dSi, potentially enhancing primary production in coastal and shelf seas (Hatton et al., 2023; Ng et al., 2024).

Pro-glacial rivers are characterized by a lighter isotopic signature in both dSi and aSi, lower than the average of non-glacial rivers, from 0.16‰ to 1.38‰ respectively for the dissolved fraction (Hatton et al., 2019b) and lower than the surrounding sediment and bedrock (Hawkings et al., 2018). Under glacial conditions, enhanced chemical weathering — driven by processes such as dissolution–reprecipitation and the leaching of freshly abraded mineral surfaces — produces highly reactive inorganic aSi. Long water residence times and intense erosion further promote silicate dissolution, even at low temperatures (Hatton et al., 2021). Additionally, suspended fine particulate matter from intense erosion carries a substantial fraction of dissolvable aSi (Baronas et al., 2021; Hatton et al., 2019a; Hawkings et al., 2017). This highly soluble aSi can represent up to 95% of total potentially bioavailable silica dSi and aSi in areas receiving glacial meltwaters. Up to 20% of this aSi can dissolve rapidly after two weeks in low-nutrient seawater ($\text{dSi} < 1\mu\text{M}$) at 18°C (Hawkings et al., 2017; Hendry et al., 2025). An even less studied and potentially highly bioavailable, colloidal-nanoparticulate size Si seems to represent a significant fraction of total bioavailable Si, only present in pro-glacial rivers, which may be a similar order of magnitude to the concentration of dSi and aSi (Pryer et al., 2020). Dissolution, precipitation, sedimentation, resuspension and uptake are key processes in glacial estuary environments controlling the fate of glacial dSi and aSi inputs to the coastal environment (Hendry et al., 2025). In addition, complex, heterogeneous and still poorly understood processes in pro-glacial environments and fjords lead to lower dSi concentrations in interstitial fluids near glacial outputs than in coastal shelf sediments, which may impact the dSi cycle in the water column and its offshore dynamics (Hendry et al., 2025; Ng et al., 2020, 2022).

832 Sea ice consists of frozen seawater floating on the ocean's surface, and it can be formed seasonally or be perennial. During
833 its formation, small pockets of brine are formed due to salt expulsion (Eicken, 2003). As the expulsion of brine increases the
834 salinity of the mixing layer, it can enhance sea water circulation (Wang and Danilov, 2022), therefore promoting the upwelling
835 of deep water and affecting the nutrient supply to surface waters. Furthermore, sea ice supports diverse communities, including
836 diatoms, inhabiting these brine pockets, as well as the sea ice surface and attached underneath the sea ice (Arrigo, 2017). The
837 recycling of bSi within these habitats directly sustains the growth of such silicifying organisms under extreme polar conditions.
838 For example, by focusing on the distribution of natural Si isotopes within the Antarctic pack ice, Fripiat et al. (2014) found
839 that bSi dissolution contributes significantly to silica production, with a dissolution-to-production ratio between 0.4 and 0.9.
840 This suggests that there is considerable regeneration of Si within the brine network, which fuels new bSi production. This
841 study was crucial in filling a gap in the understanding of sea ice Si cycling, a topic that is still poorly studied due to the
842 difficulty of measuring rates in such environments.

843 The role of permafrost in the polar regions and their influence on the Si cycle remains uncertain, particularly in the context
844 of a warming climate. Seasonal isotopic variations observed in the Lena River (Russian Siberia) suggest that Si sources shift
845 throughout the year—clay minerals dominate in winter, while summer brings increased dissolution of silicate minerals and
846 phytoliths from the upper active layer (Sun et al., 2018). These findings imply that permafrost thawing, driven by climate
847 change, could significantly alter Si fluxes and isotopic compositions in high-latitude rivers. However, a study by Mavromatis
848 et al. (2016) in the Yenisey River and its tributaries found that mineral dissolution in the watershed plays a crucial role in
849 defining the riverine dissolved $\delta^{30}\text{Si}$, regardless of permafrost coverage. Their findings highlight the influence of suspended
850 particles (e.g. clays), plant material decomposition (both contributing lower $\delta^{30}\text{Si}$), and groundwater discharge enriched in
851 heavier isotopes due to secondary silicate formation. These contrasting findings underscore the complexity of Si cycling in
852 regions covered by permafrost where multiple processes occur, with potential downstream implications for the availability and
853 isotopic composition of silica supplied to silicifying organisms in Arctic rivers and coastal zones. Further studies are essential
854 for predicting how ongoing climate change might reshape the Si export to the ocean and how these signals can be interpreted
855 in palaeorecords.

856 In a recent study, Opfergelt et al. (2024) investigated how winter river ice formation in the Lena River affects the
857 biogeochemical cycling of key nutrients like N and Si, and their transport to the Arctic Ocean. During very cold periods, *frazil*
858 *ice* forms microzones that slow water flow and create favourable conditions for microbial activity. These zones allow organic
859 matter recycling and alter nutrient processing. The formation of ice crystals leads to the precipitation of aSi, which changes
860 $\delta^{30}\text{Si}$ and the Ge/Si ratio in the remaining water. Through isotope mass balance, Opfergelt et al. (2024) estimate that about
861 39% of Lena River water passes through this ice-induced filter during winter, leading to notable silica loss and a shift in river
862 biogeochemistry.

863 These cryosphere–Si interactions are particularly relevant for silicifying organisms. For instance, the input of highly soluble
864 amorphous silica and colloidal-nanoparticulate Si from glaciers and pro-glacial rivers provides an important source of
865 bioavailable silica that can stimulate diatom blooms in coastal and shelf seas. Similarly, brine pockets in sea ice sustain diverse

diatom communities, where rapid recycling of bSi supports continued growth under extreme conditions. Changes in the magnitude, timing, and isotopic composition of these fluxes therefore have direct consequences for the ecology and distribution of silicifiers, as well as for the interpretation of palaeoceanographic records based on their silica remains. For example, climate change is accelerating the melting of glaciers, permafrost and sea ice, reducing ice-covered areas and increasing open-water regions, altering habitats, species distributions, and nutrient dynamics. The melting of sea ice, glaciers and ice sheets also releases previously trapped trace metals and nutrients into seawater, further influencing marine productivity and biogeochemical cycles (Hopwood et al., 2020). Given their vast size and prolonged melting periods, ice sheets may have a more significant global impact on Si input compared to smaller glaciers with more seasonal contributions. While glacial retreat and melting are expected to increase Si fluxes to the ocean, the long-term effects remain uncertain, as they could reshape marine ecosystems and biogeochemical cycles (Hatton et al., 2019b; Pryer et al., 2020). Palaeorecords of $\delta^{30}\text{Si}$ and Ge/Si signatures in sedimentary bSi are emerging as a useful tool to reconstruct and quantify the effects of glaciation on the Si cycle and weathering (Hou et al., 2025). Understanding the role of glaciers in the Si cycle — particularly how their contributions interact with other sources and evolve under future climate scenarios — remains a key area of research.

5 Perspectives and conclusions

Despite major advances in our understanding of silicification, silicifiers' diversity, and the global Si cycle, critical knowledge gaps persist across taxonomic, physiological, ecological, and geochemical dimensions. To move the field forward, we outline key research priorities that we believe will be pivotal in developing a more integrated and predictive understanding of biosilicification and its role in the marine Si cycle. Addressing these challenges will require integrative and interdisciplinary research approaches that bridge molecular biology, ecology, biogeochemistry, (palae)oceanography, and Earth system science.

1. Expand taxonomic and functional knowledge across silicifiers: Research remains heavily biased toward a few model organisms such as diatoms and terrestrial plants. Many other silicifying taxa, including Rhizaria, silicoflagellates, sponges, macrophytes, and even some prokaryotes, are understudied despite their potential significant contributions to the Si cycle. Broader taxonomic coverage, including the development of new model systems and comparative studies, will be essential to capture the evolutionary, functional, and ecological diversity of silicification strategies across domains of life.

2. Elucidate cellular mechanisms and physiological regulation: Much remains to be understood about how organisms control Si uptake, intra- and intercellular transport, polymerization, and efflux. For instance, the mechanisms of Si efflux, crucial for homeostasis in diatoms, are poorly characterized in most groups. Investigating the molecular basis of silicification — including gene expression, transporter function, and nanoscale silica assembly — will benefit from the use of high-resolution imaging, omics technologies, and experimental manipulation under variable environmental conditions.

3. Integrate silicifiers into ecosystem and global models: Current biogeochemical models often overlook key silicifiers such as sponges and Rhizaria. Their omission limits our ability to predict Si fluxes and understand how Si cycling interacts with

897 other elemental cycles like C and N. Incorporating a broader range of silicifiers into these models is essential, particularly
898 under changing climate regimes.

899 **4. Clarify interactions between biotic and abiotic Si processes:** The interplay between biological silicification, bSi
900 dissolution, silicate weathering, and authigenic clay formation remains insufficiently understood. This is especially true in
901 transitional environments like estuaries and coastal margins, where complex feedbacks occur. Further research is needed to
902 disentangle the contributions and temporal dynamics of biotic versus abiotic Si pathways.

903 **5. Assess environmental and climatic influences on silicification and Si fluxes:** While the environmental drivers of
904 silicification are well studied in diatoms, their effects on other silicifiers are largely unknown. Additionally, how climate-
905 related stressors — such as warming, acidification, altered precipitation, and sea-level rise — affect Si cycling and silicifiers
906 distribution is not well constrained. These processes may reshape the ecological roles of silicifiers and the fate of Si at critical
907 interfaces such as the land–ocean boundary.

908 **6. Foster cross-disciplinary integration:** Bridging disciplinary divides — between marine and terrestrial science, biology
909 and geochemistry — will enhance our understanding of the Si cycle. Cross-comparisons (e.g. between plant and algal
910 silicification), training in diverse analytical techniques, and collaboration across fields will enable more holistic interpretations
911 of both modern processes and palaeoenvironmental records.

912

913 Silicon plays a pivotal yet still underappreciated role in shaping biological and geochemical processes across marine and
914 terrestrial systems. This review highlights the remarkable diversity of silicifying organisms and their crucial, but often
915 overlooked, roles in shaping the global marine Si cycle. From unicellular diatoms to multicellular sponges, and from well-
916 studied phytoplankton to enigmatic protists and prokaryotes, silicifiers contribute to a wide array of ecological functions and
917 influence biogeochemical feedbacks across spatial and temporal scales. As research expands beyond classical models, a more
918 nuanced and integrative picture of the Si cycle is emerging — one that includes diverse silicifiers, complex environmental
919 feedbacks, and deep-time dynamics. Despite significant progress over the last decade, major uncertainties persist regarding
920 the cellular machinery of silicification, the environmental controls of Si fluxes and the integration of silicifiers into predictive
921 models. These gaps are especially pressing in the context of global change, where shifts in climate and nutrient regimes are
922 likely to affect the distribution, abundance and ecological function of silicifiers in ways that are still poorly understood.
923 Addressing these challenges will require coordinated, cross-disciplinary efforts that link biological, ecological and
924 geochemical research. Leveraging recent advances in molecular biology, high-resolution imaging, in situ monitoring, and
925 Earth system modelling will be key to unravelling the complexity of Si cycling. Advancing our understanding of
926 biosilicification is not only essential for reconstructing past marine environments but also for predicting the future of ocean
927 biogeochemistry in an era of rapid planetary change.

- 929 Abelman, A., Gersonde, R., Knorr, G., Zhang, X., Chaplign, B., Maier, E., Esper, O., Friedrichsen, H., Lohmann, G., Meyer,
930 H., and Tiedemann, R.: The seasonal sea-ice zone in the glacial Southern Ocean as a carbon sink, *Nat. Commun.*, 6, 8136,
931 <https://doi.org/10.1038/ncomms9136>, 2015.
- 932 Abramson, J., Adler, J., Dunger, J., Evans, R., Green, T., Pritzel, A., Ronneberger, O., Willmore, L., Ballard, A. J., Bambrick,
933 J., Bodenstein, S. W., Evans, D. A., Hung, C.-C., O'Neill, M., Reiman, D., Tunyasuvunakool, K., Wu, Z., Žemgulytė, A.,
934 Arvaniti, E., Beattie, C., Bertolli, O., Bridgland, A., Cherepanov, A., Congreve, M., Cowen-Rivers, A. I., Cowie, A., Figurnov,
935 M., Fuchs, F. B., Gladman, H., Jain, R., Khan, Y. A., Low, C. M. R., Perlin, K., Potapenko, A., Savy, P., Singh, S., Stecula,
936 A., Thillaisundaram, A., Tong, C., Yakneen, S., Zhong, E. D., Zielinski, M., Židek, A., Bapst, V., Kohli, P., Jaderberg, M.,
937 Hassabis, D., and Jumper, J. M.: Accurate structure prediction of biomolecular interactions with AlphaFold 3, *Nature*, 630,
938 493–500, <https://doi.org/10.1038/s41586-024-07487-w>, 2024.
- 939 Ács, É., Földi, A., Vad, C. F., Trábert, Z., Kiss, K. T., Duleba, M., Borics, G., Grigorszky, I., and Botta-Dukát, Z.: Trait-based
940 community assembly of epiphytic diatoms in saline astatic ponds: a test of the stress-dominance hypothesis, *Sci. Rep.*, 9,
941 15749, <https://doi.org/10.1038/s41598-019-52304-4>, 2019.
- 942 Adl, S.: *Rhizoa*, Protistol. Elsevier, 2024.
- 943 Aguilera, A., Lundin, D., Charalampous, E., Churakova, Y., Tellgren-Roth, C., Śliwińska-Wilczewska, S., Conley, D. J.,
944 Farnelid, H., and Pinhassi, J.: The evaluation of biogenic silica in brackish and freshwater strains reveals links between
945 phylogeny and silica accumulation in picocyanobacteria, *Appl. Environ. Microbiol.*, 91, [https://doi.org/10.1128/aem.02527-](https://doi.org/10.1128/aem.02527-24)
946 24, 2025.
- 947 Alexandre, A., Meunier, J.-D., Colin, F., and Koud, J.-M.: Plant impact on the biogeochemical cycle of silicon and related
948 weathering processes, *Geochim. Cosmochim. Acta*, 61, 677–682, [https://doi.org/10.1016/s0016-7037\(97\)00001-x](https://doi.org/10.1016/s0016-7037(97)00001-x), 1997.
- 949 Alfredsson, H., Hugelius, G., Clymans, W., Stadmark, J., Kuhry, P., and Conley, D. J.: Amorphous silica pools in permafrost
950 soils of the Central Canadian Arctic and the potential impact of climate change, *Biogeochemistry*, 124, 441–459,
951 <https://doi.org/10.1007/s10533-015-0108-1>, 2015.
- 952 Aller, R. C. and Wehrmann, L. M.: Sedimentary diagenesis, depositional environments, and benthic fluxes, in: *Treatise on*
953 *Geochemistry*, vol. 4, edited by: Anbar, A. and Weis, D., Elsevier, 573–629, [https://doi.org/10.1016/b978-0-323-99762-](https://doi.org/10.1016/b978-0-323-99762-1.00095-4)
954 1.00095-4, 2025.
- 955 Alley, K., Patacca, K., Pike, J., Dunbar, R., and Leventer, A.: Iceberg Alley, East Antarctic Margin: Continuously laminated
956 diatomaceous sediments from the late Holocene, *Mar. Micropaleontol.*, 140, 56–68,
957 <https://doi.org/10.1016/j.marmicro.2017.12.002>, 2018.
- 958 Anderson, O. R.: Protozoa, Radiolarians, in: *Encyclopedia of Ocean Sciences*, edited by: Steele, J. H., Thorpe, S. A., and
959 Turekian, K. K., Academic Press, Oxford, 2315–2320, 2001.
- 960 Aparicio, M., Le Bihan, A., Jeandel, C., Fabre, S., Almar, R., and Mingo, I. M.: Contribution of sandy beaches to the global
961 marine silicon cycle, *Nat. Geosci.*, 18, 154–159, <https://doi.org/10.1038/s41561-024-01628-6>, 2025.
- 962 Armbrust, E. V.: The life of diatoms in the world's oceans, *Nature*, 459, 185–192, <https://doi.org/10.1038/nature08057>, 2009.
- 963 Arrigo, K. R.: Sea ice as a habitat for primary producers, in: *Sea Ice*, edited by: Thomas, D. N., Wiley, 352–369,
964 <https://doi.org/10.1002/9781118778371.ch14>, 2017.

Assmy, P., Henjes, J., Smetacek, V., and Montresor, M.: Auxospore formation by the silica-sinking, oceanic diatom *Fragilariopsis kerguelensis* (Bacillariophyceae), J. Phycol., 42, 1002–1006, <https://doi.org/10.1111/j.1529-8817.2006.00260.x>, 2006.

Azam, F., Fenchel, T., Field, J. G., Gray, J. S., Meyer-Reil, L. A., and Thingstad, F.: The Ecological Role of Water-Column Microbes in the Sea, Mar. Ecol. Prog. Ser., 10, 257–263, <https://doi.org/10.3354/meps010257>, 1983.

Baines, S. B., Twining, B. S., Brzezinski, M. A., Krause, J. W., Vogt, S., Assael, D., and McDaniel, H.: Significant silicon accumulation by marine picocyanobacteria, Nat. Geosci., 5, 886–891, <https://doi.org/10.1038/ngeo1641>, 2012.

Bárcena, M. A., Cacho, I., Abrantes, F., Sierro, F. J., Grimalt, J. O., and Flores, J. A.: Paleoproductivity variations related to climatic conditions in the Alboran Sea (western Mediterranean) during the last glacial–interglacial transition: the diatom record, Palaeogeogr. Palaeoclimatol. Palaeoecol., 167, 337–357, [https://doi.org/10.1016/S0031-0182\(00\)00246-7](https://doi.org/10.1016/S0031-0182(00)00246-7), 2001.

Baronas, J. J., Hammond, D. E., Berelson, W. M., McManus, J., and Severmann, S.: Germanium–silicon fractionation in a river-influenced continental margin: The Northern Gulf of Mexico, Geochim. Cosmochim. Acta, 178, 124–142, <https://doi.org/10.1016/j.gca.2016.01.028>, 2016.

Baronas, J. J., Torres, M. A., West, A. J., Rouxel, O., Georg, B., Bouchez, J., Gaillardet, J., and Hammond, D. E.: Ge and Si isotope signatures in rivers: A quantitative multi-proxy approach, Earth Planet. Sci. Lett., 503, 194–215, <https://doi.org/10.1016/j.epsl.2018.09.022>, 2018.

Baronas, J. J., Hammond, D. E., Rouxel, O. J., and Monteverde, D. R.: A First Look at Dissolved Ge Isotopes in Marine Sediments, Front. Earth Sci., 7, <https://doi.org/10.3389/feart.2019.00162>, 2019.

Baronas, J. J., West, A. J., Burton, K. W., Hammond, D. E., Opfergelt, S., Pogge Von Strandmann, P. A. E., James, R. H., and Rouxel, O. J.: Ge and Si Isotope Behavior During Intense Tropical Weathering and Ecosystem Cycling, Glob. Biogeochem. Cycles, 34, <https://doi.org/10.1029/2019gb006522>, 2020.

Baronas, J. J., Hammond, D. E., Bennett, M. M., Rouxel, O., Pitcher, L. H., and Smith, L. C.: Ge/Si and Ge Isotope Fractionation During Glacial and Non-glacial Weathering: Field and Experimental Data From West Greenland, Front. Earth Sci., 9, <https://doi.org/10.3389/feart.2021.551900>, 2021.

Barrio-Hernandez, I., Yeo, J., Jänes, J., Mirdita, M., Gilchrist, C. L. M., Wein, T., Varadi, M., Velankar, S., Beltrao, P., and Steinegger, M.: Clustering predicted structures at the scale of the known protein universe, Nature, 622, 637–645, <https://doi.org/10.1038/s41586-023-06510-w>, 2023.

Barron, J. A., Bukry, D. B., and Gersonde, R.: Diatom and silicoflagellate biostratigraphy for the late Eocene: ODP 1090 (sub-Antarctic Atlantic), in: Diatom research over time and space Morphology, taxonomy, ecology and distribution of diatoms - from fossil to recent, marine to freshwater, established species and genera to new ones, edited by: Kociolek, J., Kulikovskiy, M., Witkowski, J., and Harwood, D., Nova Hedwigia, Stuttgart, 1–32, 2014.

Battershill, C. and Bergquist, P.: The influence of storms on asexual reproduction, recruitment, and survivorship of sponges., in: New perspectives in sponge biology, edited by: Rutzler, K., Smithsonian Institution Press, Washington, DC, 397–403, 1990.

Beazley, L. I., Kenchington, E. L., Murillo, F. J., and Sacau, M. D. M.: Deep-sea sponge grounds enhance diversity and abundance of epibenthic megafauna in the Northwest Atlantic, ICES J. Mar. Sci., 70, 1471–1490, <https://doi.org/10.1093/icesjms/fst124>, 2013.

1002 Behrenfeld, M. J., Halsey, K. H., Boss, E., Karp-Boss, L., Milligan, A. J., and Peers, G.: Thoughts on the evolution and
1003 ecological niche of diatoms, *Ecol. Monogr.*, 91, <https://doi.org/10.1002/ecm.1457>, 2021.

1004 Bell, J. J.: The functional roles of marine sponges, *Estuar. Coast. Shelf Sci.*, 79, 341–353,
1005 <https://doi.org/10.1016/j.ecss.2008.05.002>, 2008.

1006 Bell, J. J., Strano, F., Broadribb, M., Wood, G., Harris, B., Resende, A. C., Novak, E., and Micaroni, V.: Chapter Two - Sponge
1007 functional roles in a changing world, in: *Advances in Marine Biology*, vol. 95, edited by: Sheppard, C., Academic Press, 27–
1008 89, <https://doi.org/10.1016/bs.amb.2023.07.002>, 2023.

1009 Biard, T. and Ohman, M. D.: Vertical niche definition of test-bearing protists (Rhizaria) into the twilight zone revealed by in
1010 situ imaging, *Limnol. Oceanogr.*, 65, 2583–2602, <https://doi.org/10.1002/lno.11472>, 2020.

1011 Biard, T., Stemmann, L., Picheral, M., Mayot, N., Vandromme, P., Hauss, H., Gorsky, G., Guidi, L., Kiko, R., and Not, F.: In
1012 situ imaging reveals the biomass of giant protists in the global ocean, *Nature*, 532, 504–507,
1013 <https://doi.org/10.1038/nature17652>, 2016.

1014 Biard, T., Krause, J. W., Stukel, M. R., and Ohman, M. D.: The Significance of Giant Phaeodarians (Rhizaria) to Biogenic
1015 Silica Export in the California Current Ecosystem, *Glob. Biogeochem. Cycles*, 32, 987–1004,
1016 <https://doi.org/10.1029/2018GB005877>, 2018.

1017 Biller, S. J., Berube, P. M., Lindell, D., and Chisholm, S. W.: *Prochlorococcus*: the structure and function of collective
1018 diversity, *Nat. Rev. Microbiol.*, 13, 13–27, <https://doi.org/10.1038/nrmicro3378>, 2015.

1019 Booth, B. C. and Marchant, H. J.: *Parmales*, a New Order of Marine Chrysophytes, with Descriptions of Three New Genera
1020 and Seven New Species, *J. Phycol.*, 23, 245–260, <https://doi.org/10.1111/j.1529-8817.1987.tb04132.x>, 1987.

1021 Bowler, C., De Martino, A., and Falciatore, A.: Diatom cell division in an environmental context, *Curr. Opin. Plant Biol.*, 13,
1022 623–630, <https://doi.org/10.1016/j.pbi.2010.09.014>, 2010.

1023 Brylka, K., Alverson, A. J., Pickering, R. A., Richoz, S., and Conley, D. J.: Uncertainties surrounding the oldest fossil record
1024 of diatoms, *Sci. Rep.*, 13, <https://doi.org/10.1038/s41598-023-35078-8>, 2023.

1025 Brylka, K., Ashworth, M. P., Alverson, A. J., and Conley, D. J.: The Cretaceous Diatom Database: A tool for investigating
1026 early diatom evolution, *J. Phycol.*, 60, 1090–1104, <https://doi.org/10.1111/jpy.13499>, 2024.

1027 Brzezinski, M., Olson, R., and Chisholm, S.: Silicon availability and cell-cycle progression in marine diatoms, *Mar. Ecol.*
1028 *Prog. Ser.*, 67, 83–96, <https://doi.org/10.3354/meps067083>, 1990.

1029 Brzezinski, M. A.: THE Si:C:N RATIO OF MARINE DIATOMS: INTERSPECIFIC VARIABILITY AND THE EFFECT
1030 OF SOME ENVIRONMENTAL VARIABLES, *J. Phycol.*, 21, 347–357, <https://doi.org/10.1111/j.0022-3646.1985.00347.x>,
1031 1985.

1032 Brzezinski, M. A., Villareal, T. A., and Lipschultz, F.: Silica production and the contribution of diatoms to new and primary
1033 production in the central North Pacific, *Mar. Ecol. Prog. Ser.*, 167, 89–104, <https://doi.org/10.3354/meps167089>, 1998.

1034 Brzezinski, M. A., Krause, J. W., Baines, S. B., Collier, J. L., Ohnemus, D. C., and Twining, B. S.: Patterns and regulation of
1035 silicon accumulation in *Synechococcus* spp., *J. Phycol.*, 53, 746–761, <https://doi.org/10.1111/jpy.12545>, 2017.

1036 Buitenhuis, E. T., Li, W. K. W., Vaultot, D., Lomas, M. W., Landry, M. R., Partensky, F., Karl, D. M., Ulloa, O., Campbell,
1037 L., Jacquet, S., Lantoiné, F., Chavez, F., Macias, D., Gosselin, M., and McManus, G. B.: Picophytoplankton biomass
1038 distribution in the global ocean, *Earth Syst. Sci. Data*, 4, 37–46, <https://doi.org/10.5194/essd-4-37-2012>, 2012.

1039 Burki, F. and Keeling, P. J.: Rhizaria, *Curr. Biol.*, 24, R103–R107, <https://doi.org/10.1016/j.cub.2013.12.025>, 2014.

1040 Busch, K., Slaby, B. M., Bach, W., Boetius, A., Clefsen, I., Colaço, A., Creemers, M., Cristobo, J., Federwisch, L., Franke,
1041 A., Gavriilidou, A., Hethke, A., Kenchington, E., Mienis, F., Mills, S., Riesgo, A., Ríos, P., Roberts, E. M., Sipkema, D., Pita,
1042 L., Schupp, P. J., Xavier, J., Rapp, H. T., and Hentschel, U.: Biodiversity, environmental drivers, and sustainability of the
1043 global deep-sea sponge microbiome, *Nat. Commun.*, 13, <https://doi.org/10.1038/s41467-022-32684-4>, 2022.

1044 Cahoon, L. B.: The role of benthic microalgae in neritic ecosystems, in: *Oceanography and Marine Biology*, vol. 37, CRC
1045 Press, 40, 1999.

1046 Calvert, S. E.: Silica Balance in the Ocean and Diagenesis, *Nature*, 219, 919–920, <https://doi.org/10.1038/219919a0>, 1968.

1047 Cardinal, D., Alleman, L. Y., Dehairs, F., Savoye, N., Trull, T. W., and André, L.: Relevance of silicon isotopes to Si-nutrient
1048 utilization and Si-source assessment in Antarctic waters, *Glob. Biogeochem. Cycles*, 19, 2004GB002364,
1049 <https://doi.org/10.1029/2004GB002364>, 2005.

1050 Carvajal-Landinez, F. M., Helenes, J., and Murcia, L.-A. G.: Quantitative biostratigraphy and paleoecology of Neogene
1051 tropical dinoflagellate cysts, *J. South Am. Earth Sci.*, 134, 104776, <https://doi.org/10.1016/j.jsames.2023.104776>, 2024.

1052 Cassarino, L., Hendry, K. R., Henley, S. F., MacDonald, E., Arndt, S., Freitas, F. S., Pike, J., and Firing, Y. L.: Sedimentary
1053 Nutrient Supply in Productive Hot Spots off the West Antarctic Peninsula Revealed by Silicon Isotopes, *Glob. Biogeochem.*
1054 *Cycles*, 34, <https://doi.org/10.1029/2019gb006486>, 2020.

1055 Cassarino, L., Curnow, P., and Hendry, K. R.: A biomimetic peptide has no effect on the isotopic fractionation during in vitro
1056 silica precipitation, *Sci. Rep.*, 11, 9698, <https://doi.org/10.1038/s41598-021-88881-6>, 2021.

1057 Chadwick, M., Allen, C. S., Sime, L. C., Crosta, X., and Hillenbrand, C.-D.: Reconstructing Antarctic winter sea-ice extent
1058 during Marine Isotope Stage 5e, *Clim. Past*, 18, 129–146, <https://doi.org/10.5194/cp-18-129-2022>, 2022.

1059 Chang, F. H. and Gall, M.: Autecology, pigment composition and toxicology of *Dictyocha octonaria* (Dictyochophyceae,
1060 Ochrophyta) from Wellington Harbor, New Zealand, *Phycol. Res.*, 64, 65–71, <https://doi.org/10.1111/pre.12122>, 2016.

1061 Chang, F. H., McVeagh, M., Gall, M., and Smith, P.: *Chattonella globosa* is a member of Dictyochophyceae: reassignment to
1062 *Vicicitus* gen. nov., based on molecular phylogeny, pigment composition, morphology and life history, *Phycologia*, 51, 403–
1063 420, <https://doi.org/10.2216/10-104.1>, 2012.

1064 Chang, F. H., Sutherland, J., and Bradford-Grieve, J.: Taxonomic revision of Dictyochaes (Dictyochophyceae) based on
1065 morphological, ultrastructural, biochemical and molecular data, *Phycol. Res.*, 65, 235–247, <https://doi.org/10.1111/pre.12181>,
1066 2017a.

1067 Chang, S., Feng, Q., Clausen, S., and Zhang, L.: Sponge spicules from the lower Cambrian in the Yanjiahe Formation, South
1068 China: The earliest biomineralizing sponge record, *Palaeogeogr. Palaeoclimatol. Palaeoecol.*, 474, 36–44,
1069 <https://doi.org/10.1016/j.palaeo.2016.06.032>, 2017b.

1070 Chang, S., Zhang, L., Clausen, S., Bottjer, D. J., and Feng, Q.: The Ediacaran-Cambrian rise of siliceous sponges and
 1071 development of modern oceanic ecosystems, *Precambrian Res.*, 333, 105438,
 1072 <https://doi.org/10.1016/j.precamres.2019.105438>, 2019.

1073 Chen, C., Feng, Q., Algeo, T. J., Zhang, L., Chang, S., and Li, M.: New sponge spicules from the Ediacaran-Cambrian
 1074 transition in deep-water facies of South China, *Palaeogeogr. Palaeoclimatol. Palaeoecol.*, 627, 111714,
 1075 <https://doi.org/10.1016/j.palaeo.2023.111714>, 2023.

1076 Chepurnov, V. A., Mann, D. G., Vyverman, W., Sabbe, K., and Danielidis, D. B.: Sexual Reproduction, mating system, and
 1077 protoplast dynamics of *Seminavis* (Bacillariophyceae), *J. Phycol.*, 38, 1004–1019, <https://doi.org/10.1046/j.1529-8817.2002.t01-1-01233.x>, 2002.

1079 Cho, H.-M., Kim, G., Kwon, E. Y., Moosdorf, N., Garcia-Orellana, J., and Santos, I. R.: Radium tracing nutrient inputs through
 1080 submarine groundwater discharge in the global ocean, *Sci. Rep.*, 8, 2439, <https://doi.org/10.1038/s41598-018-20806-2>, 2018.

1081 Chong, L. S., Berelson, W. M., McManus, J., Hammond, D. E., Rollins, N. E., and Yager, P. L.: Carbon and biogenic silica
 1082 export influenced by the Amazon River Plume: Patterns of remineralization in deep-sea sediments, *Deep Sea Res. Part*
 1083 *Oceanogr. Res. Pap.*, 85, 124–137, <https://doi.org/10.1016/j.dsr.2013.12.007>, 2014.

1084 Chu, J., Maldonado, M., Yahel, G., and Leys, S.: Glass sponge reefs as a silicon sink, *Mar. Ecol. Prog. Ser.*, 441, 1–14,
 1085 <https://doi.org/10.3354/meps09381>, 2011.

1086 Churakova, Y., Aguilera, A., Charalampous, E., Conley, D. J., Lundin, D., Pinhassi, J., and Farnelid, H.: Biogenic silica
 1087 accumulation in picoeukaryotes: Novel players in the marine silica cycle, *Environ. Microbiol. Rep.*, 15, 282–290,
 1088 <https://doi.org/10.1111/1758-2229.13144>, 2023.

1089 Civel-Mazens, M., Cortese, G., Crosta, X., Lawler, K. A., Lowe, V., Ikehara, M., and Itaki, T.: New Southern Ocean transfer
 1090 function for subsurface temperature prediction using radiolarian assemblages, *Mar. Micropaleontol.*, 178, 102198,
 1091 <https://doi.org/10.1016/j.marmicro.2022.102198>, 2023.

1092 Civel-Mazens, M., Crosta, X., Cortese, G., Lowe, V., Itaki, T., Ikehara, M., and Kohfeld, K.: Subantarctic jet migrations
 1093 regulate vertical mixing in the Southern Indian, *Earth Planet. Sci. Lett.*, 642, 118877,
 1094 <https://doi.org/10.1016/j.epsl.2024.118877>, 2024.

1095 Closset, I., McNair, H. M., Brzezinski, M. A., Krause, J. W., Thamatrakoln, K., and Jones, J. L.: Diatom response to alterations
 1096 in upwelling and nutrient dynamics associated with climate forcing in the California Current System, *Limnol. Oceanogr.*, 66,
 1097 1578–1593, <https://doi.org/10.1002/lno.11705>, 2021.

1098 Closset, I., Brzezinski, M. A., Cardinal, D., Dapoigny, A., Jones, J. L., and Robinson, R. S.: A silicon isotopic perspective on
 1099 the contribution of diagenesis to the sedimentary silicon budget in the Southern Ocean, *Geochim. Cosmochim. Acta*, 327, 298–
 1100 313, <https://doi.org/10.1016/j.gca.2022.04.010>, 2022.

1101 Conley, D. J.: Terrestrial ecosystems and the global biogeochemical silica cycle, *Glob. Biogeochem. Cycles*, 16,
 1102 <https://doi.org/10.1029/2002gb001894>, 2002.

1103 Conley, D. J. and Carey, J. C.: Silica cycling over geologic time, *Nat. Geosci.*, 8, 431–432, <https://doi.org/10.1038/ngeo2454>,
 1104 2015.

1105 Conley, D. J., Frings, P. J., Fontorbe, G., Clymans, W., Stadmark, J., Hendry, K. R., Marron, A. O., and De La Rocha, C. L.:
1106 Biosilicification Drives a Decline of Dissolved Si in the Oceans through Geologic Time, *Front. Mar. Sci.*, 4, 397,
1107 <https://doi.org/10.3389/fmars.2017.00397>, 2017.

1108 Cooke, J. and Leishman, M. R.: Consistent alleviation of abiotic stress with silicon addition: a meta-analysis, *Funct. Ecol.*, 30,
1109 1340–1357, <https://doi.org/10.1111/1365-2435.12713>, 2016.

1110 Cornelis, J. and Delvaux, B.: Soil processes drive the biological silicon feedback loop, *Funct. Ecol.*, 30, 1298–1310,
1111 <https://doi.org/10.1111/1365-2435.12704>, 2016.

1112 Crosta, X. and Koç, N.: Diatoms: From Micropaleontology to Isotope Geochemistry, in: *Developments in Marine Geology*,
1113 vol. 1, edited by: Hillaire-Marcel, C. and De Vernal, A., Elsevier, 327–369, [https://doi.org/10.1016/S1572-5480\(07\)01013-5](https://doi.org/10.1016/S1572-5480(07)01013-5),
1114 2007.

1115 Crosta, X. and Shemesh, A.: Reconciling down core anticorrelation of diatom carbon and nitrogen isotopic ratios from the
1116 Southern Ocean, *Paleoceanography*, 17, <https://doi.org/10.1029/2000PA000565>, 2002.

1117 Crosta, X., Etourneau, J., Orme, L. C., Dalaiden, Q., Campagne, P., Swingedouw, D., Goosse, H., Massé, G., Miettinen, A.,
1118 McKay, R. M., Dunbar, R. B., Escutia, C., and Ikehara, M.: Multi-decadal trends in Antarctic sea-ice extent driven by ENSO–
1119 SAM over the last 2,000 years, *Nat. Geosci.*, 14, 156–160, <https://doi.org/10.1038/s41561-021-00697-1>, 2021.

1120 Cumming, B. F., Wilson, S. E., and Smol, J. P.: Paleolimnological potential of chrysophyte cysts and scales and of sponge
1121 spicules as indicators of lake salinity, *Int. J. Salt Lake Res.*, 2, 87–92, <https://doi.org/10.1007/BF02905055>, 1993.

1122 Currie, H. A. and Perry, C. C.: Silica in Plants: Biological, Biochemical and Chemical Studies, *Ann. Bot.*, 100, 1383–1389,
1123 <https://doi.org/10.1093/aob/mcm247>, 2007.

1124 De Freitas Oliveira, M. R., da Costa, C., and Benedito, E.: Trends and gaps in scientific production on freshwater sponges,
1125 *Oecologia Aust.*, 24, 61–75, <https://doi.org/10.4257/oeco.2020.2401.05>, 2020.

1126 De Goeij, J. M., Van Oevelen, D., Vermeij, M. J. A., Osinga, R., Middelburg, J. J., De Goeij, A. F. P. M., and Admiraal, W.:
1127 Surviving in a Marine Desert: The Sponge Loop Retains Resources Within Coral Reefs, *Science*, 342, 108–110,
1128 <https://doi.org/10.1126/science.1241981>, 2013.

1129 De La Rocha, C. L., Brzezinski, M. A., and DeNiro, M. J.: Fractionation of silicon isotopes by marine diatoms during biogenic
1130 silica formation, *Geochim. Cosmochim. Acta*, 61, 5051–5056, [https://doi.org/10.1016/S0016-7037\(97\)00300-1](https://doi.org/10.1016/S0016-7037(97)00300-1), 1997.

1131 De La Rocha, C. L., Brzezinski, M. A., DeNiro, M. J., and Shemesh, A.: Silicon-isotope composition of diatoms as an indicator
1132 of past oceanic change, *Nature*, 395, 680–683, <https://doi.org/10.1038/27174>, 1998.

1133 De Tommasi, E., Gielis, J., and Rogato, A.: Diatom Frustule Morphogenesis and Function: a Multidisciplinary Survey, *Mar.*
1134 *Genomics*, 35, 1–18, <https://doi.org/10.1016/j.margen.2017.07.001>, 2017.

1135 De Wever, P., Dumitrica, P., Caulet, J. P., Nigrini, C., and Caridroit, M.: Radiolarians in the Sedimentary Record, 0 ed., Gordan
1136 and Breach Science Publishers, <https://doi.org/10.1201/9781482283181>, 2001.

1137 Decelle, J., Veronesi, G., LeKieffre, C., Gallet, B., Chevalier, F., Stryhanyuk, H., Marro, S., Ravanel, S., Tucoulou, R.,
1138 Schieber, N., Finazzi, G., Schwab, Y., and Musat, N.: Subcellular architecture and metabolic connection in the planktonic
1139 photosymbiosis between Collodaria (radiolarians) and their microalgae, *Environ. Microbiol.*, 23, 6569–6586,
1140 <https://doi.org/10.1111/1462-2920.15766>, 2021.

1141 Demarest, M. S., Brzezinski, M. A., and Beucher, C. P.: Fractionation of silicon isotopes during biogenic silica dissolution,
1142 *Geochim. Cosmochim. Acta*, 73, 5572–5583, <https://doi.org/10.1016/j.gca.2009.06.019>, 2009.

1143 DeMaster, D. J.: The supply and accumulation of silica in the marine environment, *Geochim. Cosmochim. Acta*, 45, 1715–
1144 1732, [https://doi.org/10.1016/0016-7037\(81\)90006-5](https://doi.org/10.1016/0016-7037(81)90006-5), 1981.

1145 DeMaster, D. J.: The Diagenesis of Biogenic Silica: Chemical Transformations Occurring in the Water Column, Seabed, and
1146 Crust, *Treatise Geochem.*, 7, 407, <https://doi.org/10.1016/B0-08-043751-6/07095-X>, 2003.

1147 DeMaster, D. J.: The Global Marine Silica Budget: Sources and Sinks, in: *Encyclopedia of Ocean Sciences*, vol. 1, edited by:
1148 Cochran, J. K., Bokuniewicz, H. J., and Yager, P. L., Elsevier, 473–483, [https://doi.org/10.1016/b978-0-12-409548-9.10799-](https://doi.org/10.1016/b978-0-12-409548-9.10799-7)
1149 7, 2019.

1150 Deshmukh, R., Sonah, H., and Belanger, R. R.: New evidence defining the evolutionary path of aquaporins regulating silicon
1151 uptake in land plants, *J. Exp. Bot.*, 71, 6775–6788, <https://doi.org/10.1093/jxb/eraa342>, 2020.

1152 Doering, K., Erdem, Z., Ehlert, C., Fleury, S., Frank, M., and Schneider, R.: Changes in diatom productivity and upwelling
1153 intensity off Peru since the Last Glacial Maximum: Response to basin-scale atmospheric and oceanic forcing,
1154 *Paleoceanography*, 31, 1453–1473, <https://doi.org/10.1002/2016PA002936>, 2016.

1155 Doering, K., Ehlert, C., Pahnke, K., Frank, M., Schneider, R., and Grasse, P.: Silicon Isotope Signatures of Radiolaria Reveal
1156 Taxon-Specific Differences in Isotope Fractionation, *Front. Mar. Sci.*, 8, <https://doi.org/10.3389/fmars.2021.666896>, 2021.

1157 Dumitrica, P.: Double skeletons of silicoflagellates: Their reciprocal position and taxonomical and paleobiological values,
1158 *Rev. Micropaléontologie*, 57, 57–74, <https://doi.org/10.1016/j.revmic.2014.04.001>, 2014.

1159 Durak, G. M., Taylor, A. R., Walker, C. E., Probert, I., De Vargas, C., Audic, S., Schroeder, D., Brownlee, C., and Wheeler,
1160 G. L.: A role for diatom-like silicon transporters in calcifying coccolithophores, *Nat. Commun.*, 7, 10543,
1161 <https://doi.org/10.1038/ncomms10543>, 2016.

1162 Durbin, E. G.: Studies on the autecology of the marine diatom *Thalassiosira nordenskiöldii* II. The influence of cell size
1163 on growth rate, and carbon, nitrogen, chlorophyll *a* and silica content, *J. Phycol.*, 13, 150–155, [https://doi.org/10.1111/j.1529-](https://doi.org/10.1111/j.1529-8817.1977.tb02904.x)
1164 8817.1977.tb02904.x, 1977.

1165 Durkin, C. A., Koester, J. A., Bender, S. J., and Armbrust, E. V.: The evolution of silicon transporters in diatoms, *J. Phycol.*,
1166 52, 716–731, <https://doi.org/10.1111/jpy.12441>, 2016.

1167 Eckford-Soper, L. and Daugbjerg, N.: The ichthyotoxic genus *Pseudochattonella* (Dictyochophyceae): Distribution, toxicity,
1168 enumeration, ecological impact, succession and life history – A review, *Harmful Algae*, 58, 51–58,
1169 <https://doi.org/10.1016/j.hal.2016.08.002>, 2016.

1170 Egan, K. E., Rickaby, R. E. M., Leng, M. J., Hendry, K. R., Hermoso, M., Sloane, H. J., Bostock, H., and Halliday, A. N.:
1171 Diatom silicon isotopes as a proxy for silicic acid utilisation: A Southern Ocean core top calibration, *Geochim. Cosmochim.*
1172 *Acta*, 96, 174–192, <https://doi.org/10.1016/j.gca.2012.08.002>, 2012.

1173 Ehlert, C., Doering, K., Wallmann, K., Scholz, F., Sommer, S., Grasse, P., Geilert, S., and Frank, M.: Stable silicon isotope
1174 signatures of marine pore waters – Biogenic opal dissolution versus authigenic clay mineral formation, *Geochim. Cosmochim.*
1175 *Acta*, 191, 102–117, <https://doi.org/10.1016/j.gca.2016.07.022>, 2016.

1176 Ehrenberg: Ueber das Massenverhältniss der jetzt lebenden Kiesel-Infusorien und über ein neues Infusorien-Conglomerat als
1177 Polirschiefer von Jastraba in Ungarn, *Ann. Phys.*, 117, 555–558, <https://doi.org/10.1002/andp.18371170712>, 1837.

1178 Ehrlich, H., Deutzmann, R., Brunner, E., Cappellini, E., Koon, H., Solazzo, C., Yang, Y., Ashford, D., Thomas-Oates, J.,
1179 Lubeck, M., Baessmann, C., Langrock, T., Hoffmann, R., Wörheide, G., Reitner, J., Simon, P., Tsurkan, M., Ereskovsky, A.
1180 V., Kurek, D., Bazhenov, V. V., Hunoldt, S., Mertig, M., Vyalikh, D. V., Molodtsov, S. L., Kummer, K., Worch, H., Smetacek,
1181 V., and Collins, M. J.: Mineralization of the metre-long biosilica structures of glass sponges is templated on hydroxylated
1182 collagen, *Nat. Chem.*, 2, 1084–1088, <https://doi.org/10.1038/nchem.899>, 2010.

1183 Eicken, H.: From the Microscopic, to the Macroscopic, to the Regional Scale: Growth, Microstructure and Properties of Sea
1184 Ice, in: *Sea Ice: An Introduction to its Physics, Chemistry, Biology and Geology*, edited by: Thomas, D. N. and Dieckmann,
1185 G. S., Wiley, 22–81, <https://doi.org/10.1002/9780470757161.ch2>, 2003.

1186 Esenkulova, S., Sutherland, B. J. G., Tabata, A., Haigh, N., Pearce, C. M., and Miller, K. M.: Comparing metabarcoding and
1187 morphological approaches to identify phytoplankton taxa associated with harmful algal blooms, *Facets*, 5, 784–811,
1188 <https://doi.org/10.1139/facets-2020-0025>, 2020.

1189 Fabre, S., Jeandel, C., Zambardi, T., Roustan, M., and Almar, R.: An Overlooked Silica Source of the Modern Oceans: Are
1190 Sandy Beaches the Key?, *Front. Earth Sci.*, 7, <https://doi.org/10.3389/feart.2019.00231>, 2019.

1191 Fagerness, V. L.: The spring bloom of the silicoflagellate *Dictyocha speculum* in East Sound, Washington, with respect to
1192 certain environmental factors, 1984.

1193 Falkowski, P. G., Katz, M. E., Knoll, A. H., Quigg, A., Raven, J. A., Schofield, O., and Taylor, F. J. R.: The Evolution of
1194 Modern Eukaryotic Phytoplankton, *Science*, 305, 354–360, <https://doi.org/10.1126/science.1095964>, 2004.

1195 Falkowski, P. G., Fenchel, T., and Delong, E. F.: The Microbial Engines That Drive Earth’s Biogeochemical Cycles, *Science*,
1196 320, 1034–1039, <https://doi.org/10.1126/science.1153213>, 2008.

1197 Farooq, M. A. and Dietz, K.-J.: Silicon as Versatile Player in Plant and Human Biology: Overlooked and Poorly Understood,
1198 *Front. Plant Sci.*, 6, <https://doi.org/10.3389/fpls.2015.00994>, 2015.

1199 Faure, E., Not, F., Benoiston, A.-S., Labadie, K., Bittner, L., and Ayata, S.-D.: Mixotrophic protists display contrasted
1200 biogeographies in the global ocean, *ISME J.*, 13, 1072–1083, <https://doi.org/10.1038/s41396-018-0340-5>, 2019.

1201 Ferguson, A. and Davis, A.: Heart of glass: spicule armament and physical defense in temperate reef sponges, *Mar. Ecol. Prog.*
1202 *Ser.*, 372, 77–86, <https://doi.org/10.3354/meps07680>, 2008.

1203 Fernandez, N. M., Bouchez, J., Derry, L. A., Chorover, J., Gaillardet, J., Giesbrecht, I., Fries, D., and Druhan, J. L.: Resiliency
1204 of Silica Export Signatures When Low Order Streams Are Subject to Storm Events, *J. Geophys. Res. Biogeosciences*, 127,
1205 <https://doi.org/10.1029/2021jg006660>, 2022.

1206 Field, C. B., Behrenfeld, M. J., Randerson, J. T., and Falkowski, P.: Primary Production of the Biosphere: Integrating
1207 Terrestrial and Oceanic Components, *Science*, 281, 237–240, <https://doi.org/10.1126/science.281.5374.237>, 1998.

1208 Flombaum, P., Wang, W.-L., Primeau, F. W., and Martiny, A. C.: Global picophytoplankton niche partitioning predicts overall
1209 positive response to ocean warming, *Nat. Geosci.*, 13, 116–120, <https://doi.org/10.1038/s41561-019-0524-2>, 2020.

1210 Flynn, K. J. and Martin-Jézéquel, V.: Modelling Si-N-limited growth of diatoms, *J. Plankton Res.*, 22, 447–472,
1211 <https://doi.org/10.1093/plankt/22.3.447>, 2000.

1212 Folkers, M. and Rombouts, T.: Sponges Revealed: A Synthesis of Their Overlooked Ecological Functions Within Aquatic
1213 Ecosystems, in: *YOUMARES 9 - The Oceans: Our Research, Our Future*, edited by: Jungblut, S., Liebich, V., and Bode-
1214 Dalby, M., Springer International Publishing, Cham, 181–193, https://doi.org/10.1007/978-3-030-20389-4_9, 2020.

1215 Fontorbe, G., Frings, P. J., De La Rocha, C. L., Hendry, K. R., and Conley, D. J.: A silicon depleted North Atlantic since the
1216 Palaeogene: Evidence from sponge and radiolarian silicon isotopes, *Earth Planet. Sci. Lett.*, 453, 67–77,
1217 <https://doi.org/10.1016/j.epsl.2016.08.006>, 2016.

1218 Fontorbe, G., Frings, P. J., De La Rocha, C. L., Hendry, K. R., Carstensen, J., and Conley, D. J.: Enrichment of dissolved silica
1219 in the deep equatorial Pacific during the Eocene-Oligocene, *Paleoceanography*, 32, 848–863,
1220 <https://doi.org/10.1002/2017PA003090>, 2017.

1221 Fortey, R. A. and Holdsworth, B. K.: The oldest known well-preserved Radiolaria, *Boll. Della Soc. Paleontol. Ital.*, 10, 35–
1222 41, 1971.

1223 Frings, P. J., Clymans, W., Fontorbe, G., De La Rocha, C. L., and Conley, D. J.: The continental Si cycle and its impact on the
1224 ocean Si isotope budget, *Chem. Geol.*, 425, 12–36, <https://doi.org/10.1016/j.chemgeo.2016.01.020>, 2016.

1225 Frings, P. J., Schubring, F., Oelze, M., and Von Blanckenburg, F.: Quantifying biotic and abiotic Si fluxes in the Critical Zone
1226 with Ge/Si ratios along a gradient of erosion rates, *Am. J. Sci.*, 321, 1204–1245, <https://doi.org/10.2475/08.2021.03>, 2021.

1227 Frings, P. J., Panizzo, V. N., Sutton, J. N., and Ehlert, C.: Diatom silicon isotope ratios in Quaternary research: Where do we
1228 stand?, *Quat. Sci. Rev.*, 344, 108966, <https://doi.org/10.1016/j.quascirev.2024.108966>, 2024.

1229 Fripiat, F., Cardinal, D., Tison, J.-L., Worby, A., and André, L.: Diatom-induced silicon isotopic fractionation in Antarctic sea
1230 ice, *J. Geophys. Res. Biogeosciences*, 112, <https://doi.org/10.1029/2006JG000244>, 2007.

1231 Fripiat, F., Tison, J.-L., André, L., Notz, D., and Delille, B.: Biogenic silica recycling in sea ice inferred from Si-isotopes:
1232 constraints from Arctic winter first-year sea ice, *Biogeochemistry*, 119, 25–33, <https://doi.org/10.1007/s10533-013-9911-8>,
1233 2014.

1234 Fuhrman, J. A.: Marine viruses and their biogeochemical and ecological effects, *Nature*, 399, 541–548,
1235 <https://doi.org/10.1038/21119>, 1999.

1236 Gaino, E., Scoccia, F., Piersanti, S., Rebora, M., Bellucci, L. G., and Ludovisi, A.: Spicule records of *Ephydatia fluviatilis* as
1237 a proxy for hydrological and environmental changes in the shallow Lake Trasimeno (Umbria, Italy), *Hydrobiologia*, 679, 139–
1238 153, <https://doi.org/10.1007/s10750-011-0861-7>, 2012.

1239 Geilert, S., Grasse, P., Doering, K., Wallmann, K., Ehlert, C., Scholz, F., Frank, M., Schmidt, M., and Hensen, C.: Impact of
1240 ambient conditions on the Si isotope fractionation in marine pore fluids during early diagenesis, [https://doi.org/10.5194/bg-](https://doi.org/10.5194/bg-2019-481)
1241 2019-481, 8 January 2020.

1242 Geilert, S., Frick, D. A., Garbe-Schönberg, D., Scholz, F., Sommer, S., Grasse, P., Vogt, C., and Dale, A. W.: Coastal El Niño
1243 triggers rapid marine silicate alteration on the seafloor, *Nat. Commun.*, 14, <https://doi.org/10.1038/s41467-023-37186-5>, 2023.

1244 Gentil, J., Hempel, F., Moog, D., Zauner, S., and Maier, U. G.: Review: origin of complex algae by secondary endosymbiosis:
1245 a journey through time, *J. Soil Sci. Plant Nutr.*, 254, 1835–1843, <https://doi.org/10.1007/s00709-017-1098-8>, 2017.

1246 Gereá, M., Saad, J., Izaguirre, I., Queimaliños, C., Gasol, J., and Unrein, F.: Presence, abundance and bacterivory of the
1247 mixotrophic algae *Pseudopedinella* (Dictyochophyceae) in freshwater environments, *Aquat. Microb. Ecol.*, 76, 219–232,
1248 <https://doi.org/10.3354/ame01780>, 2016.

1249 Ghobara, M. M., Ghobara, M. M., Mazumder, N., Vinayak, V., Reissig, L., Gebeshuber, I. C., Tiffany, M. A., Gordon, R., and
1250 Gordon, R.: On Light and Diatoms: A Photonics and Photobiology Review, in: *Diatoms: Fundamentals and Applications*, John
1251 Wiley & Sons, Ltd, 129–189, <https://doi.org/10.1002/9781119370741.ch7>, 2019.

1252 Giesbrecht, K. E. and Varela, D. E.: Summertime Biogenic Silica Production and Silicon Limitation in the Pacific Arctic
1253 Region From 2006 to 2016, *Glob. Biogeochem. Cycles*, 35, e2020GB006629, <https://doi.org/10.1029/2020GB006629>, 2021.

1254 Görlich, S., Pawolski, D., Zlotnikov, I., and Kröger, N.: Control of biosilica morphology and mechanical performance by the
1255 conserved diatom gene *Silicanin-1*, *Commun. Biol.*, 2, <https://doi.org/10.1038/s42003-019-0436-0>, 2019.

1256 Gouretski, V. V. and Koltermann, K. P.: WOCE - Global Hydrographic Climatology: A Technical Report, Bundesamt für
1257 Seeschifffahrt und Hydrographie (BSH), Hamburg & Rostock, <https://doi.org/10.57802/azf1-r757>, 2004.

1258 Gouvêa, L., Fragkopoulou, E., B. Araújo, M., Serrão, E. A., and Assis, J.: Seagrass Biodiversity Under the Latest-Generation
1259 Scenarios of Projected Climate Change, *J. Biogeogr.*, 52, 172–185, <https://doi.org/10.1111/jbi.15021>, 2024.

1260 Grasse, P., Closset, I., Jones, J. L., Geilert, S., and Brzezinski, M. A.: Controls on Dissolved Silicon Isotopes Along the U.S.
1261 GEOTRACES Eastern Pacific Zonal Transect (GP16), *Glob. Biogeochem. Cycles*, 34, e2020GB006538,
1262 <https://doi.org/10.1029/2020GB006538>, 2020.

1263 Grenne, T. and Slack, J. F.: Paleozoic and Mesozoic silica-rich seawater: Evidence from hematitic chert (jasper) deposits,
1264 *Geology*, 31, 319, [https://doi.org/10.1130/0091-7613\(2003\)031%253C0319:pamsrs%253E2.0.co;2](https://doi.org/10.1130/0091-7613(2003)031%253C0319:pamsrs%253E2.0.co;2), 2003.

1265 Gutierrez-Rodriguez, A., Stukel, M. R., Lopes dos Santos, A., Biard, T., Scharek, R., Vaultot, D., Landry, M. R., and Not, F.:
1266 High contribution of Rhizaria (Radiolaria) to vertical export in the California Current Ecosystem revealed by DNA
1267 metabarcoding, *ISME J.*, 13, 964–976, <https://doi.org/10.1038/s41396-018-0322-7>, 2019.

1268 Haeckel, E.: Report on the Radiolaria collected by H.M.S. Challenger during the years 1873-1876, *Zoology*, 18, 1–1803, 1887.

1269 Halbach, L., Vihtakari, M., Duarte, P., Everett, A., Granskog, M. A., Hop, H., Kauko, H. M., Kristiansen, S., Myhre, P. I.,
1270 Pavlov, A. K., Pramanik, A., Tatarek, A., Torsvik, T., Wiktor, J. M., Wold, A., Wulff, A., Steen, H., and Assmy, P.: Tidewater
1271 Glaciers and Bedrock Characteristics Control the Phytoplankton Growth Environment in a Fjord in the Arctic, *Front. Mar.*
1272 *Sci.*, 6, <https://doi.org/10.3389/fmars.2019.00254>, 2019.

1273 Hamm, C. E., Merkel, R., Springer, O., Jurkojc, P., Maier, C., Prectel, K., and Smetacek, V.: Architecture and material
1274 properties of diatom shells provide effective mechanical protection, *Nature*, 421, 841–843,
1275 <https://doi.org/10.1038/nature01416>, 2003.

1276 Harper, H. E. and Knoll, A. H.: Silica, diatoms, and Cenozoic radiolarian evolution, *Geology*, 3, 175,
1277 [https://doi.org/10.1130/0091-7613\(1975\)3%253C175:sdacre%253E2.0.co;2](https://doi.org/10.1130/0091-7613(1975)3%253C175:sdacre%253E2.0.co;2), 1975.

1278 Harrison, F. W.: Sponges (Porifera: Spongillidae), in: *Pollution Ecology of Freshwater Invertebrates*, edited by: Hart, C. W.
1279 and Fuller, S. L. H., Academic Press New York, New York, 29–66, 1974.

1280 Hartley, S. E. and DeGabriel, J. L.: The ecology of herbivore-induced silicon defences in grasses, *Funct. Ecol.*, 30, 1311–1322,
1281 <https://doi.org/10.1111/1365-2435.12706>, 2016.

1282 Hatton, J. E., Hendry, K. R., Hawkings, J. R., Wadham, J. L., Kohler, T. J., Stibal, M., Beaton, A. D., Bagshaw, E. A., and
1283 Telling, J.: Investigation of subglacial weathering under the Greenland Ice Sheet using silicon isotopes, *Geochim. Cosmochim.*
1284 *Acta*, 247, 191–206, <https://doi.org/10.1016/j.gca.2018.12.033>, 2019a.

1285 Hatton, J. E., Hendry, K. R., Hawkings, J. R., Wadham, J. L., Opfergelt, S., Kohler, T. J., Yde, J. C., Stibal, M., and Žárský,
1286 J. D.: Silicon isotopes in Arctic and sub-Arctic glacial meltwaters: the role of subglacial weathering in the silicon cycle, *Proc.*
1287 *R. Soc. Math. Phys. Eng. Sci.*, 475, 20190098, <https://doi.org/10.1098/rspa.2019.0098>, 2019b.

1288 Hatton, J. E., Hendry, K. R., Hawkings, J. R., Wadham, J. L., Benning, L. G., Blukis, R., Roddatis, V., Ng, H. C., and Wang,
1289 T.: Physical weathering by glaciers enhances silicon mobilisation and isotopic fractionation, *Geochem. Perspect. Lett.*, 7–12,
1290 <https://doi.org/10.7185/geochemlet.2126>, 2021.

1291 Hatton, J. E., Ng, H. C., Meire, L., Woodward, E. M. S., Leng, M. J., Coath, C. D., Stuart-Lee, A., Wang, T., Annett, A. L.,
1292 and Hendry, K. R.: Silicon Isotopes Highlight the Role of Glaciated Fjords in Modifying Coastal Waters, *J. Geophys. Res.*
1293 *Biogeosciences*, 128, <https://doi.org/10.1029/2022jg007242>, 2023.

1294 Hawkings, J. R., Wadham, J. L., Benning, L. G., Hendry, K. R., Tranter, M., Tedstone, A., Nienow, P., and Raiswell, R.: Ice
1295 sheets as a missing source of silica to the polar oceans, *Nat. Commun.*, 8, <https://doi.org/10.1038/ncomms14198>, 2017.

1296 Hawkings, J. R., Hatton, J. E., Hendry, K. R., De Souza, G. F., Wadham, J. L., Ivanovic, R., Kohler, T. J., Stibal, M., Beaton,
1297 A., Lamarche-Gagnon, G., Tedstone, A., Hain, M. P., Bagshaw, E., Pike, J., and Tranter, M.: The silicon cycle impacted by
1298 past ice sheets, *Nat. Commun.*, 9, <https://doi.org/10.1038/s41467-018-05689-1>, 2018.

1299 Hendry, K. R. and Robinson, L. F.: The relationship between silicon isotope fractionation in sponges and silicic acid
1300 concentration: Modern and core-top studies of biogenic opal, *Geochim. Cosmochim. Acta*, 81, 1–12,
1301 <https://doi.org/10.1016/j.gca.2011.12.010>, 2012.

1302 Hendry, K. R., Georg, R. B., Rickaby, R. E. M., Robinson, L. F., and Halliday, A. N.: Deep ocean nutrients during the Last
1303 Glacial Maximum deduced from sponge silicon isotopic compositions, *Earth Planet. Sci. Lett.*, 292, 290–300,
1304 <https://doi.org/10.1016/j.epsl.2010.02.005>, 2010.

1305 Hendry, K. R., Swann, G. E. A., Leng, M. J., Sloane, H. J., Goodwin, C., Berman, J., and Maldonado, M.: Silica stable isotopes
1306 and silicification in a carnivorous sponge *Asbestopluma* sp., *Biogeosciences Discuss.*, 11, 16573–16597,
1307 <https://doi.org/10.5194/bgd-11-16573-2014>, 2014.

1308 Hendry, K. R., Marron, A. O., Vincent, F., Conley, D. J., Gehlen, M., Ibarbalz, F. M., Quéguiner, B., and Bowler, C.:
1309 Competition between Silicifiers and Non-silicifiers in the Past and Present Ocean and Its Evolutionary Impacts, *Front. Mar.*
1310 *Sci.*, 5, 22, <https://doi.org/10.3389/fmars.2018.00022>, 2018.

1311 Hendry, K. R., Sales De Freitas, F., Arndt, S., Beaton, A., Friberg, L., Hatton, J. E., Hawkings, J. R., Jones, R. L., Krause, J.
1312 W., Meire, L., Ng, H. C., Pryer, H., Tingey, S., Van De Velde, S. J., Wadham, J., Wang, T., and Woodward, E. M. S.: Insights
1313 into silicon cycling from ice sheet to coastal ocean from isotope geochemistry, *Commun. Earth Environ.*, 6,
1314 <https://doi.org/10.1038/s43247-025-02264-7>, 2025.

1315 Heneghan, R. F., Holloway-Brown, J., Gasol, J. M., Herndl, G. J., Morán, X. A. G., and Galbraith, E. D.: The global
1316 distribution and climate resilience of marine heterotrophic prokaryotes, *Nat. Commun.*, 15, <https://doi.org/10.1038/s41467-024-50635-z>, 2024.

1318 Henriksen, P., Knipschildt, F., Moestrup, Ø., and Thomsen, H. A.: Autecology, life history and toxicology of the
1319 silicoflagellate *Dictyocha speculum* (Silicoflagellata, Dictyochophyceae), *Phycologia*, 32, 29–39,
1320 <https://doi.org/10.2216/i0031-8884-32-1-29.1>, 1993.

1321 Herman, P. M. J., Hemminga, M. A., Nienhuis, P. H., Verschuure, J. M., and Wessel, E. G. J.: Wax and wane of eelgrass
1322 *Zostera marina* and water column silicon levels, *Mar. Ecol. Prog. Ser.*, 144, 303–307, <https://doi.org/10.3354/meps144303>,
1323 1996.

1324 Hernández-Almeida, I., Cortese, G., Yu, P. -S., Chen, M. -T., and Kucera, M.: Environmental determinants of radiolarian
1325 assemblages in the western Pacific since the last deglaciation, *Paleoceanography*, 32, 830–847,
1326 <https://doi.org/10.1002/2017PA003159>, 2017.

1327 Hernández-Becerril, D. U. and Bravo-Sierra, E.: Planktonic Silicoflagellates (Dictyochophyceae) from the Mexican Pacific
1328 Ocean, *Bot. Mar.*, 44, <https://doi.org/10.1515/bot.2001.050>, 2001.

1329 Hervé, V., Derr, J., Douady, S., Quinet, M., Moisan, L., and Lopez, P. J.: Multiparametric Analyses Reveal the pH-Dependence
1330 of Silicon Biomineralization in Diatoms, *PLOS ONE*, 7, e46722, <https://doi.org/10.1371/journal.pone.0046722>, 2012.

1331 Hiebert, T. C., Thompson, A. W., and Sutherland, K. R.: Diverse microbial prey in the guts of gelatinous grazers revealed by
1332 microscopy, *Mar. Biol.*, 172, <https://doi.org/10.1007/s00227-025-04615-6>, 2025.

1333 Hildebrand, M. and Lerch, S. J. L.: Diatom silica biomineralization: Parallel development of approaches and understanding,
1334 *Semin. Cell Dev. Biol.*, 46, 27–35, <https://doi.org/10.1016/j.semcdb.2015.06.007>, 2015.

1335 Hildebrand, M., Volcani, B. E., Gassmann, W., and Schroeder, J. I.: A gene family of silicon transporters, *Nature*, 385, 688–
1336 689, <https://doi.org/10.1038/385688b0>, 1997.

1337 Hildebrand, M., Lerch, S. J. L., and Shrestha, R. P.: Understanding Diatom Cell Wall Silicification—Moving Forward, *Front.*
1338 *Mar. Sci.*, 5, <https://doi.org/10.3389/fmars.2018.00125>, 2018.

1339 Hirota, R., Hata, Y., Ikeda, T., Ishida, T., and Kuroda, A.: The Silicon Layer Supports Acid Resistance of *Bacillus cereus*
1340 Spores, *J. Bacteriol.*, 192, 111–116, <https://doi.org/10.1128/jb.00954-09>, 2010.

1341 Hobbie, J. E., Daley, R. J., and Jasper, S.: Use of nuclepore filters for counting bacteria by fluorescence microscopy, *Appl.*
1342 *Environ. Microbiol.*, 33, 1225–1228, <https://doi.org/10.1128/aem.33.5.1225-1228.1977>, 1977.

1343 Hodell, D. A., Kanfoush, S. L., Shemesh, A., Crosta, X., Charles, C. D., and Guilderson, T. P.: Abrupt Cooling of Antarctic
1344 Surface Waters and Sea Ice Expansion in the South Atlantic Sector of the Southern Ocean at 5000 cal yr B.P., *Quat. Res.*, 56,
1345 191–198, <https://doi.org/10.1006/qres.2001.2252>, 2001.

1346 Hodson, M. J., White, P. J., Mead, A., and Broadley, M. R.: Phylogenetic Variation in the Silicon Composition of Plants, *Ann.*
1347 *Bot.*, 96, 1027–1046, <https://doi.org/10.1093/aob/mci255>, 2005.

1348 Hong, W.-L., Sun, X., Torres, M. E., Huang, T.-H., and Pickering, R. A.: The role of silicate alteration in regulating marine
1349 carbon cycling, *Chem. Geol.*, 684, 122769, <https://doi.org/10.1016/j.chemgeo.2025.122769>, 2025.

1350 Hooper, J. N. A. and Van Soest, R. W. M.: *Systema Porifera. A Guide to the Classification of Sponges*, in: *Systema Porifera*,
1351 Springer US, Boston, MA, 1–7, https://doi.org/10.1007/978-1-4615-0747-5_1, 2002.

1352 Hopwood, M. J., Carroll, D., Dunse, T., Hodson, A., Holding, J. M., Iriarte, J. L., Ribeiro, S., Achterberg, E. P., Cantoni, C.,
1353 Carlson, D. F., Chierici, M., Clarke, J. S., Cozzi, S., Fransson, A., Juul-Pedersen, T., Winding, M. H. S., and Meire, L.: Review
1354 article: How does glacier discharge affect marine biogeochemistry and primary production in the Arctic?, *The Cryosphere*, 14,
1355 1347–1383, <https://doi.org/10.5194/tc-14-1347-2020>, 2020.

1356 Hopwood, M. J., Carroll, D., Gu, Y., Huang, X., Krause, J., Cozzi, S., Cantoni, C., Gastelu Barcena, M. F., Carroll, S., and
1357 Körtzinger, A.: A Close Look at Dissolved Silica Dynamics in Disko Bay, West Greenland, *Glob. Biogeochem. Cycles*, 39,
1358 <https://doi.org/10.1029/2023gb008080>, 2025.

1359 Hou, Y., Baronas, J., Kemeny, P., Bouchez, J., Geirsdóttir, Á., Miller, G., and Torres, M.: Glacially enhanced silicate
1360 weathering revealed by Holocene lake records, <https://doi.org/10.31223/X5RM73>, 8 February 2025.

1361 Ignatiades, L.: The Relationship of the Seasonality of Silicoflagellates to Certain Environmental Factors, *Bot. Mar.*, 13,
1362 <https://doi.org/10.1515/botm.1970.13.1.44>, 1970.

1363 Iler, R. K.: The chemistry of silica, Solubility, Polymerization, *Colloid Surf. Prop. Biochem.*, 866, 1979.

1364 Inagaki, F., Motomura, Y., and Ogata, S.: Microbial silica deposition in geothermal hot waters, *Appl. Microbiol. Biotechnol.*,
1365 60, 605–611, <https://doi.org/10.1007/s00253-002-1100-y>, 2003.

1366 Isson, T. T. and Planavsky, N. J.: Reverse weathering as a long-term stabilizer of marine pH and planetary climate, *Nature*,
1367 560, 471–475, <https://doi.org/10.1038/s41586-018-0408-4>, 2018.

1368 Iwai, M., Motoyama, I., Lin, W., Takashima, R., Yamada, Y., and Eguchi, N.: Diatom and Radiolarian Biostratigraphy in the
1369 Vicinity of the 2011 Tohoku Earthquake Source Fault in IODP Hole 343- C0019E of JFAST, *Isl. Arc*, 34, e70009,
1370 <https://doi.org/10.1111/iar.70009>, 2025.

1371 Jeong, Y. and Lee, J.: Comparative analysis of organelle genomes provides conflicting evidence between morphological
1372 similarity and phylogenetic relationship in diatoms, *Front. Mar. Sci.*, 10, <https://doi.org/10.3389/fmars.2023.1283893>, 2024.

1373 Jewson, D. H.: Size reduction, reproductive strategy and the life cycle of a centric diatom, *Philos. Trans. R. Soc. Lond.*, 336,
1374 191–213, <https://doi.org/10.1098/rstb.1992.0056>, 1997.

1375 Jin, X., Gruber, N., Dunne, J. P., Sarmiento, J. L., and Armstrong, R. A.: Diagnosing the contribution of phytoplankton
1376 functional groups to the production and export of particulate organic carbon, CaCO₃, and opal from global nutrient and
1377 alkalinity distributions, *Glob. Biogeochem. Cycles*, 20, <https://doi.org/10.1029/2005gb002532>, 2006.

1378 Jochem, F. and Babenerd, B.: Naked Dictyocha speculum – a new type of phytoplankton bloom in the Western Baltic, *Mar.*
1379 *Biol.*, 103, 373–379, <https://doi.org/10.1007/bf00397272>, 1989.

1380 Johnson, S. N., Waterman, J. M., Hartley, S. E., Cooke, J., Ryalls, J. M. W., Lagisz, M., and Nakagawa, S.: Plant Silicon
1381 Defences Suppress Herbivore Performance, but Mode of Feeding Is Key, *Ecol. Lett.*, 27, e14519,
1382 <https://doi.org/10.1111/ele.14519>, 2024.

1383 Jordan, R. and McCartney, K.: *Stephanocha* nom. nov., a replacement name for the illegitimate silicoflagellate genus
1384 *Distephanus* Stöhr., *Phytotaxa*, 201, 177–187, 2015.

1385 Jumper, J., Evans, R., Pritzel, A., Green, T., Figurnov, M., Ronneberger, O., Tunyasuvunakool, K., Bates, R., Žídek, A.,
1386 Potapenko, A., Bridgland, A., Meyer, C., Kohl, S. A. A., Ballard, A. J., Cowie, A., Romera-Paredes, B., Nikolov, S., Jain, R.,
1387 Adler, J., Back, T., Petersen, S., Reiman, D., Clancy, E., Zielinski, M., Steinegger, M., Pacholska, M., Berghammer, T.,

1388 Bodenstein, S., Silver, D., Vinyals, O., Senior, A. W., Kavukcuoglu, K., Kohli, P., and Hassabis, D.: Highly accurate protein
1389 structure prediction with AlphaFold, *Nature*, 596, 583–589, <https://doi.org/10.1038/s41586-021-03819-2>, 2021.

1390 Jurkowska, A. and Świerczewska-Gładysz, E.: The evolution of the marine Si cycle in the Archean-Palaeozoic - an overlooked
1391 Si source?, *Earth-Sci. Rev.*, 248, 104629, <https://doi.org/10.1016/j.earscirev.2023.104629>, 2024.

1392 Kemp, A. E. S., Pearce, R. B., Grigorov, I., Rance, J., Lange, C. B., Quilty, P., and Salter, I.: Production of giant marine
1393 diatoms and their export at oceanic frontal zones: Implications for Si and C flux from stratified oceans, *Glob. Biogeochem.*
1394 *Cycles*, 20, 2006GB002698, <https://doi.org/10.1029/2006GB002698>, 2006.

1395 Kidder, D. L. and Tomescu, I.: Biogenic chert and the Ordovician silica cycle, *Palaeogeogr. Palaeoclimatol. Palaeoecol.*, 458,
1396 29–38, <https://doi.org/10.1016/j.palaeo.2015.10.013>, 2016.

1397 Kim, H. H., Laufkötter, C., Lovato, T., Doney, S. C., and Ducklow, H. W.: Projected 21st-century changes in marine
1398 heterotrophic bacteria under climate change, *Front. Microbiol.*, 14, <https://doi.org/10.3389/fmicb.2023.1049579>, 2023.

1399 Klitgaard, A. B.: The fauna associated with outer shelf and upper slope sponges (Porifera, Demospongiae) at the Faroe Islands,
1400 northeastern Atlantic, *Sarsia*, 80, 1–22, <https://doi.org/10.1080/00364827.1995.10413574>, 1995.

1401 Knight, M. J., Senior, L., Nancolas, B., Ratcliffe, S., and Curnow, P.: Direct evidence of the molecular basis for biological
1402 silicon transport, *Nat. Commun.*, 7, 11926, <https://doi.org/10.1038/ncomms11926>, 2016.

1403 Knight, M. J., Hardy, B. J., Wheeler, G. L., and Curnow, P.: Computational modelling of diatom silicic acid transporters
1404 predicts a conserved fold with implications for their function and evolution, *Biochim. Biophys. Acta BBA - Biomembr.*, 1865,
1405 184056, <https://doi.org/10.1016/j.bbamem.2022.184056>, 2023.

1406 Koltun, V. M.: Spicule analysis and its application in geology: *Izvestiya Akademii Nauk SSR, Seriya Geol.*, 4, 73–77, 1960.

1407 Kotzsch, A., Gröger, P., Pawolski, D., Bomans, P. H. H., Sommerdijk, N. A. J. M., Schlierf, M., and Kröger, N.: Silicanin-1
1408 is a conserved diatom membrane protein involved in silica biomineralization, *BMC Biol.*, 15, <https://doi.org/10.1186/s12915-017-0400-8>, 2017.

1410 Krause, J. W., Nelson, D. M., and Brzezinski, M. A.: Biogenic silica production and the diatom contribution to primary
1411 production and nitrate uptake in the eastern equatorial Pacific Ocean, *Deep Sea Res. Part II Top. Stud. Oceanogr.*, 58, 434–
1412 448, <https://doi.org/10.1016/j.dsr2.2010.08.010>, 2011.

1413 Krause, J. W., Brzezinski, M. A., Baines, S. B., Collier, J. L., Twining, B. S., and Ohnemus, D. C.: Picoplankton contribution
1414 to biogenic silica stocks and production rates in the Sargasso Sea, *Glob. Biogeochem. Cycles*, 31, 762–774,
1415 <https://doi.org/10.1002/2017gb005619>, 2017.

1416 Krause, J. W., Schulz, I. K., Rowe, K. A., Dobbins, W., Winding, M. H. S., Sejr, M. K., Duarte, C. M., and Agustí, S.: Silicic
1417 acid limitation drives bloom termination and potential carbon sequestration in an Arctic bloom, *Sci. Rep.*, 9, 8149,
1418 <https://doi.org/10.1038/s41598-019-44587-4>, 2019.

1419 Kristiansen, S., Farbro, T., and Naustvoll, L.-J.: Production of biogenic silica by spring diatoms, *Limnol. Oceanogr.*, 45, 472–
1420 478, <https://doi.org/10.4319/lo.2000.45.2.0472>, 2000.

1421 Kröger, N., Deutzmann, R., and Sumper, M.: Polycationic Peptides from Diatom Biosilica That Direct Silica Nanosphere
1422 Formation, *Science*, 286, 1129–1132, <https://doi.org/10.1126/science.286.5442.1129>, 1999.

1423 Kröger, N., Lorenz, S., Brunner, E., and Sumper, M.: Self-Assembly of Highly Phosphorylated Silaffins and Their Function
1424 in Biosilica Morphogenesis, *Science*, 298, 584–586, <https://doi.org/10.1126/science.1076221>, 2002.

1425 Kuerten, S., Parolin, M., Assine, M. L., and McGlue, M. M.: Sponge spicules indicate Holocene environmental changes on
1426 the Nabileque River floodplain, southern Pantanal, Brazil, *J. Paleolimnol.*, 49, 171–183, [https://doi.org/10.1007/s10933-012-](https://doi.org/10.1007/s10933-012-9652-z)
1427 9652-z, 2013.

1428 Kumar, S., Milstein, Y., Bami, Y., Elbaum, M., and Elbaum, R.: Mechanism of silica deposition in sorghum silica cells, *New*
1429 *Phytol.*, 213, 791–798, <https://doi.org/10.1111/nph.14173>, 2017a.

1430 Kumar, S., Soukup, M., and Elbaum, R.: Silicification in Grasses: Variation between Different Cell Types, *Front. Plant Sci.*,
1431 8, <https://doi.org/10.3389/fpls.2017.00438>, 2017b.

1432 Kumar, S., Rechav, K., Kaplan-Ashiri, I., and Gal, A.: Imaging and quantifying homeostatic levels of intracellular silicon in
1433 diatoms, *Sci. Adv.*, 6, eaaz7554, <https://doi.org/10.1126/sciadv.aaz7554>, 2020a.

1434 Kumar, S., Adiram-Filiba, N., Blum, S., Sanchez-Lopez, J. A., Tzfadia, O., Omid, A., Volpin, H., Heifetz, Y., Goobes, G., and
1435 Elbaum, R.: Siliplant1 protein precipitates silica in sorghum silica cells, *J. Exp. Bot.*, 71, 6830–6843,
1436 <https://doi.org/10.1093/jxb/eraa258>, 2020b.

1437 Kumar, S., Natalio, F., and Elbaum, R.: Protein-driven biomineralization: Comparing silica formation in grass silica cells to
1438 other biomineralization processes, *J. Struct. Biol.*, 213, 107665, <https://doi.org/10.1016/j.jsb.2020.107665>, 2021.

1439 Kuwata, A., Yamada, K., Ichinomiya, M., Yoshikawa, S., Tragin, M., Vaultot, D., and Lopes dos Santos, A.: Bolidophyceae,
1440 a Sister Picoplanktonic Group of Diatoms – A Review, *Front. Mar. Sci.*, 5, <https://doi.org/10.3389/fmars.2018.00370>, 2018.

1441 Laget, M., Drago, L., Panaiotis, T., Kiko, R., Stemmann, L., Rogge, A., Llopis-Monferrer, N., Leynaert, A., Irisson, J.-O., and
1442 Biard, T.: Global census of the significance of giant mesopelagic protists to the marine carbon and silicon cycles, *Nat.*
1443 *Commun.*, 15, 3341, <https://doi.org/10.1038/s41467-024-47651-4>, 2024.

1444 Lalonde, S. V., Konhauser, K. O., Reysenbach, A.-L., and Ferris, F. G.: The experimental silicification of Aquificales and
1445 their role in hot spring sinter formation, *Geobiology*, 3, 41–52, <https://doi.org/10.1111/j.1472-4669.2005.00042.x>, 2005.

1446 Lampitt, R. S., Briggs, N., Cael, B. B., Espinola, B., Hélaouët, P., Henson, S. A., Norrbin, F., Pebody, C. A., and Smeed, D.:
1447 Deep ocean particle flux in the Northeast Atlantic over the past 30 years: carbon sequestration is controlled by ecosystem
1448 structure in the upper ocean, *Front. Earth Sci.*, 11, <https://doi.org/10.3389/feart.2023.1176196>, 2023.

1449 Laruelle, G. G., Roubéix, V., Sferratore, A., Brodherr, B., Ciuffa, D., Conley, D. J., Dürr, H. H., Garnier, J., Lancelot, C., Le
1450 Thi Phuong, Q., Meunier, J. -D., Meybeck, M., Michalopoulos, P., Moriceau, B., Ní Longphuirt, S., Loucaides, S., Papush, L.,
1451 Presti, M., Ragueneau, O., Regnier, P., Saccone, L., Slomp, C. P., Spiteri, C., and Van Cappellen, P.: Anthropogenic
1452 perturbations of the silicon cycle at the global scale: Key role of the land-ocean transition, *Glob. Biogeochem. Cycles*, 23, 1–
1453 17, <https://doi.org/10.1029/2008GB003267>, 2009.

1454 Läubli, C., Gaviria-Lugo, N., Bernhardt, A., Wittmann, H., Sachse, D., Mohtadi, M., Lückge, A., and Frings, P. J.: Constraints
1455 on the Role of Marine Authigenic Clay Formation in Determining Seawater Lithium Isotope Composition, *Geochim. Geophys.*
1456 *Geosystems*, 26, e2024GC012099, <https://doi.org/10.1029/2024GC012099>, 2025.

1457 Le Quéré, C., Harrison, S. P., Prentice, I. C., Buitenhuis, E. T., Aumont, O., Bopp, L., Claustre, H., Cotrim Da Cunha, L.,
1458 Geider, R., Giraud, X., Klaas, C., Kohfeld, K. E., Legendre, L., Manizza, M., Platt, T., Rivkin, R. B., Sathyendranath, S., Uitz,

1459 J., Watson, A. J., and Wolf-Gladrow, D.: Ecosystem dynamics based on plankton functional types for global ocean
1460 biogeochemistry models, *Glob. Change Biol.*, 11, 2016–2040, <https://doi.org/10.1111/j.1365-2486.2005.1004.x>, 2005.

1461 Leblanc, K. and Hutchins, D. A.: New applications of a biogenic silica deposition fluorophore in the study of oceanic diatoms,
1462 *Limnol. Oceanogr. Methods*, 3, 462–476, <https://doi.org/10.4319/lom.2005.3.462>, 2005.

1463 Leventer, A., Dunbar, R. B., and DeMaster, D. J.: Diatom Evidence for Late Holocene Climatic Events in Granite Harbor,
1464 Antarctica, *Paleoceanography*, 8, 373–386, <https://doi.org/10.1029/93PA00561>, 1993.

1465 Leventer, A., Domack, E., Dunbar, R., Pike, J., Stickley, C., Maddison, E., Brachfeld, S., Manley, P., and McClennen, C.:
1466 Marine sediment record from the East Antarctic margin reveals dynamics of ice sheet recession, *GSA Today*, 16, 4,
1467 <https://doi.org/10.1130/GSAT01612A.1>, 2006.

1468 Leys, S. P. and Lauzon, N. R. J.: Hexactinellid sponge ecology: growth rates and seasonality in deep water sponges, *J. Exp.*
1469 *Mar. Biol. Ecol.*, 230, 111–129, [https://doi.org/10.1016/S0022-0981\(98\)00088-4](https://doi.org/10.1016/S0022-0981(98)00088-4), 1998.

1470 Li, J., Zhang, K., Ke, Z., Liu, J., Tan, Y., Chen, Z., and Liu, H.: Composition and genetic diversity of picoeukaryotes in the
1471 northeastern South China Sea during the Luzon winter bloom, *Reg. Stud. Mar. Sci.*, 57, 102752,
1472 <https://doi.org/10.1016/j.rsma.2022.102752>, 2023.

1473 Liang, Y., Hua, H., Zhu, Y.-G., Zhang, J., Cheng, C., and Römheld, V.: Importance of plant species and external silicon
1474 concentration to active silicon uptake and transport, *New Phytol.*, 172, 63–72, <https://doi.org/10.1111/j.1469-8137.2006.01797.x>, 2006.

1476 Likhoshway, Ye. V., Masyukova, Yu. A., Sherbakova, T. A., Petrova, D. P., and Grachev, M. A.: Detection of the gene
1477 responsible for silicic acid transport in chrysophycean algae, *Dokl. Biol. Sci.*, 408, 256–260,
1478 <https://doi.org/10.1134/S001249660603015X>, 2006.

1479 Litchman, E.: Trait-Based Diatom Ecology, in: *The Molecular Life of Diatoms*, edited by: Falciatore, A. and Mock, T.,
1480 Springer International Publishing, Cham, 3–27, https://doi.org/10.1007/978-3-030-92499-7_1, 2022.

1481 Livage, J.: Bioinspired nanostructured materials, *Comptes Rendus Chim.*, 21, 969–973,
1482 <https://doi.org/10.1016/j.crci.2018.08.001>, 2018.

1483 Llopis Monferrer, N., Boltovskoy, D., Tréguer, P., Sandin, M. M., Not, F., and Leynaert, A.: Estimating Biogenic Silica
1484 Production of Rhizaria in the Global Ocean, *Glob. Biogeochem. Cycles*, 34, <https://doi.org/10.1029/2019gb006286>, 2020.

1485 Llopis Monferrer, N., Romac, S., Laget, M., Nakamura, Y., Biard, T., and Sandin, M. M.: Is the Gelatinous Matrix of
1486 Nassellaria (Radiolaria) a Strategy for Coping With Oligotrophy?, *Environ. Microbiol.*, 27, e70098,
1487 <https://doi.org/10.1111/1462-2920.70098>, 2025.

1488 Lohman, K. E.: The ubiquitous diatom—a brief survey of the present state of knowledge, *Am. J. Sci.*, 258, 180–191, 1960.

1489 López-Acosta, M., Leynaert, A., and Maldonado, M.: Silicon consumption in two shallow-water sponges with contrasting
1490 biological features: Si consumption by sponges, *Limnol. Oceanogr.*, 61, 2139–2150, <https://doi.org/10.1002/lno.10359>, 2016.

1491 López-Acosta, M., Leynaert, A., Grall, J., and Maldonado, M.: Silicon consumption kinetics by marine sponges: An
1492 assessment of their role at the ecosystem level, *Limnol. Oceanogr.*, 63, 2508–2522, <https://doi.org/10.1002/lno.10956>, 2018.

1493 López-Acosta, M., Maldonado, M., Grall, J., Ehrhold, A., Sitjà, C., Galobart, C., Pérez, F. F., and Leynaert, A.: Sponge
1494 contribution to the silicon cycle of a diatom-rich shallow bay, *Limnol. Oceanogr.*, 67, 2431–2447,
1495 <https://doi.org/10.1002/Ino.12211>, 2022.

1496 Loucaides, S., Michalopoulos, P., Presti, M., Koning, E., Behrends, T., and Van Cappellen, P.: Seawater-mediated interactions
1497 between diatomaceous silica and terrigenous sediments: Results from long-term incubation experiments, *Chem. Geol.*, 270,
1498 68–79, <https://doi.org/10.1016/j.chemgeo.2009.11.006>, 2010.

1499 Łukowiak, M.: Fossil and modern sponge fauna of southern Australia and adjacent regions compared: interpretation,
1500 evolutionary and biogeographic significance of the late Eocene ‘soft’ sponges, *Contrib. Zool.*, 85, 13–35,
1501 <https://doi.org/10.1163/18759866-08501002>, 2016.

1502 Luo, M., Li, W., Geilert, S., Dale, A. W., Song, Z., and Chen, D.: Active Silica Diagenesis in the Deepest Hadal Trench
1503 Sediments, *Geophys. Res. Lett.*, 49, e2022GL099365, <https://doi.org/10.1029/2022GL099365>, 2022.

1504 Luo, M., Zheng, M., Wallmann, K., Dale, A. W., Strasser, M., Torres, M. E., Koelling, M., Riedinger, N., März, C., Rasbury,
1505 T., Bao, R., Itaki, T., Ikehara, K., Johnson, J. E., Bellanova, P., Nakamura, Y., Yu, M., Xie, J., and Chen, D.: Rapid burial and
1506 intense degradation of organic matter drive active silicate weathering in the subsurface sediments of the ocean’s deepest realm,
1507 *Geology*, 53, 636–641, <https://doi.org/10.1130/G53131.1>, 2025.

1508 Maavara, T., Dürr, H. H., and Van Cappellen, P.: Worldwide retention of nutrient silicon by river damming: From sparse data
1509 set to global estimate, *Glob. Biogeochem. Cycles*, 28, 842–855, <https://doi.org/10.1002/2014gb004875>, 2014.

1510 Mackenzie, F. T. and Garrels, R. M.: Chemical mass balance between rivers and oceans, *Am. J. Sci.*, 264, 507–525,
1511 <https://doi.org/10.2475/ajs.264.7.507>, 1966.

1512 Mackie, G. O. and Singla, C. L.: Studies on hexactinellid sponges. I. Histology of *Rhabdocalyptus dawsoni* (Lambe, 1873),
1513 *Philos. Trans. R. Soc. Lond. B Biol. Sci.*, 301, 365–400, <https://doi.org/10.1098/rstb.1983.0028>, 1997.

1514 Maddison, E. J., Pike, J., Leventer, A., Dunbar, R., Brachfeld, S., Domack, E. W., Manley, P., and McClellenn, C.: Post-glacial
1515 seasonal diatom record of the Mertz Glacier Polynya, East Antarctica, *Mar. Micropaleontol.*, 60, 66–88,
1516 <https://doi.org/10.1016/j.marmicro.2006.03.001>, 2006.

1517 Maldonado, M. and Abdul Wahab, M. A.: Phylum Porifera, in: *Atlas of Marine Invertebrate Larvae*, edited by: Boyle, M. J.,
1518 Young, C. M., and Sewell, M. A., Elsevier Science & Technology, Chantilly, 626, 2025.

1519 Maldonado, M. and Hendry, K. R.: Revisiting the silicon isotopic signal of sponge skeletons and its implications, *Limnol.*
1520 *Oceanogr.*, Ino.70138, <https://doi.org/10.1002/Ino.70138>, 2025.

1521 Maldonado, M. and Riesgo, A.: Reproduction in Porifera: a synoptic overview, *Treballs de la Societat Catalana de Biologia*,
1522 24–49 pp., 2008.

1523 Maldonado, M., Navarro, L., Grasa, A., Gonzalez, A., and Vaquerizo, I.: Silicon uptake by sponges: a twist to understanding
1524 nutrient cycling on continental margins, *Sci. Rep.*, 1, <https://doi.org/10.1038/srep00030>, 2011.

1525 Maldonado, M., Ribes, M., and Van Duyl, F. C.: Nutrient Fluxes Through Sponges: biology, budgets, and ecological
1526 implications, *Adv. Mar. Biol.*, 62, 113–182, <https://doi.org/10.1016/b978-0-12-394283-8.00003-5>, 2012.

1527 Maldonado, M., Aguilar, R., Bannister, R. J., Bell, J. J., Conway, K. W., Dayton, P. K., Díaz, C., Gutt, J., Kelly, M.,
1528 Kenchington, E. L. R., Leys, S. P., Pomponi, S. A., Rapp, H. T., Rützler, K., Tendal, O. S., Vacelet, J., and Young, C. M.:

1529 Sponge Grounds as Key Marine Habitats: A Synthetic Review of Types, Structure, Functional Roles, and Conservation
1530 Concerns, in: *Marine Animal Forests: The Ecology of Benthic Biodiversity Hotspots*, vol. 1, edited by: Rossi, S., Bramanti,
1531 L., Gori, A., and Orejas Saco del Valle, C., Springer International Publishing, Cham, 145–184, [https://doi.org/10.1007/978-3-](https://doi.org/10.1007/978-3-319-17001-5_24-1)
1532 319-17001-5_24-1, 2017.

1533 Maldonado, M., López-Acosta, M., Sitjà, C., García-Puig, M., Galobart, C., Ercilla, G., and Leynaert, A.: Sponge skeletons as
1534 an important sink of silicon in the global oceans, *Nat. Geosci.*, 12, 815–822, <https://doi.org/10.1038/s41561-019-0430-7>, 2019.

1535 Maldonado, M., López-Acosta, M., Beazley, L., Kenchington, E., Koutsouveli, V., and Riesgo, A.: Cooperation between
1536 passive and active silicon transporters clarifies the ecophysiology and evolution of biosilicification in sponges, *Sci. Adv.*, 6,
1537 eaba9322, <https://doi.org/10.1126/sciadv.aba9322>, 2020.

1538 Maldonado, M., Beazley, L., López-Acosta, M., Kenchington, E., Casault, B., Hanz, U., and Mienis, F.: Massive silicon
1539 utilization facilitated by a benthic-pelagic coupled feedback sustains deep-sea sponge aggregations, *Limnol. Oceanogr.*, 66,
1540 366–391, <https://doi.org/10.1002/lno.11610>, 2021.

1541 Maldonado, M., López-Acosta, M., Abalde, S., Martos, I., Ehrlich, H., and Leynaert, A.: On the dissolution of sponge silica:
1542 Assessing variability and biogeochemical implications, *Front. Mar. Sci.*, 9, <https://doi.org/10.3389/fmars.2022.1005068>, 2022.

1543 Malinverno, E.: Extant morphotypes of *Distephanus speculum* (Silicoflagellata) from the Australian sector of the Southern
1544 Ocean: Morphology, morphometry and biogeography, *Mar. Micropaleontol.*, 77, 154–174,
1545 <https://doi.org/10.1016/j.marmicro.2010.09.002>, 2010.

1546 Maliva, R. G., Knoll, A. H., and Siever, R.: Secular Change in Chert Distribution: A Reflection of Evolving Biological
1547 Participation in the Silica Cycle, *PALAIOS*, 4, 519, <https://doi.org/10.2307/3514743>, 1989.

1548 Maliva, R. G., Knoll, A. H., and Simonson, B. M.: Secular change in the Precambrian silica cycle: Insights from chert
1549 petrology, *Geol. Soc. Am. Bull.*, 117, 835–845, <https://doi.org/10.1130/b25555.1>, 2005.

1550 Maniscalco, M. A., Brzezinski, M. A., Lampe, R. H., Cohen, N. R., McNair, H. M., Ellis, K. A., Brown, M., Till, C. P.,
1551 Twining, B. S., Bruland, K. W., Marchetti, A., and Thametrakoln, K.: Diminished carbon and nitrate assimilation drive changes
1552 in diatom elemental stoichiometry independent of silicification in an iron-limited assemblage, *ISME Commun.*, 2, 57,
1553 <https://doi.org/10.1038/s43705-022-00136-1>, 2022.

1554 Mann, D. G. and Vanormelingen, P.: An Inordinate Fondness? The Number, Distributions, and Origins of Diatom Species, *J.*
1555 *Eukaryot. Microbiol.*, 60, 414–420, <https://doi.org/10.1111/jeu.12047>, 2013.

1556 Marron, A., Cassarino, L., Hatton, J., Curnow, P., and Hendry, K. R.: Technical note: The silicon isotopic composition of
1557 choanoflagellates: implications for a mechanistic understanding of isotopic fractionation during biosilicification,
1558 *Biogeosciences*, 16, 4805–4813, <https://doi.org/10.5194/bg-16-4805-2019>, 2019.

1559 Marron, A. O., Alston, M. J., Heavens, D., Akam, M., Caccamo, M., Holland, P. W. H., and Walker, G.: A family of diatom-
1560 like silicon transporters in the siliceous loricate choanoflagellates, *Proc. R. Soc. B Biol. Sci.*, 280, 20122543,
1561 <https://doi.org/10.1098/rspb.2012.2543>, 2013.

1562 Marron, A. O., Ratcliffe, S., Wheeler, G. L., Goldstein, R. E., King, N., Not, F., De Vargas, C., and Richter, D. J.: The Evolution
1563 of Silicon Transport in Eukaryotes, *Mol. Biol. Evol.*, 33, 3226–3248, <https://doi.org/10.1093/molbev/msw209>, 2016.

1564 Martin-Jézéquel, V., Hildebrand, M., and Brzezinski, M. A.: Silicon metabolism in diatoms: implications for growth, *J.*
1565 *Phycol.*, 36, 821–840, <https://doi.org/10.1046/j.1529-8817.2000.00019.x>, 2000.

1566 Massey, F. P., Ennos, A. R., and Hartley, S. E.: Silica in grasses as a defence against insect herbivores: contrasting effects on
1567 folivores and a phloem feeder, *J. Anim. Ecol.*, 75, 595–603, <https://doi.org/10.1111/j.1365-2656.2006.01082.x>, 2006.

1568 Mavromatis, V., Rinder, T., Prokushkin, A. S., Pokrovsky, O. S., Korets, M. A., Chmeleff, J., and Oelkers, E. H.: The effect
1569 of permafrost, vegetation, and lithology on Mg and Si isotope composition of the Yenisey River and its tributaries at the end
1570 of the spring flood, *Geochim. Cosmochim. Acta*, 191, 32–46, <https://doi.org/10.1016/j.gca.2016.07.003>, 2016.

1571 Mayzel, B., Aram, L., Varsano, N., Wolf, S. G., and Gal, A.: Structural evidence for extracellular silica formation by diatoms,
1572 *Nat. Commun.*, 12, <https://doi.org/10.1038/s41467-021-24944-6>, 2021.

1573 McCartney, K., Churchill, S., and Woestendiek, L.: Silicoflagellates and Ebridians from Leg 138, Eastern Equatorial Pacific,
1574 *Proc. Ocean Drill. Program*, <https://doi.org/10.2973/odp.proc.sr.138.108.1995>, 1995.

1575 McCartney, K., Witkowski, J., Jordan, R. W., Daugbjerg, N., Malinverno, E., Van Wezel, R., Kano, H., Abe, K., Scott, F.,
1576 Schweizer, M., Young, J. R., Hallegraeff, G. M., and Shiozawa, A.: Fine structure of silicoflagellate double skeletons, *Mar.*
1577 *Micropaleontol.*, 113, 10–19, <https://doi.org/10.1016/j.marmicro.2014.08.006>, 2014.

1578 McCartney, K., Witkowski, J., and Szaruga, A.: Palaeocene–early Eocene southern subtropical to subpolar silicoflagellate
1579 biostratigraphy, *Acta Geol. Pol.*, 68, 219–248, 2018.

1580 McCartney, K., Witkowski, J., Jordan, R. W., Abe, K., Januszkiewicz, A., Wróbel, R., Bąk, M., and Soeding, E.:
1581 Silicoflagellate evolution through the Cenozoic, *Mar. Micropaleontol.*, 172, 102108,
1582 <https://doi.org/10.1016/j.marmicro.2022.102108>, 2022.

1583 McCutchin, C. A., Edgar, K. J., Chen, C.-L., and Dove, P. M.: Silica–Biomacromolecule Interactions: Toward a Mechanistic
1584 Understanding of Silicification, *Biomacromolecules*, 26, 43–84, <https://doi.org/10.1021/acs.biomac.4c00674>, 2025.

1585 McGrath, E. C., Woods, L., Jompa, J., Haris, A., and Bell, J. J.: Growth and longevity in giant barrel sponges: Redwoods of
1586 the reef or Pines in the Indo-Pacific?, *Sci. Rep.*, 8, <https://doi.org/10.1038/s41598-018-33294-1>, 2018.

1587 McKenzie, L., Nordlund, L. M., Jones, B. L., Cullen-Unsworth, L. C., Roelfsema, C. M., and Unsworth, R.: The global
1588 distribution of seagrass meadows, *Environ. Res. Lett.*, 15, 074041, <https://doi.org/10.1088/1748-9326/ab7d06>, 2020.

1589 McManus, J., Hammond, D. E., Berelson, W. M., Kilgore, T. E., Demaster, D. J., Ragueneau, O. G., and Collier, R. W.: Early
1590 diagenesis of biogenic opal: Dissolution rates, kinetics, and paleoceanographic implications, *Deep Sea Res. Part II Top. Stud.*
1591 *Oceanogr.*, 42, 871–903, [https://doi.org/10.1016/0967-0645\(95\)00035-o](https://doi.org/10.1016/0967-0645(95)00035-o), 1995.

1592 McMurray, S. E., Blum, J. E., and Pawlik, J. R.: Redwood of the reef: growth and age of the giant barrel sponge *Xestospongia*
1593 *muta* in the Florida Keys, *Mar. Biol.*, 155, 159–171, <https://doi.org/10.1007/s00227-008-1014-z>, 2008.

1594 McNair, H. M., Brzezinski, M. A., and Krause, J. W.: Quantifying diatom silicification with the fluorescent dye, PDMPO,
1595 *Limnol. Oceanogr. Methods*, 13, 587–599, <https://doi.org/10.1002/lom3.10049>, 2015.

1596 McNair, H. M., Brzezinski, M. A., and Krause, J. W.: Diatom populations in an upwelling environment decrease silica content
1597 to avoid growth limitation, *Environ. Microbiol.*, 20, 4184–4193, <https://doi.org/10.1111/1462-2920.14431>, 2018.

1598 Meire, L., Meire, P., Struyf, E., Krawczyk, D. W., Arendt, K. E., Yde, J. C., Juul Pedersen, T., Hopwood, M. J., Rysgaard, S.,
1599 and Meysman, F. J. R.: High export of dissolved silica from the Greenland Ice Sheet, *Geophys. Res. Lett.*, 43, 9173–9182,
1600 <https://doi.org/10.1002/2016gl070191>, 2016.

1601 Meister, P., Alexandre, A., Bailey, H., Barker, P., Biskaborn, B. K., Broadman, E., Cartier, R., Chaplign, B., Couapel, M.,
1602 Dean, J. R., Diekmann, B., Harding, P., Henderson, A. C. G., Hernandez, A., Herzsuh, U., Kostrova, S. S., Lacey, J., Leng,
1603 M. J., Lücke, A., Mackay, A. W., Magyari, E. K., Narancic, B., Porchier, C., Rosqvist, G., Shemesh, A., Sonzogni, C., Swann,
1604 G. E. A., Sylvestre, F., and Meyer, H.: A global compilation of diatom silica oxygen isotope records from lake sediment –
1605 trends and implications for climate reconstruction, *Clim. Past*, 20, 363–392, <https://doi.org/10.5194/cp-20-363-2024>, 2024.

1606 Michalopoulos, P. and Aller, R. C.: Rapid Clay Mineral Formation in Amazon Delta Sediments: Reverse Weathering and
1607 Oceanic Elemental Cycles, *Science*, 270, 614–617, <https://doi.org/10.1126/science.270.5236.614>, 1995.

1608 Michalopoulos, P. and Aller, R. C.: Early diagenesis of biogenic silica in the Amazon delta: alteration, authigenic clay
1609 formation, and storage, *Geochim. Cosmochim. Acta*, 68, 1061–1085, <https://doi.org/10.1016/j.gca.2003.07.018>, 2004.

1610 Michalopoulos, P., Aller, R. C., and Reeder, R. J.: Conversion of diatoms to clays during early diagenesis in tropical,
1611 continental shelf muds, *Geology*, 28, 1095–1098, [https://doi.org/10.1130/0091-7613\(2000\)028%253C1095:codtcd%253E2.3.co;2](https://doi.org/10.1130/0091-7613(2000)028%253C1095:codtcd%253E2.3.co;2), 2000.

1613 Mirdita, M., Schütze, K., Moriwaki, Y., Heo, L., Ovchinnikov, S., and Steinegger, M.: ColabFold: making protein folding
1614 accessible to all, *Nat. Methods*, 19, 679–682, <https://doi.org/10.1038/s41592-022-01488-1>, 2022.

1615 Mitani-Ueno, N., Yamaji, N., Huang, S., Yoshioka, Y., Miyaji, T., and Ma, J. F.: A silicon transporter gene required for healthy
1616 growth of rice on land, *Nat. Commun.*, 14, 6522, <https://doi.org/10.1038/s41467-023-42180-y>, 2023.

1617 Moestrup, Ø. and Thomsen, H. A.: Dictyocha speculum (Silicoflagellata, Dictyochophyceae). Studies on armoured and
1618 unarmoured stages, *Biol. Skr. Det K. Dan. Vidensk. Selsk.*, 37, 1–57, 1990.

1619 Molina-Cruz, A.: Holocene palaeo-oceanography of the northern Iceland Sea, indicated by Radiolaria and sponge spicules, *J.*
1620 *Quat. Sci.*, 6, 303–312, <https://doi.org/10.1002/jqs.3390060405>, 1991.

1621 Morais, L., Fairchild, T. R., Lahr, D. J. G., Rudnitzki, I. D., Schopf, J. W., Garcia, A. K., Kudryavtsev, A. B., and Romero, G.
1622 R.: Carbonaceous and siliceous Neoproterozoic vase-shaped microfossils (Urucum Formation, Brazil) and the question of
1623 early protistan biomineralization, *J. Paleontol.*, 91, 393–406, <https://doi.org/10.1017/jpa.2017.16>, 2017.

1624 Morozov, A. A. and Galachyants, Y. P.: Diatom genes originating from red and green algae: Implications for the secondary
1625 endosymbiosis models, *Mar. Genomics*, 45, 72–78, <https://doi.org/10.1016/j.margen.2019.02.003>, 2019.

1626 Mouget, J.-L., Gastineau, R., Davidovich, O., Gaudin, P., and Davidovich, N. A.: Light is a key factor in triggering sexual
1627 reproduction in the pennate diatom *Haslea ostrearia*: Light induction of sexual reproduction in diatoms, *FEMS Microbiol.*
1628 *Ecol.*, 69, 194–201, <https://doi.org/10.1111/j.1574-6941.2009.00700.x>, 2009.

1629 Müller, W. E. G., Boreiko, A., Wang, X., Belikov, S. I., Wiens, M., Grebenjuk, V. A., Schloßmacher, U., and Schröder, H. C.:
1630 Silicateins, the major biosilica forming enzymes present in demosponges: Protein analysis and phylogenetic relationship, *Gene*,
1631 395, 62–71, <https://doi.org/10.1016/j.gene.2007.02.014>, 2007.

1632 Müller, W. E. G., Mugnaioli, E., Schröder, H. C., Schloßmacher, U., Giovine, M., Kolb, U., and Wang, X.: Hierarchical
1633 composition of the axial filament from spicules of the siliceous sponge *Suberites domuncula*: from biosilica-synthesizing
1634 nanofibrils to structure- and morphology-guiding triangular stems, *Cell Tissue Res.*, 351, 49–58,
1635 <https://doi.org/10.1007/s00441-012-1519-0>, 2013.

1636 Murray, D. and Schrader, H.: Distribution of silicoflagellates in plankton and core top samples from the Gulf of California,
1637 *Mar. Micropaleontol.*, 7, 517–539, [https://doi.org/10.1016/0377-8398\(83\)90013-0](https://doi.org/10.1016/0377-8398(83)90013-0), 1983.

1638 Naidoo-Bagwell, A. A., Monteiro, F. M., Hendry, K. R., Burgan, S., Wilson, J. D., Ward, B. A., Ridgwell, A., and Conley, D.
1639 J.: A diatom extension to the cGENIE Earth system model – EcoGENIE 1.1, *Geosci. Model Dev.*, 17, 1729–1748,
1640 <https://doi.org/10.5194/gmd-17-1729-2024>, 2024.

1641 Nakagawa Y., Endo Y., and Taki K.: Contributions of heterotrophic and autotrophic prey to the diet of euphausiid, *Euphausia*
1642 *pacifica* in the coastal waters off northeastern Japan, *Polar Biosci.*, 15, 52–65, <https://doi.org/10.15094/00006183>, 2002.

1643 Nakamura, Y., Tuji, A., Kimoto, K., Yamaguchi, A., Hori, R. S., and Suzuki, N.: Ecology, Morphology, Phylogeny and
1644 Taxonomic Revision of Giant Radiolarians, *Orodaria* ord. nov. (Radiolaria; Rhizaria; SAR), *Protist*, 172, 125808,
1645 <https://doi.org/10.1016/j.protis.2021.125808>, 2021.

1646 Nakov, T., Beaulieu, J. M., and Alverson, A. J.: Accelerated diversification is related to life history and locomotion in a
1647 hyperdiverse lineage of microbial eukaryotes (Diatoms, Bacillariophyta), *New Phytol.*, 219, 462–473,
1648 <https://doi.org/10.1111/nph.15137>, 2018.

1649 Nantke, C. K. M., Frings, P. J., Stadmark, J., Czymzik, M., and Conley, D. J.: Correction to: Si cycling in transition zones: a
1650 study of Si isotopes and biogenic silica accumulation in the Chesapeake Bay through the Holocene, *Biogeochemistry*, 146,
1651 171–171, <https://doi.org/10.1007/s10533-019-00618-w>, 2019.

1652 Naumova, E. Yu., Zaidykov, I. Yu., Tauson, V. L., and Likhoshway, Y. V.: Features of the Fine Structure and SI Content of
1653 the Mandibular Gnathobase of Four Freshwater Species of *Epischura* (Copepoda: Calanoida), *J. Crustac. Biol.*, 35, 741–746,
1654 <https://doi.org/10.1163/1937240X-00002385>, 2015.

1655 Nawaz, M. A., Azeem, F., Zakharenko, A. M., Lin, X., Atif, R. M., Baloch, F. S., Chan, T.-F., Chung, G., Ham, J., Sun, S.,
1656 and Golokhvast, K. S.: In-silico Exploration of Channel Type and Efflux Silicon Transporters and Silicification Proteins in 80
1657 Sequenced Viridiplantae Genomes, *Plants*, 9, 1612, <https://doi.org/10.3390/plants9111612>, 2020.

1658 Nelson, D. M. and Goering, J. J.: A stable isotope tracer method to measure silicic acid uptake by marine phytoplankton, *Anal.*
1659 *Biochem.*, 78, 139–147, [https://doi.org/10.1016/0003-2697\(77\)90017-3](https://doi.org/10.1016/0003-2697(77)90017-3), 1977.

1660 Nelson, D. M., Tréguer, P., Brzezinski, M. A., Leynaert, A., and Quéguiner, B.: Production and dissolution of biogenic silica
1661 in the ocean: Revised global estimates, comparison with regional data and relationship to biogenic sedimentation, *Glob.*
1662 *Biogeochem. Cycles*, 9, 359–372, <https://doi.org/10.1029/95gb01070>, 1995.

1663 Neuweiler, F., Larmagnat, S., Molson, J., and Fortin-Morin, F.: Sponge Spicules, Silicification, and Sequence Stratigraphy, *J.*
1664 *Sediment. Res.*, 84, 1107–1119, <https://doi.org/10.2110/jsr.2014.86>, 2014.

1665 Ng, H. C., Cassarino, L., Pickering, R. A., Woodward, E. M. S., Hammond, S. J., and Hendry, K. R.: Sediment efflux of silicon
1666 on the Greenland margin and implications for the marine silicon cycle, *Earth Planet. Sci. Lett.*, 529, 115877,
1667 <https://doi.org/10.1016/j.epsl.2019.115877>, 2020.

1668 Ng, H. C., Hawkings, J. R., Bertrand, S., Summers, B. A., Sieber, M., Conway, T. M., Freitas, F. S., Ward, J. P. J., Pryer, H.
1669 V., Wadham, J. L., Arndt, S., and Hendry, K. R.: Benthic Dissolved Silicon and Iron Cycling at Glaciated Patagonian Fjord
1670 Heads, *Glob. Biogeochem. Cycles*, 36, <https://doi.org/10.1029/2022gb007493>, 2022.

1671 Ng, H. C., Hendry, K. R., Ward, R., Woodward, E. M. S., Leng, M. J., Pickering, R. A., and Krause, J. W.: Detrital Input
1672 Sustains Diatom Production off a Glaciated Arctic Coast, *Geophys. Res. Lett.*, 51, e2024GL108324,
1673 <https://doi.org/10.1029/2024GL108324>, 2024.

1674 Nikolaev, S. I., Berney, C., Fahrni, J. F., Bolivar, I., Polet, S., Mylnikov, A. P., Aleshin, V. V., Petrov, N. B., and Pawlowski,
1675 J.: The twilight of Heliozoa and rise of Rhizaria, an emerging supergroup of amoeboid eukaryotes, *Proc. Natl. Acad. Sci.*, 101,
1676 8066–8071, <https://doi.org/10.1073/pnas.0308602101>, 2004.

1677 Ogane, K., Tuji, A., Suzuki, N., Kurihara, T., and Matsuoka, A.: First application of PDMPO to examine silicification in
1678 polycystine Radiolaria, *Plankton Benthos Res.*, 4, 89–94, <https://doi.org/10.3800/pbr.4.89>, 2009.

1679 Ohnemus, D. C., Rauschenberg, S., Krause, J. W., Brzezinski, M. A., Collier, J. L., Geraci-Yee, S., Baines, S. B., and Twining,
1680 B. S.: Silicon content of individual cells of *Synechococcus* from the North Atlantic Ocean, *Mar. Chem.*, 187, 16–24,
1681 <https://doi.org/10.1016/j.marchem.2016.10.003>, 2016.

1682 Oksman, M., Juggins, S., Miettinen, A., Witkowski, A., and Weckström, K.: The biogeography and ecology of common diatom
1683 species in the northern North Atlantic, and their implications for paleoceanographic reconstructions, *Mar. Micropaleontol.*,
1684 148, 1–28, <https://doi.org/10.1016/j.marmicro.2019.02.002>, 2019.

1685 Olofsson, M., Robertson, E. K., Edler, L., Arneborg, L., Whitehouse, M. J., and Ploug, H.: Nitrate and ammonium fluxes to
1686 diatoms and dinoflagellates at a single cell level in mixed field communities in the sea, *Sci. Rep.*, 9, 1424,
1687 <https://doi.org/10.1038/s41598-018-38059-4>, 2019.

1688 Onodera, J., Watanabe, E., Nishino, S., and Harada, N.: Distribution and vertical fluxes of silicoflagellates, ebridians, and the
1689 endoskeletal dinoflagellate *Actiniscus* in the western Arctic Ocean, *Polar Biol.*, 39, 327–341, [https://doi.org/10.1007/s00300-](https://doi.org/10.1007/s00300-015-1784-y)
1690 015-1784-y, 2016.

1691 Opfergelt, S., Gaspard, F., Hirst, C., Monin, L., Juhls, B., Morgenstern, A., Angelopoulos, M., and Overduin, P. P.: Frazil ice
1692 changes winter biogeochemical processes in the Lena River, *Commun. Earth Environ.*, 5, [https://doi.org/10.1038/s43247-024-](https://doi.org/10.1038/s43247-024-01884-9)
1693 01884-9, 2024.

1694 Otero-Ferrer, J. L., Cermeño, P., Bode, A., Fernández-Castro, B., Gasol, J. M., Morán, X. A. G., Marañón, E., Moreira-Coello,
1695 V., Varela, M. M., Villamaña, M., and Mouriño-Carballido, B.: Factors controlling the community structure of picoplankton
1696 in contrasting marine environments, *Biogeosciences*, 15, 6199–6220, <https://doi.org/10.5194/bg-15-6199-2018>, 2018.

1697 Ou, Q., Xu, H., Zhang, Z., Ma, J., and Pan, K.: Effects of ambient silicic acid concentration on the physiology of marine
1698 cyanobacterial *Synechococcus*, *Mar. Environ. Res.*, 209, 107220, <https://doi.org/10.1016/j.marenvres.2025.107220>, 2025.

1699 Painting, S. J., Lucas, M. I., Peterson, W. T., Brown, P. C., Hutchings, L., and Mitchell-Innes, B. A.: Dynamics of
1700 bacterioplankton, phytoplankton and mesozooplankton communities during the development of an upwelling plume in the
1701 southern Benguela, *Mar. Ecol. Prog. Ser.*, 100, 35–53, 1993.

1702 Pančić, M., Torres, R. R., Almeda, R., and Kiørboe, T.: Silicified cell walls as a defensive trait in diatoms, *Proc. R. Soc. B*
1703 *Biol. Sci.*, 286, 20190184, <https://doi.org/10.1098/rspb.2019.0184>, 2019.

1704 Passmore, A. J., Jarman, S. N., Swadling, K. M., Kawaguchi, S., McMinn, A., and Nicol, S.: DNA as a Dietary Biomarker in
1705 Antarctic Krill, *Euphausia superba*, *Mar. Biotechnol.*, 8, 686–696, <https://doi.org/10.1007/s10126-005-6088-8>, 2006.

1706 Pasternak, A. F. and Schnack-Schiel, S. B.: Seasonal feeding patterns of the dominant Antarctic copepods *Calanus propinquus*
1707 and *Calanoides acutus* in the Weddell Sea, *Polar Biol.*, 24, 771–784, <https://doi.org/10.1007/s003000100283>, 2001.

1708 Perry, E. C. and Lefticariu, L.: Formation and Geochemistry of Precambrian Cherts, in: *Treatise on Geochemistry*, Elsevier,
1709 1–21, <https://doi.org/10.1016/B0-08-043751-6/07138-3>, 2007.

1710 Petrucciani, A., Chaerle, P., and Norici, A.: Diatoms Versus Copepods: Could Frustule Traits Have a Role in Avoiding
1711 Predation?, *Front. Mar. Sci.*, 8, <https://doi.org/10.3389/fmars.2021.804960>, 2022a.

1712 Petrucciani, A., Knoll, A. H., and Norici, A.: Si decline and diatom evolution: Insights from physiological experiments, *Front.*
1713 *Mar. Sci.*, 9, 924452, <https://doi.org/10.3389/fmars.2022.924452>, 2022b.

1714 Petrucciani, A., Moretti, P., Ortore, M. G., and Norici, A.: Integrative effects of morphology, silicification, and light on diatom
1715 vertical movements, *Front. Plant Sci.*, 14, <https://doi.org/10.3389/fpls.2023.1143998>, 2023.

1716 Phoenix, V. R., Adams, D. G., and Konhauser, K. O.: Cyanobacterial viability during hydrothermal biomineralisation, *Chem.*
1717 *Geol.*, 169, 329–338, [https://doi.org/10.1016/S0009-2541\(00\)00212-6](https://doi.org/10.1016/S0009-2541(00)00212-6), 2000.

1718 Pike, J. and Kemp, A. E. S.: Early Holocene decadal-scale ocean variability recorded in Gulf of California laminated sediments,
1719 *Paleoceanography*, 12, 227–238, <https://doi.org/10.1029/96PA03132>, 1997.

1720 Pisera, A. and Sáez, A.: Paleoenvironmental significance of a new species of freshwater sponge from the Late Miocene
1721 Quillagua Formation (N Chile), *J. South Am. Earth Sci.*, 15, 847–852, [https://doi.org/10.1016/S0895-9811\(03\)00012-9](https://doi.org/10.1016/S0895-9811(03)00012-9), 2003.

1722 Pokrovsky, O. S., Reynolds, B. C., Prokushkin, A. S., Schott, J., and Viers, J.: Silicon isotope variations in Central Siberian
1723 rivers during basalt weathering in permafrost-dominated larch forests, *Chem. Geol.*, 355, 103–116,
1724 <https://doi.org/10.1016/j.chemgeo.2013.07.016>, 2013.

1725 Pondaven, P., Gallinari, M., Chollet, S., Bucciarelli, E., Sarthou, G., Schultes, S., and Jean, F.: Grazing-induced Changes in
1726 Cell Wall Silicification in a Marine Diatom, *Protist*, 158, 21–28, <https://doi.org/10.1016/j.protis.2006.09.002>, 2007.

1727 Porter, S. M. and Knoll, A. H.: Testate amoebae in the Neoproterozoic Era: evidence from vase-shaped microfossils in the
1728 Chuar Group, Grand Canyon, Paleobiology, 26, 360–385, [https://doi.org/10.1666/0094-8373\(2000\)026%253C0360:taitne%253E2.0.co;2](https://doi.org/10.1666/0094-8373(2000)026%253C0360:taitne%253E2.0.co;2), 2000.

1730 Presti, M. and Michalopoulos, P.: Estimating the contribution of the authigenic mineral component to the long-term reactive
1731 silica accumulation on the western shelf of the Mississippi River Delta, *Cont. Shelf Res.*, 28, 823–838,
1732 <https://doi.org/10.1016/j.csr.2007.12.015>, 2008.

1733 Preston, C. M., Durkin, C. A., and Yamahara, K. M.: DNA metabarcoding reveals organisms contributing to particulate matter
1734 flux to abyssal depths in the North East Pacific ocean, *Deep Sea Res. Part II Top. Stud. Oceanogr.*, 173, 104708,
1735 <https://doi.org/10.1016/j.dsr2.2019.104708>, 2020.

1736 Pryer, H. V., Hawkings, J. R., Wadham, J. L., Robinson, L. F., Hendry, K. R., Hatton, J. E., Kellerman, A. M., Bertrand, S.,
1737 Gill-Olivas, B., Marshall, M. G., Brooker, R. A., Daneri, G., and Häussermann, V.: The Influence of Glacial Cover on Riverine
1738 Silicon and Iron Exports in Chilean Patagonia, *Glob. Biogeochem. Cycles*, 34, <https://doi.org/10.1029/2020gb006611>, 2020.

1739 Ragueneau, O., Schultes, S., Bidle, K., Claquin, P., and Moriceau, B.: Si and C interactions in the world ocean: Importance of
1740 ecological processes and implications for the role of diatoms in the biological pump, *Glob. Biogeochem. Cycles*, 20,
1741 <https://doi.org/10.1029/2006GB002688>, 2006.

1742 Rahman, S., Aller, R. C., and Cochran, J. K.: The Missing Silica Sink: Revisiting the Marine Sedimentary Si Cycle Using
1743 Cosmogenic ³²Si, *Glob. Biogeochem. Cycles*, 31, 1559–1578, <https://doi.org/10.1002/2017gb005746>, 2017.

1744 Rahman, S., Tamborski, J. J., Charette, M. A., and Cochran, J. K.: Dissolved silica in the subterranean estuary and the impact
1745 of submarine groundwater discharge on the global marine silica budget, *Mar. Chem.*, 208, 29–42,
1746 <https://doi.org/10.1016/j.marchem.2018.11.006>, 2019.

1747 Ran, L., Wiesner, M. G., Liang, Y., Liang, W., Zhang, L., Yang, Z., Li, H., and Chen, J.: Differential dissolution of biogenic
1748 silica significantly affects the utility of sediment diatoms as paleoceanographic proxies, *Limnol. Oceanogr.*, 69, 467–481,
1749 <https://doi.org/10.1002/lno.12492>, 2024.

1750 Ran, X., Wu, W., Song, Z., Wang, H., Chen, H., Yao, Q., Xin, M., Liu, P., and Yu, Z.: Decadal change in dissolved silicate
1751 concentration and flux in the Changjiang (Yangtze) River, *Sci. Total Environ.*, 839, 156266,
1752 <https://doi.org/10.1016/j.scitotenv.2022.156266>, 2022.

1753 Ratcliffe, S., Meyer, E. M., Walker, C. E., Knight, M., McNair, H. M., Matson, P. G., Iglesias-Rodriguez, D., Brzezinski, M.,
1754 Langer, G., Sadekov, A., Greaves, M., Brownlee, C., Curnow, P., Taylor, A. R., and Wheeler, G. L.: Characterization of the
1755 molecular mechanisms of silicon uptake in coccolithophores, *Env. Microbiol.*, 25, 315–330, <https://doi.org/10.1111/1462-2920.16280>, 2023a.

1757 Ratcliffe, S., Meyer, E. M., Walker, C. E., Knight, M., McNair, H. M., Matson, P. G., Iglesias-Rodriguez, D., Brzezinski, M.,
1758 Langer, G., Sadekov, A., Greaves, M., Brownlee, C., Curnow, P., Taylor, A. R., and Wheeler, G. L.: Characterization of the
1759 molecular mechanisms of silicon uptake in coccolithophores, *Environ. Microbiol.*, 25, 315–330, <https://doi.org/10.1111/1462-2920.16280>, 2023b.

1761 Raven, J.: Blue carbon: past, present and future, with emphasis on macroalgae, *Biol. Lett.*, 14, 20180336,
1762 <https://doi.org/10.1098/rsbl.2018.0336>, 2018.

1763 Ray, N., Al-Haj, A., Maguire, T., Henning, M., and Fulweiler, R.: Coastal silicon cycling amplified by oyster aquaculture,
1764 *Mar. Ecol. Prog. Ser.*, 673, 29–41, <https://doi.org/10.3354/meps13803>, 2021.

1765 Riesgo, A., Maldonado, M., López-Legentil, S., and Giribet, G.: A Proposal for the Evolution of Cathepsin and Silicatein in
1766 Sponges, *J. Mol. Evol.*, 80, 278–291, <https://doi.org/10.1007/s00239-015-9682-z>, 2015.

1767 Rigual-Hernández, A. S., Trull, T. W., Bray, S. G., and Armand, L. K.: The fate of diatom valves in the Subantarctic and Polar
1768 Frontal Zones of the Southern Ocean: Sediment trap versus surface sediment assemblages, *Palaeogeogr. Palaeoclimatol.*
1769 *Palaeoecol.*, 457, 129–143, <https://doi.org/10.1016/j.palaeo.2016.06.004>, 2016.

1770 Rizos, I., Frada, M. J., Bittner, L., and Not, F.: Life cycle strategies in free-living unicellular eukaryotes: Diversity, evolution,
1771 and current molecular tools to unravel the private life of microorganisms, *J. Eukaryot. Microbiol.*, 71, e13052,
1772 <https://doi.org/10.1111/jeu.13052>, 2024.

1773 Robinson, R. S., Moore, T. C., Erhardt, A. M., and Scher, H. D.: Evidence for changes in subsurface circulation in the late
1774 Eocene equatorial Pacific from radiolarian-bound nitrogen isotope values, *Paleoceanography*, 30, 912–922,
1775 <https://doi.org/10.1002/2015PA002777>, 2015.

1776 Robinson, R. S., Jones, C. A., Kelly, R. P., Love, A., Closset, I., Rafter, P. A., and Brzezinski, M.: A Test of the Diatom-
1777 Bound Paleoproxy: Tracing the Isotopic Composition of Nutrient-Nitrogen Into Southern Ocean Particles and Sediments,
1778 *Glob. Biogeochem. Cycles*, 34, e2019GB006508, <https://doi.org/10.1029/2019GB006508>, 2020.

1779 Rohde, S. and Schupp, P. J.: Allocation of chemical and structural defenses in the sponge *Melophlus sarasinorum*, *J. Exp. Mar.*
1780 *Biol. Ecol.*, 399, 76–83, <https://doi.org/10.1016/j.jembe.2011.01.012>, 2011.

1781 Rong, B., Zhang, L., Liu, Z., Bai, W., Gu, W., Wei, X., Hou, W., and Ge, C.: Role of phytoliths in carbon stabilization of
1782 *Zostera marina* L. plants: One unreported mechanism of carbon sequestration in eelgrass beds, *Estuar. Coast. Shelf Sci.*, 301,
1783 108751, <https://doi.org/10.1016/j.ecss.2024.108751>, 2024.

1784 Roseby, Z. A., Smith, J. A., Hillenbrand, C.-D., Allen, C. S., Leventer, A., Hogan, K., Cartigny, M. J. B., Rosenheim, B. E.,
1785 Kuhn, G., and Larter, R. D.: History of Anvers-Hugo Trough, western Antarctic Peninsula shelf, since the Last Glacial
1786 Maximum. Part II: Palaeo-productivity and palaeoceanographic changes during the Last Glacial Transition, *Quat. Sci. Rev.*,
1787 294, 107503, <https://doi.org/10.1016/j.quascirev.2022.107503>, 2022.

1788 Roth, J., Gallinari, M., Schoelynck, J., Hernán, G., Máñez-Crespo, J., Ricart, A. M., and López-Acosta, M.: Chemical
1789 determination of silica in seagrass leaves reveals two operational silica pools in *Zostera marina*, *Biogeochemistry*, 168,
1790 <https://doi.org/10.1007/s10533-024-01189-1>, 2025.

1791 Round, F. E., Crawford, R. M., and Mann, D. G.: *Diatoms: Biology and Morphology of the Genera*, Cambridge University
1792 Press, 768 pp., 1990.

1793 Ryderheim, F., Grønning, J., and Kiørboe, T.: Thicker shells reduce copepod grazing on diatoms, *Limnol. Oceanogr. Lett.*, 7,
1794 435–442, <https://doi.org/10.1002/lol2.10243>, 2022.

1795 Sancetta, C.: Seasonal occurrence of silicoflagellate morphologies in different environments of the eastern Pacific Ocean, *Mar.*
1796 *Micropaleontol.*, 16, 285–291, [https://doi.org/10.1016/0377-8398\(90\)90007-9](https://doi.org/10.1016/0377-8398(90)90007-9), 1990.

1797 Santos, I. R., Chen, X., Lecher, A. L., Sawyer, A. H., Moosdorf, N., Rodellas, V., Tamborski, J., Cho, H.-M., Dimova, N.,
1798 Sugimoto, R., Bonaglia, S., Li, H., Hajati, M.-C., and Li, L.: Submarine groundwater discharge impacts on coastal nutrient
1799 biogeochemistry, *Nat. Rev. Earth Environ.*, 2, 307–323, <https://doi.org/10.1038/s43017-021-00152-0>, 2021.

1800 Schiller, J.: Die planktonischen Vegetationen des Adriatischen Meeres, *Arch Protistenkd*, 53, 59–123, 1925.

1801 Schneider-Mor, A., Yam, R., Bianchi, C., Kunz-Pirrung, M., Gersonde, R., and Shemesh, A.: Diatom stable isotopes, sea ice
1802 presence and sea surface temperature records of the past 640 ka in the Atlantic sector of the Southern Ocean, *Geophys. Res.*
1803 *Lett.*, 32, 2005GL022543, <https://doi.org/10.1029/2005GL022543>, 2005.

1804 Schoelynck, J. and Struyf, E.: Silicon in aquatic vegetation, *Funct. Ecol.*, 30, 1323–1330, <https://doi.org/10.1111/1365->
1805 2435.12614, 2016.

1806 Schoelynck, J., Bal, K., Puijalon, S., Meire, P., and Struyf, E.: Hydrodynamically mediated macrophyte silica dynamics, *Plant*
1807 *Biol.*, 14, 997–1005, <https://doi.org/10.1111/j.1438-8677.2012.00583.x>, 2012.

1808 Schröder, H. C., Brandt, D., Schloßmacher, U., Wang, X., Tahir, M. N., Tremel, W., Belikov, S. I., and Müller, W. E. G.:
1809 Enzymatic production of biosilica glass using enzymes from sponges: basic aspects and application in nanobiotechnology
1810 (material sciences and medicine), *Naturwissenschaften*, 94, 339–359, <https://doi.org/10.1007/s00114-006-0192-0>, 2007.

1811 Schröder, H.-C., Perović-Ottstadt, S., Rothenberger, M., Wiens, M., Schwertner, H., Batel, R., Korzhev, M., Müller, I. M., and
1812 Müller, W. E. G.: Silica transport in the demosponge *Suberites domuncula* : fluorescence emission analysis using the PDMPO
1813 probe and cloning of a potential transporter, *Biochem. J.*, 381, 665–673, <https://doi.org/10.1042/BJ20040463>, 2004.

1814 Sekiguchi, H., Moriya, M., Nakayama, T., and Inouye, I.: Vestigial Chloroplasts in Heterotrophic Stramenopiles *Pteridomonas*
1815 *danica* and *Ciliophrys infusionum* (Dictyochophyceae), *Protist*, 153, 157–167, <https://doi.org/10.1078/1434-4610-00094>,
1816 2002.

1817 Sheath, R. and Wehr, J.: Freshwater Algae of North America, Elsevier, <https://doi.org/10.1016/b978-0-12-741550-5.x5000-4>,
1818 2003.

1819 Shemesh, A., Rietti-Shati, M., Rioual, P., Battarbee, R., De Beaulieu, J., Reille, M., Andrieu, V., and Svobodova, H.: An
1820 oxygen isotope record of lacustrine opal from a European Maar indicates climatic stability during the Last Interglacial,
1821 Geophys. Res. Lett., 28, 2305–2308, <https://doi.org/10.1029/2000GL012720>, 2001.

1822 Shimizu, K., Cha, J., Stucky, G. D., and Morse, D. E.: Silicatein α : Cathepsin L-like protein in sponge biosilica, Proc. Natl.
1823 Acad. Sci., 95, 6234–6238, <https://doi.org/10.1073/pnas.95.11.6234>, 1998.

1824 Shimizu, K., Amo, Y. D., Brzezinski, M. A., Stucky, G. D., and Morse, D. E.: A novel fluorescent silica tracer for biological
1825 silicification studies, Chem. Biol., 8, 1051–1060, [https://doi.org/10.1016/S1074-5521\(01\)00072-2](https://doi.org/10.1016/S1074-5521(01)00072-2), 2001.

1826 Shimizu, K., Amano, T., Bari, Md. R., Weaver, J. C., Arima, J., and Mori, N.: Glassin, a histidine-rich protein from the siliceous
1827 skeletal system of the marine sponge *Euplectella*, directs silica polycondensation, Proc. Natl. Acad. Sci., 112, 11449–
1828 11454, <https://doi.org/10.1073/pnas.1506968112>, 2015.

1829 Shimizu, K., Nishi, M., Sakate, Y., Kawanami, H., Bito, T., Arima, J., Leria, L., and Maldonado, M.: Silica-associated proteins
1830 from hexactinellid sponges support an alternative evolutionary scenario for biomineralization in Porifera, Nat. Commun., 15,
1831 <https://doi.org/10.1038/s41467-023-44226-7>, 2024.

1832 Shrestha, R. P., Tesson, B., Norden-Krichmar, T., Federowicz, S., Hildebrand, M., and Allen, A. E.: Whole transcriptome
1833 analysis of the silicon response of the diatom *Thalassiosira pseudonana*, BMC Genomics, 13, <https://doi.org/10.1186/1471-2164-13-499>, 2012.

1835 Sieradzki, E. T., Ignacio-Espinoza, J. C., Needham, D. M., Fichot, E. B., and Fuhrman, J. A.: Dynamic marine viral infections
1836 and major contribution to photosynthetic processes shown by spatiotemporal picoplankton metatranscriptomes, Nat.
1837 Commun., 10, 1169, <https://doi.org/10.1038/s41467-019-09106-z>, 2019.

1838 Siever, R.: Silica in the oceans: biological-geochemical interplay, in: Scientists on Gaia, edited by: S. H., S. and P. J., B., MIT
1839 Press, Cambridge, 287–295, 1991.

1840 Siever, R.: The silica cycle in the Precambrian, Geochim. Cosmochim. Acta, 56, 3265–3272, [https://doi.org/10.1016/0016-7037\(92\)90303-z](https://doi.org/10.1016/0016-7037(92)90303-z), 1992.

1842 Silva, P. C.: Algae. A Taxonomic Survey. Fasc. 1, Phycologia, 21, 192–194, <https://doi.org/10.2216/i0031-8884-21-2-192.1>,
1843 1982.

1844 Sim-Smith, C., Ellwood, M., and Kelly, M.: Sponges as Proxies for Past Climate Change Events, in: Climate Change, Ocean
1845 Acidification and Sponges: Impacts Across Multiple Levels of Organization, edited by: Carballo, J. L. and Bell, J. J., Springer
1846 International Publishing, Cham, 49–78, https://doi.org/10.1007/978-3-319-59008-0_3, 2017.

1847 Sperling, E. A., Robinson, J. M., Pisani, D., and Peterson, K. J.: Where’s the glass? Biomarkers, molecular clocks, and
1848 microRNAs suggest a 200-Myr missing Precambrian fossil record of siliceous sponge spicules, Geobiology, 8, 24–36,
1849 <https://doi.org/10.1111/j.1472-4669.2009.00225.x>, 2010.

1850 Struyf, E. and Conley, D. J.: Emerging understanding of the ecosystem silica filter, Biogeochemistry, 107, 9–18,
1851 <https://doi.org/10.1007/s10533-011-9590-2>, 2012.

1852 Struyf, E., Smis, A., Van Damme, S., Meire, P., and Conley, D. J.: The Global Biogeochemical Silicon Cycle, *Silicon*, 1, 207–
1853 213, <https://doi.org/10.1007/s12633-010-9035-x>, 2009.

1854 Strydom, S., McCallum, R., Lafratta, A., Webster, C. L., O’Dea, C. M., Said, N. E., Dunham, N., Inostroza, K., Salinas, C.,
1855 Billingham, S., Phelps, C. M., Campbell, C., Gorham, C., Bernasconi, R., Frouws, A. M., Werner, A., Vitelli, F., Puigcorb ,
1856 V., D’Cruz, A., McMahon, K. M., Robinson, J., Huggett, M. J., McNamara, S., Hyndes, G. A., and Serrano, O.: Global dataset
1857 on seagrass meadow structure, biomass and production, *Earth Syst. Sci. Data*, 15, 511–519, [https://doi.org/10.5194/essd-15-](https://doi.org/10.5194/essd-15-511-2023)
1858 511-2023, 2023.

1859 Stukel, M. R., Biard, T., Krause, J., and Ohman, M. D.: Large Phaeodaria in the twilight zone: Their role in the carbon cycle,
1860 *Limnol. Oceanogr.*, 63, 2579–2594, <https://doi.org/10.1002/lno.10961>, 2018.

1861 Su, Y., Lundholm, N., and Ellegaard, M.: The effect of different light regimes on diatom frustule silicon concentration, *Algal*
1862 *Res.*, 29, 36–40, <https://doi.org/10.1016/j.algal.2017.11.014>, 2018.

1863 Sun, X., M rth, C.-M., Porcelli, D., Kutscher, L., Hirst, C., Murphy, M. J., Maximov, T., Petrov, R. E., Humborg, C., Schmitt,
1864 M., and Andersson, P. S.: Stable silicon isotopic compositions of the Lena River and its tributaries: Implications for silicon
1865 delivery to the Arctic Ocean, *Geochim. Cosmochim. Acta*, 241, 120–133, <https://doi.org/10.1016/j.gca.2018.08.044>, 2018.

1866 Sutton, J. N., Varela, D. E., Brzezinski, M. A., and Beucher, C.: Species-dependent silicon isotope fractionation in unialgal
1867 cultures of marine diatoms, AGU Fall Meeting Abstracts, ADS Bibcode: 2011AGUFMPP51B1831S, PP51B-1831, 2011.

1868 Sutton, J. N., Varela, D. E., Brzezinski, M. A., and Beucher, C. P.: Species-dependent silicon isotope fractionation by marine
1869 diatoms, *Geochim. Cosmochim. Acta*, 104, 300–309, <https://doi.org/10.1016/j.gca.2012.10.057>, 2013.

1870 Suzuki, N. and Not, F.: Biology and Ecology of Radiolaria, in: *Marine Protists: Diversity and Dynamics*, edited by: Ohtsuka,
1871 S., Suzaki, T., Horiguchi, T., Suzuki, N., and Not, F., Springer Japan, Tokyo, 179–222, [https://doi.org/10.1007/978-4-431-](https://doi.org/10.1007/978-4-431-55130-0_8)
1872 55130-0_8, 2015.

1873 Swann, G. E. A., Leng, M. J., Juschus, O., Melles, M., Brigham-Grette, J., and Sloane, H. J.: A combined oxygen and silicon
1874 diatom isotope record of Late Quaternary change in Lake El’gygytyn, North East Siberia, *Quat. Sci. Rev.*, 29, 774–786,
1875 <https://doi.org/10.1016/j.quascirev.2009.11.024>, 2010.

1876 Taguchi, S. and Laws, E. A.: Application of a single-cell isolation technique to studies of carbon assimilation by the subtropical
1877 silicoflagellate *Dictyocha perlae vis*, *Mar. Ecol. Prog. Ser.*, 23, 251–255, 1985a.

1878 Taguchi, S. and Laws, E. A.: Application of a single-cell isolation technique to studies of carbon assimilation by the subtropical
1879 silicoflagellate *Dictyocha perlaevis*, *Mar. Ecol. Prog. Ser.*, 23, 251–255, 1985b.

1880 Takahashi, K.: Radiolaria: Sinking population, standing stock, and production rate, *Mar. Micropaleontol.*, 8, 171–181,
1881 [https://doi.org/10.1016/0377-8398\(83\)90022-1](https://doi.org/10.1016/0377-8398(83)90022-1), 1983.

1882 Takahashi, K.: Silicoflagellates as productivity indicators: Evidence from long temporal and spatial flux variability responding
1883 to hydrography in the northeastern Pacific, *Glob. Biogeochem. Cycles*, 3, 43–61, <https://doi.org/10.1029/gb003i001p00043>,
1884 1989.

1885 Takahashi, K., Onodera, J., and Katsuki, K.: Significant populations of seven-sided *Distephanus* (Silicoflagellata) in the sea-
1886 ice covered environment of the central Arctic Ocean, summer 2004, *Micropaleontology*, 55, 313–325, 2009.

1887 Tesson, B., Lerch, S. J. L., and Hildebrand, M.: Characterization of a New Protein Family Associated With the Silica
1888 Deposition Vesicle Membrane Enables Genetic Manipulation of Diatom Silica, *Sci. Rep.*, 7, [https://doi.org/10.1038/s41598-](https://doi.org/10.1038/s41598-017-13613-8)
1889 017-13613-8, 2017.

1890 Thamatrakoln, K. and Hildebrand, M.: Silicon Uptake in Diatoms Revisited: A Model for Saturable and Nonsaturable Uptake
1891 Kinetics and the Role of Silicon Transporters, *Plant Physiol.*, 146, 1397–1407, <https://doi.org/10.1104/pp.107.107094>, 2008.

1892 Thamatrakoln, K., Alverson, A. J., and Hildebrand, M.: Comparative sequence analysis of diatom silicon transporters: toward
1893 a mechanistic model of silicon transport, *J. Phycol.*, 42, 822–834, <https://doi.org/10.1111/j.1529-8817.2006.00233.x>, 2006.

1894 de Tombeur, F., Turner, B. L., Laliberté, E., Lambers, H., Mahy, G., Faucon, M.-P., Zemunik, G., and Cornelis, J.-T.: Plants
1895 sustain the terrestrial silicon cycle during ecosystem retrogression, *Science*, 369, 1245–1248,
1896 <https://doi.org/10.1126/science.abc0393>, 2020.

1897 de Tombeur, F., Péliissier, R., Shihaan, A., Rahajaharilaza, K., Fort, F., Mahaut, L., Lemoine, T., Thorne, S. J., Hartley, S. E.,
1898 Luquet, D., Fabre, D., Lambers, H., Morel, J.-B., Ballini, E., and Violle, C.: Growth–defence trade-off in rice: fast-growing
1899 and acquisitive genotypes have lower expression of genes involved in immunity, *J. Exp. Bot.*, 74, 3094–3103,
1900 <https://doi.org/10.1093/jxb/erad071>, 2023a.

1901 de Tombeur, F., Raven, J. A., Toussaint, A., Lambers, H., Cooke, J., Hartley, S. E., Johnson, S. N., Coq, S., Katz, O., Schaller,
1902 J., and Violle, C.: Why do plants silicify?, *Trends Ecol. Evol.*, 38, 275–288, <https://doi.org/10.1016/j.tree.2022.11.002>, 2023b.

1903 de Tombeur, F., Plouzeau, L., Shaw, J., Hodson, M. J., Ranathunge, K., Kotula, J., Hayes, P. E., Tremblay, M., Coq, S., Stein,
1904 M., Nakamura, R., Wright, I. J., Lambers, H., Violle, C., and Clode, P. L.: Anatomical and Trait Analyses Reveal a Silicon-
1905 Carbon Trade-Off in the Epidermis of Sedges, *Plant Cell Environ.*, 48, 2396–2410, <https://doi.org/10.1111/pce.15307>, 2025.

1906 Torricella, F., Melis, R., Malinverno, E., Fontolan, G., Bussi, M., Capotondi, L., Del Carlo, P., Di Roberto, A., Geniram, A.,
1907 Kuhn, G., Khim, B.-K., Morigi, C., Scateni, B., and Colizza, E.: Environmental and Oceanographic Conditions at the
1908 Continental Margin of the Central Basin, Northwestern Ross Sea (Antarctica) Since the Last Glacial Maximum, *Geosciences*,
1909 11, 155, <https://doi.org/10.3390/geosciences11040155>, 2021.

1910 Torricella, F., Gamboa Sojo, V. M., Gariboldi, K., Douss, N., Musco, M. E., Caricchi, C., Lucchi, R. G., Carbonara, K., and
1911 Morigi, C.: Multiproxy investigation of the last 2,000 years BP marine paleoenvironmental record along the western
1912 Spitsbergen margin, *Arct. Antarct. Alp. Res.*, 54, 562–583, <https://doi.org/10.1080/15230430.2022.2123859>, 2022.

1913 Torricella, F., Morigi, C., Gamboa-Sojo, V., Carbonara, K., Bronzo, L., and Lucchi, R. G.: Paleooceanographic changes along
1914 the western Spitsbergen margin, evidence from planktic microfossil during the last 10 kyr BP, *Palaeogeogr. Palaeoclimatol.*
1915 *Palaeoecol.*, 670, 112940, <https://doi.org/10.1016/j.palaeo.2025.112940>, 2025.

1916 Tréguer, P., Nelson, D. M., Van Bennekom, A. J., DeMaster, D. J., Leynaert, A., and Quéguiner, B.: The Silica Balance in the
1917 World Ocean: A Reestimate, *Science*, 268, 375–379, <https://doi.org/10.1126/science.268.5209.375>, 1995.

1918 Tréguer, P., Bowler, C., Moriceau, B., Dutkiewicz, S., Gehlen, M., Aumont, O., Bittner, L., Dugdale, R., Finkel, Z., Iudicone,
1919 D., Jahn, O., Guidi, L., Lasbleiz, M., Leblanc, K., Levy, M., and Pondaven, P.: Influence of diatom diversity on the ocean
1920 biological carbon pump, *Nat. Geosci.*, 11, 27–37, <https://doi.org/10.1038/s41561-017-0028-x>, 2018.

1921 Tréguer, P. J.: The Southern Ocean silica cycle, *Comptes Rendus Géoscience*, 346, 279–286,
1922 <https://doi.org/10.1016/j.crte.2014.07.003>, 2014.

- 1923 Tréguer, P. J. and De La Rocha, C. L.: The World Ocean Silica Cycle, *Annu. Rev. Mar. Sci.*, 5, 477–501,
1924 <https://doi.org/10.1146/annurev-marine-121211-172346>, 2013.
- 1925 Tréguer, P. J., Sutton, J. N., Brzezinski, M., Charette, M. A., Devries, T., Dutkiewicz, S., Ehlert, C., Hawkings, J., Leynaert,
1926 A., Liu, S. M., Llopi Monferrer, N., López-Acosta, M., Maldonado, M., Rahman, S., Ran, L., and Rouxel, O.: Reviews and
1927 syntheses: The biogeochemical cycle of silicon in the modern ocean, *Biogeosciences*, 18, 1269–1289,
1928 <https://doi.org/10.5194/bg-18-1269-2021>, 2021.
- 1929 Trower, E. J., Strauss, J. V., Sperling, E. A., and Fischer, W. W.: Isotopic analyses of Ordovician–Silurian siliceous skeletons
1930 indicate silica-depleted Paleozoic oceans, *Geobiology*, 19, 460–472, <https://doi.org/10.1111/gbi.12449>, 2021.
- 1931 Van Cappellen, P. and Qiu, L.: Biogenic silica dissolution in sediments of the Southern Ocean. I. Solubility, *Deep Sea Res.*
1932 Part II Top. *Stud. Oceanogr.*, 44, 1109–1128, [https://doi.org/10.1016/s0967-0645\(96\)00113-0](https://doi.org/10.1016/s0967-0645(96)00113-0), 1997.
- 1933 Van Cappellen, P., Dixit, S., and Van Beusekom, J.: Biogenic silica dissolution in the oceans: Reconciling experimental and
1934 field-based dissolution rates, *Glob. Biogeochem. Cycles*, 16, <https://doi.org/10.1029/2001gb001431>, 2002.
- 1935 Van Soest, R. W. M., Boury-Esnault, N., Vacelet, J., Dohrmann, M., Erpenbeck, D., De Voogd, N. J., Santodomingo, N.,
1936 Vanhoorne, B., Kelly, M., and Hooper, J. N. A.: Global Diversity of Sponges (Porifera), *PLoS ONE*, 7, e35105,
1937 <https://doi.org/10.1371/journal.pone.0035105>, 2012.
- 1938 Van Valkenburg, S. D. and Norris, R. E.: The Growth and Morphology of the Silicoflagellate *Dictyocha Fibula* Ehrenberg in
1939 Culture, *J. Phycol.*, 6, 48–54, <https://doi.org/10.1111/j.1529-8817.1970.tb02356.x>, 1970.
- 1940 Varela, D. E., Pride, C. J., and Brzezinski, M. A.: Biological fractionation of silicon isotopes in Southern Ocean surface waters,
1941 *Glob. Biogeochem. Cycles*, 18, <https://doi.org/10.1029/2003GB002140>, 2004.
- 1942 Vaultot, D., Eikrem, W., Viprey, M., and Moreau, H.: The diversity of small eukaryotic phytoplankton ($\leq 3 \mu\text{m}$) in marine
1943 ecosystems, *FEMS Microbiol. Rev.*, 32, 795–820, <https://doi.org/10.1111/j.1574-6976.2008.00121.x>, 2008.
- 1944 Visintini, N., Martiny, A. C., and Flombaum, P.: *Prochlorococcus*, *Synechococcus*, and picoeukaryotic phytoplankton
1945 abundances in the global ocean, *Limnol. Oceanogr. Lett.*, 6, 207–215, <https://doi.org/10.1002/lol2.10188>, 2021.
- 1946 Vonk, J. A., Smulders, F. O. H., Christianen, M. J. A., and Govers, L. L.: Seagrass leaf element content: A global overview,
1947 *Mar. Pollut. Bull.*, 134, 123–133, <https://doi.org/10.1016/j.marpolbul.2017.09.066>, 2018.
- 1948 de Voogd, N., Alvarez, B., Boury-Esnault, N., Cárdenas, P., Díaz, M.-C., Dohrmann, M., Downey, R., Goodwin, C., Hajdu,
1949 E., Hooper, J., Kelly, M., Klautau, M., Lim, S.-C., Manconi, R., Morrow, C., Pinheiro, U., Pisera, A., Ríos, P., Rützler, K.,
1950 Schönberg, C., Turner, T., Vacelet, J., van Soest, R., and Xavier, J.: World Porifera Database. Accessed at
1951 <https://www.marinespecies.org/porifera> on yyyy-mm-dd, <https://doi.org/10.14284/359>, 2025.
- 1952 Vrieling, E. G., Sun, Q., Tian, M., Kooyman, P. J., Gieskes, W. W. C., Van Santen, R. A., and Sommerdijk, N. A. J. M.:
1953 Salinity-dependent diatom biosilicification implies an important role of external ionic strength, *Proc. Natl. Acad. Sci.*, 104,
1954 10441–10446, <https://doi.org/10.1073/pnas.0608980104>, 2007.
- 1955 Wallmann, K., Geilert, S., and Scholz, F.: Chemical Alteration of Riverine Particles in Seawater and Marine Sediments: Effects
1956 on Seawater Composition and Atmospheric CO₂, *Am. J. Sci.*, 323, <https://doi.org/10.2475/001c.87455>, 2023.
- 1957 Wang, Q. and Danilov, S.: A Synthesis of the Upper Arctic Ocean Circulation During 2000–2019: Understanding the Roles
1958 of Wind Forcing and Sea Ice Decline, *Front. Mar. Sci.*, 9, <https://doi.org/10.3389/fmars.2022.863204>, 2022.

- 1959 Wang, X., Schloßmacher, U., Wiens, M., Batel, R., Schröder, H. C., and Müller, W. E. G.: Silicateins, silicatein interactors
1960 and cellular interplay in sponge skeletogenesis: formation of glass fiber-like spicules, *FEBS J.*, 279, 1721–1736,
1961 <https://doi.org/10.1111/j.1742-4658.2012.08533.x>, 2012.
- 1962 Ward, J. P. J., Hendry, K. R., Arndt, S., Faust, J. C., Freitas, F. S., Henley, S. F., Krause, J. W., März, C., Tessin, A. C., and
1963 Airs, R. L.: Benthic silicon cycling in the Arctic Barents Sea: a reaction–transport model study, *Biogeosciences*, 19, 3445–
1964 3467, <https://doi.org/10.5194/bg-19-3445-2022>, 2022.
- 1965 Wei, Y., Qu, K., Cui, Z., and Sun, J.: Picocyanobacteria–A non-negligible group for the export of biomineral silica to ocean
1966 depth, *J. Environ. Manage.*, 342, 118313, <https://doi.org/10.1016/j.jenvman.2023.118313>, 2023.
- 1967 Wenzl, S., Hett, R., Richthammer, P., and Sumper, M.: Silacidins: Highly Acidic Phosphopeptides from Diatom Shells Assist
1968 in Silica Precipitation In Vitro, *Angew. Chem. Int. Ed.*, 47, 1729–1732, <https://doi.org/10.1002/anie.200704994>, 2008.
- 1969 Wetzel, F., de Souza, G. F., and Reynolds, B. C.: What controls silicon isotope fractionation during dissolution of diatom
1970 opal?, *Geochim. Cosmochim. Acta*, 131, 128–137, <https://doi.org/10.1016/j.gca.2014.01.028>, 2014.
- 1971 Wild, B., Gerrits, R., and Bonneville, S.: The contribution of living organisms to rock weathering in the critical zone, *Npj*
1972 *Mater. Degrad.*, 6, <https://doi.org/10.1038/s41529-022-00312-7>, 2022.
- 1973 Wille, M., Sutton, J., Ellwood, M. J., Sambridge, M., Maher, W., Eggins, S., and Kelly, M.: Silicon isotopic fractionation in
1974 marine sponges: A new model for understanding silicon isotopic variations in sponges, *Earth Planet. Sci. Lett.*, 292, 281–289,
1975 <https://doi.org/10.1016/j.epsl.2010.01.036>, 2010.
- 1976 Williams, O. L., Kurtz, A. C., Eagle, M. J., Kroeger, K. D., Tamborski, J. J., and Carey, J. C.: Mechanisms and magnitude of
1977 dissolved silica release from a New England salt marsh, *Biogeochemistry*, 161, 251–271, <https://doi.org/10.1007/s10533-022-00976-y>, 2022.
- 1979 Wörheide, G., Dohrmann, M., Erpenbeck, D., Larroux, C., Maldonado, M., Voigt, O., Borchellini, C., and Lavrov, D. V.:
1980 Deep Phylogeny and Evolution of Sponges (Phylum Porifera), *Adv. Mar. Biol.*, 1–78, <https://doi.org/10.1016/B978-0-12-387787-1.00007-6>, 2012.
- 1982 Wu, X., Yang, S., Wallmann, K., Scholz, F., Dou, Y., Guo, J., and Xu, X.: Strong potassium uptake in surface sediments of
1983 the Changjiang River Estuary and the East China Sea: Implications for authigenic processes and the marine potassium budget,
1984 *Earth Planet. Sci. Lett.*, 657, 119292, <https://doi.org/10.1016/j.epsl.2025.119292>, 2025.
- 1985 Xu, H., Shi, Z., Zhang, X., Pang, M., Pan, K., and Liu, H.: Diatom frustules with different silica contents affect copepod
1986 grazing due to differences in the nanoscale mechanical properties, *Limnol. Oceanogr.*, 66, 3408–3420,
1987 <https://doi.org/10.1002/lno.11887>, 2021.
- 1988 Yacano, M. R., Foster, S. Q., Ray, N. E., Oczkowski, A., Raven, J. A., and Fulweiler, R. W.: Marine macroalgae are an
1989 overlooked sink of silicon in coastal systems, *New Phytol.*, 233, 2330–2336, <https://doi.org/10.1111/nph.17889>, 2021.
- 1990 Yager, J. A., West, A. J., Trower, E. J., Fischer, W. W., Ritterbush, K., Rosas, S., Bottjer, D. J., Celestian, A. J., Berelson, W.
1991 M., and Corsetti, F. A.: Evidence for Low Dissolved Silica in mid-Mesozoic Oceans, *Am. J. Sci.*, 325,
1992 <https://doi.org/10.2475/001c.122691>, 2025.
- 1993 Yamada, K., Yoshikawa, S., Ichinomiya, M., Kuwata, A., Kamiya, M., and Ohki, K.: Effects of Silicon-Limitation on Growth
1994 and Morphology of *Triparma laevis* NIES-2565 (Parnales, Heterokontophyta), *PLOS ONE*, 9, e103289,
1995 <https://doi.org/10.1371/journal.pone.0103289>, 2014.

1996 Zexer, N., Kumar, S., and Elbaum, R.: Silica deposition in plants: scaffolding the mineralization, *Ann. Bot.*, 131, 897–908,
1997 <https://doi.org/10.1093/aob/mcad056>, 2023.

1998 Zhang, L., Wang, R., Chen, M., Liu, J., Zeng, L., Xiang, R., and Zhang, Q.: Biogenic silica in surface sediments of the South
1999 China Sea: Controlling factors and paleoenvironmental implications, *Deep Sea Res. Part II Top. Stud. Oceanogr.*, 122, 142–
2000 152, <https://doi.org/10.1016/j.dsr2.2015.11.008>, 2015.

2001 Zhang, L., Suzuki, N., Nakamura, Y., and Tuji, A.: Modern shallow water radiolarians with photosynthetic microbiota in the
2002 western North Pacific, *Mar. Micropaleontol.*, 139, 1–27, <https://doi.org/10.1016/j.marmicro.2017.10.007>, 2018.

2003 Zhang, Z., Cao, Z., Grasse, P., Dai, M., Gao, L., Kuhnert, H., Gledhill, M., Chiessi, C. M., Doering, K., and Frank, M.:
2004 Dissolved silicon isotope dynamics in large river estuaries, *Geochim. Cosmochim. Acta*, 273, 367–382,
2005 <https://doi.org/10.1016/j.gca.2020.01.028>, 2020a.

2006 Zhang, Z., Sun, X., Dai, M., Cao, Z., Fontorbe, G., and Conley, D. J.: Impact of human disturbance on the biogeochemical
2007 silicon cycle in a coastal sea revealed by silicon isotopes, *Limnol. Oceanogr.*, 65, 515–528, <https://doi.org/10.1002/lno.11320>,
2008 2020b.

2009 Zhu, D., Liu, S. M., Leynaert, A., Tréguer, P., Ren, J., Schoelynck, J., Ma, Y., and Sutton, J. N.: Muddy sediments are an
2010 important potential source of silicon in coastal and continental margin zones, *Mar. Chem.*, 258, 104350,
2011 <https://doi.org/10.1016/j.marchem.2024.104350>, 2024.

2012 Zhu, T., Zhao, S., Xu, B., Liu, D., Cardenas, M. B., Yu, H., Zhang, Y., Chen, X., Xiao, K., Yi, L., Cho, H.-M., Liu, S., Zhang,
2013 Z., Lian, E., Burnett, W. C., Chen, G., Yu, Z., and Santos, I. R.: Large scale submarine groundwater discharge dominates
2014 nutrient inputs to China’s coast, *Nat. Commun.*, 16, 2932, <https://doi.org/10.1038/s41467-025-58103-y>, 2025.

2015 Ziegler, K., Chadwick, O. A., Brzezinski, M. A., and Kelly, E. F.: Natural variations of $\delta^{30}\text{Si}$ ratios during progressive basalt
2016 weathering, Hawaiian Islands, *Geochim. Cosmochim. Acta*, 69, 4597–4610, <https://doi.org/10.1016/j.gca.2005.05.008>, 2005.

2017

2018 **Author contributions.** All authors collaborated on the conception and writing of this manuscript. Author order was determined
2019 randomly using a Python script to reflect the equal contribution of all authors to the work. Hence, neither the order of authors
2020 nor the role of corresponding authors is a reflection of their contribution to the work.

2021

2022 **Acknowledgements.** The authors would like to thank the SILICAMICS (Biogeochemistry and Genomics of Silicification and
2023 Silicifiers) and IBIS (Isotopes in Biogenic Silica) communities for fostering such welcoming, open, and intellectually engaging
2024 environments during their 2024 conferences. The vibrant exchange of ideas and collaborative spirit at these events were
2025 instrumental in inspiring and shaping the conception of this manuscript.

2026

2027 **Financial support.** Félix de Tombeur received funding from the European Union’s Horizon 2020 research and innovation
2028 programme under the Marie Skłodowska-Curie grant agreement No. 101021641 (project SiliConomic). Alessandra Petrucciani
2029 received funding from the European Union’s Horizon research and innovation actions programme under grant agreement No.
2030 101083355 (project DESIRED). Natasha Bryan received funding from the Helmholtz Association through INSPIRES Project

2031 ‘Polar-Flow’ (2025). María López-Acosta received funding by a postdoctoral fellowship and project funded by the ‘Xunta de
2032 Galicia’ (IN606C-2023/001). Antonia U. Thielecke received funding from the Helmholtz Association through the Helmholtz
2033 Young Investigator group ‘Side-Effect’ (VH-NG-1600). Natalia Llopis Monferrer received funding from the European
2034 Union’s Horizon Europe research and innovation program under grant agreement No. 101064167 (MSCA postdoctoral
2035 fellowship Si-ORHIGENS). Dongdong Zhu was supported by the China Postdoctoral Science Foundation under Grant No.
2036 2024M753048, and the Qingdao Postdoctoral Grant (QDBSH20240202136).

2038 **Boxes**

Box 1: Studying biosilicification and Si uptake: from molecular tools to radioisotope enrichment physiological experiments

Biosilicification is the molecular process by which organisms take up silicic acid and transform it into resistant, elastic biomaterials. The study of this process is crucial not only for understanding its biological and ecological significance, but also for unlocking sustainable solutions in material sciences. At the same time, insights gained at the molecular and cellular levels enhance our understanding of the marine Si cycle and improve the accuracy of global biogeochemical models. Recent advances in molecular and single-cell techniques are pushing the frontiers of this field. This toolbox highlights the key technologies currently used to investigate biosilicification.

A central focus in biosilicification research is the identification of molecular markers that signal the presence of this process. Among these, Si transporters are particularly informative. Due to their highly conserved (Hildebrand et al., 1997), these proteins are frequently identified using sequence similarity searches, hidden Markov models, and phylogenetic analyses to detect them in genome and transcriptome datasets (e.g. Durkin et al., 2016; Marron et al., 2016). Functional annotation and expression analyses can help confirm their roles in silicon transport and their regulation across different environmental conditions and taxa. However, silicon transporters are not necessarily the only proteins involved in this complex process. An indirect approach to studying silicification-related genes is to compare RNA transcript levels under limiting and excess silicate availability. By correlating the transcription of unknown genes with that of known silicifying proteins (e.g. Maniscalco et al., 2022; Thamatrakoln and Hildebrand, 2008), it is possible to identify potential candidates involved in silica metabolism. However, this approach is limited to the organisms that can be cultured or maintained in controlled conditions. Beyond genetic analyses, tools such as AlphaFold (Abramson et al., 2024; Mirdita et al., 2022) provide accurate structural predictions of proteins (Jumper et al., 2021). By modelling protein structures, it is possible to study active sites, binding interactions with silica precursors, and the molecular mechanisms driving silica deposition (Knight et al., 2023). Computational simulations and molecular docking further refine these insights by examining protein interactions with silicic acid and other biomolecules. In addition, structural alignment algorithms such as the Foldseek cluster (Barrio-

Hernandez et al., 2023) enable large-scale comparisons, helping to identify domain families and detect remote structural similarities, shedding light on protein function and evolution in diverse organisms. Integrating these predictive approaches with experimental techniques such as electron cryomicroscopy, X-ray crystallography, and biochemical assays strengthens structural interpretations, deepening our understanding of biomineralization processes.

There are also qualitative methods for studying silicification, such as the use of fluorescent compounds. More recent developments have used PDMPO ((2-(4-pyridyl)-5-[(4-(2-dimethylamino-ethylaminocarbamoyl)methoxy)-phenyl]oxazole) in sponges, diatoms, and siliceous Rhizaria (McNair et al., 2015; Ogane et al., 2009; Schröder et al., 2004). This compound is incorporated into newly polymerized bSi under acidic conditions and emits a strong green fluorescence allowing for single-cell and mortality-independent information on silicification and growth rates (Leblanc and Hutchins, 2005; McNair et al., 2015; Shimizu et al., 2001). While this technique is not fully quantitative, these fluorescent markers provide valuable insight into the silicification process, helping to determine the spatial and temporal patterns of silica deposition and offering a deeper understanding of biomineralization dynamics.

The study of radioisotopes and stable isotopes also provides valuable insights into the dynamics of silicification, including uptake mechanisms, intracellular processing, and environmental influences. Silicon stable isotope tracing (^{30}Si) has long been used to simultaneously quantify bSi production and dissolution in the ocean (Fripiat et al., 2007; Nelson and Goering, 1977). Despite the long sample preparation times and complex instrumental analysis required, they offer a powerful tool to understand and quantify nutrient uptake mechanisms, especially when used in conjunction with other stable isotopes such as carbon (^{13}C) or nitrogen (^{15}N -nitrate or ^{15}N -ammonium). Using secondary ion mass spectrometry, it is possible to obtain direct measurements of single cell uptake rates from the same sample (Olofsson et al., 2019). Beyond their use in ecosystem-scale studies, ^{30}Si has also been directly applied to investigate biosilicification pathways. For instance, Marron et al. (2019) explored silicification in cultured choanoflagellates and highlighted potential similarities with sponge pathways, complementing mechanistic modelling of sponge Si isotope fractionation (Wille et al., 2010; updated by Maldonado and Hendry, 2025). In vitro experiments have also demonstrated the role of diatom proteins in fractionating Si isotopes, using the R5 peptide as a model for natural biomolecules involved in diatom silicification (Cassarino et al., 2021).

Due to its easy applicability and increased sensitivity compared to stable isotopes, Si radioisotope tracing (^{32}Si) has gained increasing popularity in recent decades (Closset et al., 2021; Giesbrecht and Varela, 2021; Krause et al., 2019). It has been successfully applied to a variety of silicifying organisms, beginning with diatoms and later extended to others like Rhizaria (Llopis Monferrer et al., 2020). This technique may also be applicable to other organisms such as silicoflagellates and sponges, that can be maintained under controlled conditions.

Box 2: Siliceous microfossils as markers of past and present oceanic conditions

Siliceous microfossils are widely used to reconstruct past environments, from deep geological times to the recent past. Among these, radiolarians, diatoms, and dinoflagellate cysts are particularly valuable for biostratigraphic studies, especially in environments where carbonate fossils are scarce or poorly preserved (Barron et al., 2014; Carvajal-Landinez et al., 2024; Iwai et al., 2025). Siliceous microfossils also serve as proxies in palaeoclimatic reconstructions, providing insights into water masses and environmental parameters such as sea ice cover, sea surface temperature (SST), and marine productivity (Torricella et al., 2025).

Diatoms play a key role in palaeoceanographic and palaeoclimatic reconstructions, particularly at high latitudes, where carbonate preservation is poor. Their distribution is controlled by surface water parameters including light availability, salinity, nutrient levels, temperature, sea ice extent, and the concentration of dissolved silicic acid (Torricella et al., 2022). Benthic diatoms are also influenced by substrate type and water depth, typically flourishing at around 100 meters where sunlight still reaches the seafloor (Round et al., 1990). Because diatom species occupy well-defined ecological niches, their fossil assemblages can be used to infer past oceanographic variability. However, only about 1-10% of surface-dwelling diatoms are preserved in sediments. Their preservation is affected by silica dissolution during settling and at the seafloor, as well as by lateral transport, bioturbation, grazing, and diagenesis (e.g. Crosta and Koç, 2007; Ran et al., 2024). Despite these challenges, diatom assemblages provide crucial information on past surface ocean and climate conditions across a range of regions, including the Southern Ocean (e.g. Crosta et al., 2021), the Arctic (e.g. Oksman et al., 2019), and mid-latitudes (e.g. Bárcena et al., 2001). Exceptionally well-preserved, laminated diatom oozes — particularly those found in Southern Ocean coastal sites — enable high-resolution reconstructions of palaeoceanographic conditions (e.g. Alley et al., 2018; Leventer et al., 2006; Roseby et al., 2022). Seasonally laminated, diatom-rich sequences allow for annual-scale investigations of productivity and sedimentation processes (e.g. Leventer et al., 1993; Maddison et al., 2006; Pike and Kemp, 1997). In contrast, laminations formed by giant diatoms are often associated with specific oceanographic settings such as frontal systems and nutrient trapping, rather than seasonal cycles (Kemp et al., 2006). Stable isotope analyses have recently been applied to diatoms to strengthen palaeoenvironmental interpretations. Commonly measured isotopes include C and N in diatom-bound organic matter, as well as oxygen and Si in the siliceous frustules (Frings et al., 2024; Robinson et al., 2020; Swann et al., 2010). The oxygen isotope $\delta^{18}\text{O}$ provides information on ice volume, temperature, and regional oceanographic conditions (e.g. Hodell et al., 2001; Shemesh et al., 2001), while $\delta^{30}\text{Si}$ reflects the degree of dSi utilization by comparing uptake rates to ambient concentrations (Cardinal et al., 2005; De La Rocha et al., 1998; Varela et al., 2004). In addition, $\delta^{15}\text{N}$ and $\delta^{13}\text{C}$ serve as proxies for past ocean productivity (Crosta and Shemesh, 2002; Schneider-Mor et al., 2005).

Radiolarians, like diatoms, are widely employed in modern and palaeoceanographic studies due to their sensitivity to changes in SST, thermocline depth, nutrient availability, and water mass distribution (Hernández-Almeida et al., 2017; Zhang et al., 2015, 2018). Their siliceous skeletons are well preserved in sediments and form distinct assemblages that

record past temperature gradients, upwelling intensity, and ocean stratification (e.g. Civel-Mazens et al., 2024). Radiolarians can also serve as valuable palaeoceanographic proxies in regions where other silicifiers, such as diatoms, are rare or poorly preserved, particularly in certain deep-sea or oligotrophic sedimentary environments. Several studies have used both diatom and radiolarian assemblages to quantitatively estimate past sea temperature, salinity, and sea ice extent using transfer function techniques (Chadwick et al., 2022; Civel-Mazens et al., 2023; Crosta and Koç, 2007). These functions are based on three key datasets: (1) the modern species distributions in core-top sediments or water samples, (2) contemporary oceanographic parameters obtained from in situ measurements, and (3) fossil assemblages from sediment cores. A major limitation of this approach is the requirement for comprehensive coverage of all three datasets within the target study region.

Isotopic analyses can also be applied to radiolarians. The Si isotope $\delta^{30}\text{Si}$ is used to reconstruct past dSi concentrations (Doering et al., 2021), while $\delta^{18}\text{O}$ serves as a tracer for water temperature. Robinson et al. (2015) tested $\delta^{15}\text{N}$ measurements on radiolarian tests, finding that it reflects the isotopic composition of their food sources. However, $\delta^{15}\text{N}$ in radiolarians shows significant offsets compared to other siliceous microfossils, emphasizing the need to isolate radiolarian fractions carefully from other organisms. Abelmann et al. (2015) observed that $\delta^{18}\text{O}$ and $\delta^{30}\text{Si}$ from radiolarians and diatoms may not always align with changes in assemblages, but still offer valuable insights into silica uptake by different groups and changes in surface and subsurface water masses (down to ~ 400 m).

Silicoflagellates, though less abundant and less studied than diatoms and radiolarians, are still useful in micropalaeontology as proxies for palaeotemperature and palaeoceanographic reconstructions (e.g. McCartney et al., 2022; Rigual-Hernández et al., 2016; Torricella et al., 2021). Sponges also contribute to siliceous microfossil records, with their spicules commonly preserved in marine sediments. Although assigning isolated spicules to specific sponge taxa is often difficult and sponge-derived material may be scarce in some environments such as abyssal plains, they have been used to infer evolutionary, ecological, and environmental conditions (e.g. De Freitas Oliveira et al., 2020; Sim-Smith et al., 2017). Koltun (1960) first emphasized their utility in reconstructing salinity, temperature, and depth from sedimentary sequences. Sponge spicules now serve as valuable proxies for reconstructing a range of palaeoenvironmental conditions, including water flow regimes and velocities (Kuerten et al., 2013), pH (Pisera and Sáez, 2003), light availability (Harrison, 1974), temperature (Gaino et al., 2012), currents (Molina-Cruz, 1991), salinity (Cumming et al., 1993), and water depth (Łukowiak, 2016). Stable isotope analyses, particularly those focusing on $\delta^{30}\text{Si}$, are increasingly used on sponge silica to investigate Si cycling in ancient oceans (Egan et al., 2012). Sutton et al. (2011) demonstrated that $\delta^{30}\text{Si}$ in sponge spicules offers a more accurate and integrated view of whole-ocean Si cycling than surface-dominated diatom records alone.

In conclusion, siliceous microfossils offer a diverse and powerful set of tools for palaeoenvironmental and palaeoclimatic reconstruction in a range of marine environments. Each group contributes unique ecological and geochemical information: diatoms, silicoflagellates, and radiolarians are particularly valuable for deciphering past surface and subsurface oceanic

conditions, while sponge spicules provide complementary information on deeper water mass properties, benthic environments, and the Si cycle. Recent advances in stable isotope geochemistry have further expanded the potential of these microfossils, allowing for increasingly precise reconstructions of nutrient dynamics, temperature variations and Si utilisation.

Box 3: Trait-based approaches to understand the functions of silicification: are diatoms and plants the same?

Why do species or families invest more in silicification than others? Does silicification involve trade-offs with key ecological strategies? What are the costs and benefits of silicification? In land plants, integrating Si concentrations in trait-based approaches has recently proved useful to answer those fundamental questions about Si utilization (de Tombeur et al., 2023b). The question arises as to whether the same approaches could be used in marine silicifiers such as diatoms. In plants, measuring organ-scale Si concentration is relatively easy and offers a reasonable proxy for the degree of silicification, which can then be linked to other functional traits (de Tombeur et al., 2023a, 2025). In diatoms, we hypothesize that it is probably more the shape of silica-based skeletons that is linked to specific functions and associated trade-offs, and less the bulk diatom Si concentrations per se. As such, using only diatom Si concentrations, as done in plants, may not be sufficient to infer specific functions associated with silicification given the large diversity of silicification patterns. Instead, diatom shapes should be involved in current trait-based frameworks. Beyond silicification, current trait-based approaches in diatoms mostly rely on metabolic traits (e.g. nutrient uptake rates; Ács et al., 2019; Litchman, 2022), and less on morphological and chemical traits that are reasonably easy to measure, as it the case in plants (e.g. leaf thickness, leaf area, leaf N concentration). This major difference explains why trait-based approaches to better understand the role and evolution of silicification will probably not follow the same paths for diatoms and plants. Maintaining a constant dialog between trait-based ecologists working on both types of silicifiers is, however, essential.

Box 4: Silicon natural, stable isotopes as tracers of the marine silica cycle

In the natural environment, Si has three stable isotopes: ^{28}Si , ^{29}Si , and ^{30}Si . The natural isotopic composition, referred to as $\delta^{30}\text{Si}$ when expressed as the $^{30}\text{Si}/^{28}\text{Si}$ ratio relative to a reference standard, serves as a powerful tracer for elucidating the marine Si cycle by recording key processes such as biological uptake, dSi utilization, and diagenetic alteration. In the surface ocean, diatoms preferentially incorporate ^{28}Si when building their opaline frustules, leaving the residual dSi enriched in ^{30}Si (De La Rocha et al., 1997; Sutton et al., 2013). This isotopic fractionation (usually noted $^{30}\epsilon$ or $\Delta^{30}\text{Si}$) offers a window into dSi utilization: higher $\delta^{30}\text{Si}$ values in diatoms signal regions where Si is strongly depleted and efficiently used (Grasse et al., 2020). Consequently, measuring $\delta^{30}\text{Si}$ in sedimentary diatom frustules allows to reconstruct past shifts in nutrient availability and productivity, thereby shedding light on glacial-interglacial transitions and long-term variations in the Si cycle (e.g. De La Rocha et al., 1998; Doering et al., 2016; Egan et al., 2012).

In addition to diatoms, other silicifiers, such as sponges and radiolarians, provide complementary insights into Si cycling across various marine environments. Sponges, as benthic organisms, record Si isotope signatures from deeper water masses. Studies have demonstrated that isotopic fractionation in sponge spicules correlates closely with ambient dSi concentrations, and this relationship appears to be independent of factors like temperature, pH, salinity, or other nutrient levels (Hendry et al., 2010; Hendry and Robinson, 2012; Wille et al., 2010). However, a recent study suggests that the relationship between isotopic fractionation and dSi follows different trends in different sponge classes (Maldonado and Hendry, 2025). Radiolarians, on the other hand, are siliceous protozooplankton that inhabit both surface and deep waters unveiling the potential to reconstruct past dSi concentrations from different water depths (Fontorbe et al., 2016, 2017; Hendry et al., 2014). Current estimates of the isotopic fractionation of radiolarians rely on comparing $\delta^{30}\text{Si}$ values from radiolarians in surface sediments with those of the surrounding water mass (Abelmann et al., 2015; Doering et al., 2021).

Beyond these biological processes, $\delta^{30}\text{Si}$ is also a powerful tool for tracing terrestrial inputs and sedimentary recycling. Generally, silicate mineral weathering on land releases dSi with elevated $\delta^{30}\text{Si}$ compared to primary silicate minerals, due to the formation of isotopically light phases, such as secondary minerals in soils and biogenic phytoliths in vegetation (Baronas et al., 2018; Frings et al., 2021; Ziegler et al., 2005). Within marine sediments, the combined effects of bSi dissolution, silicate mineral dissolution, and authigenic clay formation are also reflected in the isotopic composition of porewaters and the buried silica pool (Closset et al., 2022; Ehlert et al., 2016; Geilert et al., 2020, 2023; Ng et al., 2022). Taken together, these processes underscore the versatility of $\delta^{30}\text{Si}$ as a geochemical tracer for both modern and ancient oceanic Si dynamics.

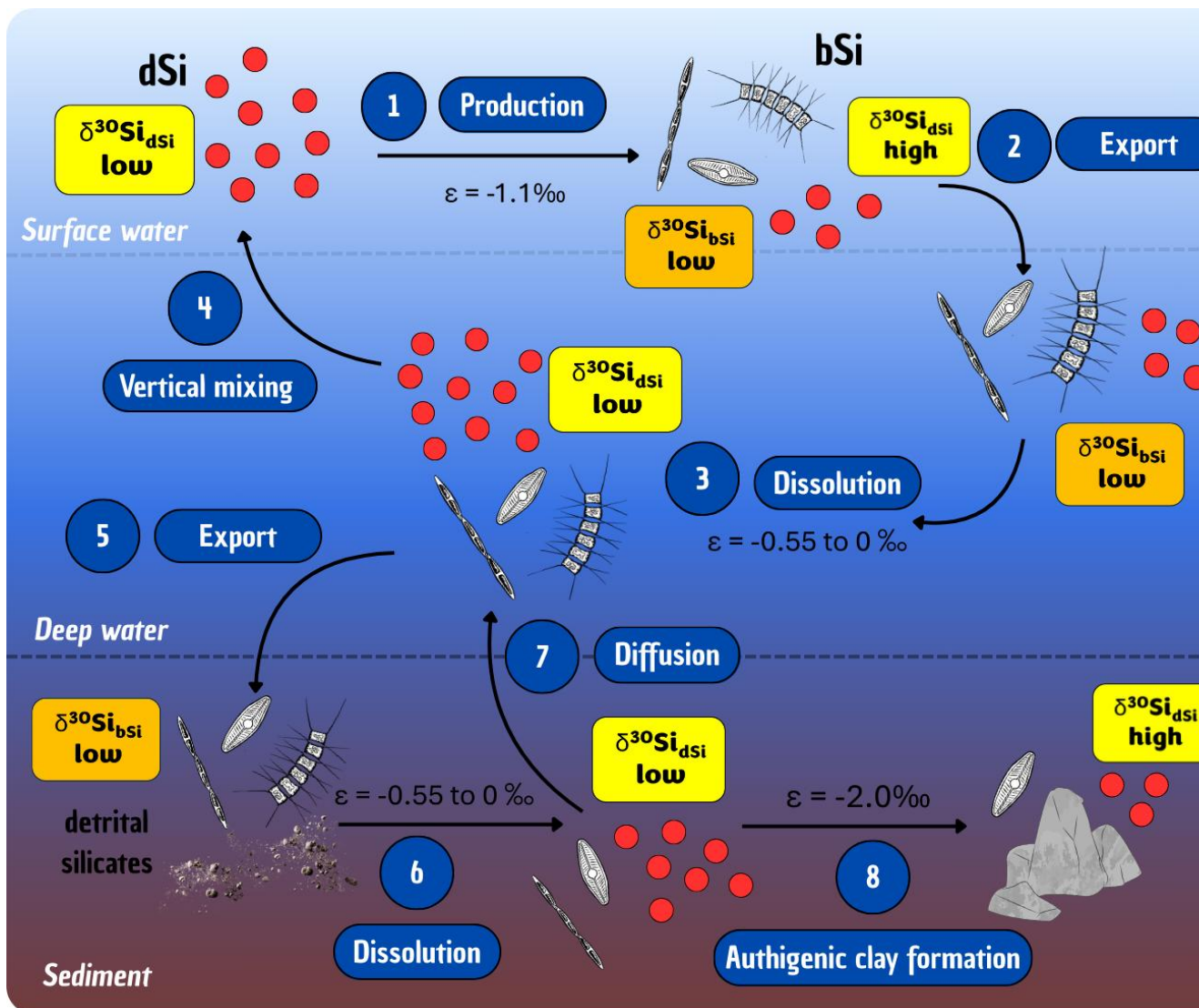


Figure 4. Schematics of the silicon (Si) cycle and isotope fractionation during various oceanic processes, using diatoms as a model for the biogenic silica (bSi) component. The dissolved silica (dSi) pool is depicted by red dots, with its isotopic composition represented by yellow squares. The bSi and detrital silicate pools are illustrated with representative symbols (diatoms, sediments, rocks), and their isotopic composition are shown as orange squares.

Various processes in the ocean affect isotopic fractionation throughout the Si cycle (**Fig. 4**). During the production of bSi, such as in the case of diatoms in surface waters, organisms preferentially incorporate lighter Si isotopes, raising the isotopic composition (high $\delta^{30}\text{Si}$ value) of the surrounding seawater. Simultaneously, the bSi itself becomes enriched in lighter Si isotopes (low $\delta^{30}\text{Si}$ value; **Fig. 4 – 1**). At the end of the productive season, the bSi, characterized by its lower $\delta^{30}\text{Si}$ value compared to dSi, is exported to deeper oceanic layers (**Fig. 4 – 2**). In the deep ocean, bSi undergoes gradual dissolution,

releasing its low $\delta^{30}\text{Si}$ signature back into the surrounding seawater. It remains uncertain whether this dissolution process actively fractionates Si isotopes — specifically, whether the release preferentially favours lighter Si isotopes (as proposed by Demarest et al., 2009) or not (as suggested by Wetzell et al., 2014). Nevertheless, the overall effect of this recycling process is the maintenance of a low $\delta^{30}\text{Si}$ signature in deep waters (**Fig. 4 – 3**). The light $\delta^{30}\text{Si}$ imprint from the deep waters is subsequently transported back to the surface through vertical mixing processes, particularly during winter periods or in upwelling regions, where it becomes available for uptake by new primary producers (**Fig. 4 – 4**). Simultaneously, the bSi that does not undergo further recycling within the water column settles and reaches the sediment (**Fig. 4 – 5**). Upon deposition in the sediment, bSi remains stored over extended timescales, during which it continues to undergo dissolution, releasing its light isotopic composition into the pore or interstitial waters (**Fig. 4 – 6**). These Si-rich pore waters with low $\delta^{30}\text{Si}$ value eventually diffuse back into the overlying bottom waters, contributing to the Si pool in the deeper ocean layers (**Fig. 4 – 7**). Under certain conditions, the dSi in pore waters may precipitate back into a mineral phase, forming authigenic clays. While the mechanisms underlying this process remain poorly understood, evidence suggests that it may involve isotopic fractionation, preferentially incorporating the lighter Si isotope into the newly formed clay minerals, thereby increasing the $\delta^{30}\text{Si}$ of the dissolved phase (**Fig. 4 – 8**).